Landscape Controls of Complex Terrain and Vegetation Heterogeneity on Carbon Cycling in a Humid, Temperate Watershed in West Virginia

Jeffrey Wayne Atkins
Wallburg, North Carolina

B.A. Western Carolina University, 2004

A dissertation presented to the Graduate Faculty
of the University of Virginia in Candidacy for the Degree of Doctor of Philosophy

Department of Environmental Sciences

University of Virginia

February, 2016

ABSTRACT

In topographically complex terrain, the spatial heterogeneity of carbon cycling is affected by vegetation heterogeneity and landscape position through the lateral and vertical redistribution of soil water. Vegetation affects carbon cycling directly through photosynthesis, tissue allocation, respiration, and litter production, but also by mediating abiotic environmental factors such as soil temperature, soil moisture, and available light. In areas of topographic complexity, such as mountain catchments, the landscape can laterally redirect soil water, resulting in areas of convergent and divergent soil moisture that create spatial heterogeneities in carbon fluxes. Our knowledge of how vegetation interacts with landscape position to affect carbon cycling within areas of cool, humid watersheds is lacking. Further, we must also understand how these systems are changing and the possible impacts of climate and climatic variability. Here I address this knowledge gap in three ways: 1) by examining landscape controls on surface soil carbon fluxes and response to inter-annual climate variability; 2) examining the landscape controls on litter decomposition, nitrogen availability, and the organic layer; 3) characterizing the spatial and temporal dynamics of the evergreen shrub community. The major findings of my dissertation are that 1) surface soil CO_2 fluxes are greater beneath evergreen shrubs across all elevations for the three years measured—a result driven not only by differences in soil moisture and soil temperature beneath shrubs, but also by differences in soil chemical and physical properties; 2) fluxes are constrained during periods of greater soil moisture, with soil moisture responding strongly to varying annual precipitation, resulting in variability of soil CO_2 fluxes; 3) litter decomposition is predominately controlled by elevation with seasonal differences possibility related to snow cover; 4) nitrogen availability is controlled by vegetation, with areas of greater

availability beneath closed forest canopies—driven by differences in nitrate abundance; 5) evergreen shrub cover in the study watershed is increasing, with the greatest increases at low and mid elevations and along southerly aspects—areas that were once water-limited on the landscape.

Table of Contents

ABSTRACT 2

ACKNOWLEDGEMENTS 7

Chapter One: Introduction 10

COMPLEX TERRAIN *10*

LANDSCAPE CONTROLS ON SOIL CARBON FLUXES *11*

LANDSCAPE CONTROLS ON DECOMPOSITION *14*

VEGETATION HETEROGENITY AND THE FOREST UNDERSTORY *16*

WATERSHED APPROACH *17*

STUDY SITE *18*

SOILS AND GEOLOGY *19*

LAND USE AND LAND CHANGE HISTORY *20*

DISSERTATION FOCUS *22*

REFERENCES *23*

Chapter Two: Vegetation heterogeneity and landscape influence the timing and magnitude of soil CO_2 efflux in a humid, Appalachian watershed 32

ABSTRACT *32*

INTRODUCTION *33*

METHODS *37*

SITE DESCRIPTION *37*

VEGETATION AND ELEVATION CLASSES *38*

Soil CO_2 efflux *38*

VOLUMETRIC WATER CONTENT *39*

SOIL TEMPERATURE *41*

SOILS *42*

DATA ANALYSIS *42*

RESULTS *44*

SOIL CO_2 EFFLUX (F_{SOIL}) *44*

WATER-FILLED PORE SPACE (WFPS) *45*

SOIL TEMPERATURE (T_{SOIL}) *46*

SOIL PHYSICAL AND CHEMICAL CHARACTERISTICS *46*

DISCUSSION *48*

CONCLUSIONS *55*

TABLES AND FIGURES *57*
APPENDIX *65*
REFERENCES *70*

Chapter Three: Nutrient cycling, litter decomposition, and the organic layer among varying vegetation cover classes along an elevation gradient in a West Virginia watershed 78

ABSTRACT *78*
INTRODUCTION *79*
METHODS *83*
SITE DESCRIPTION *83*
VEGETATION AND ELEVATION CLASSES *84*
LITTERBAG EXPERIMENT *84*
LEAF LIGNIN, CARBON, AND NITROGEN *85*
NITROGEN AVAILABILITY *85*
SOILS AND THE ORGANIC LAYER *86*
DATA ANALYSIS *86*
RESULTS *87*
LITTER BAG EXPERIMENT *87*
NITROGEN AVAILABILITY *88*
ORGANIC LAYER *88*
DISCUSSION *88*
CONCLUSIONS *92*
TABLES AND FIGURES *94*
REFERENCES *103*

Chapter Four: Characterization of Understory Shrub Expansion in a West Virginia watershed from 1986 - 2011 using Landsat Derived Vegetation Indices 107

ABSTRACT *107*
INTRODUCTION *107*
METHODS *112*
STUDY AREA *112*
LANDSAT DATA *113*
VEGETATION INDICES *113*
MODEL SELECTION AND IMAGE CLASSIFICATIONS *115*
SPATIAL ANALYSIS *116*

TREND ANALYSIS *117*
ELEVATION, ASPECT, DISTANCE-TO-STREAM *117*
RESULTS *118*
VEGETATION INDICES *118*
MODEL CLASSIFICATION COMPARISON *119*
CHANGES IN CLASSIFICATION FROM 1986 TO 2011 ..... *119*
LINEAR REGRESSION CHANGE ANALYSIS *120*
ELEVATION *120*
ASPECT *120*
DISTANCE-TO-STREAM *121*
LANDSCAPE VARIABLE COVARIANCE *122*
DISCUSSION *122*
IMPACTS OF UNDERSTORY SHRUB EXPANSION *124*
SHRUB EXPANSION AND LANDSCAPE VARIABLES *125*
EVERGREEN SHRUBS WITHIN THE SECONDARY FOREST *126*
CONCLUSIONS *128*
TABLES AND FIGURES *129*
APPENDIX *139*
REFERENCES *140*

Chapter Five: Synthesis and Conclusions 145

LANDSCAPE CONTROLS ON SOIL CO_2 EFFLUX *145*
LANDSCAPE CONTROLS ON DECOMPOSITION, NUTRIENT CYCLING, AND THE ORGANIC LAYER *146*
CHARACTERIZING THE EVERGREEN SHRUB COMMUNITY *147*
FUTURE DIRECTIONS *148*
REFERENCES *150*

ACKNOWLEDGEMENTS

I would like to acknowledge the Canaan Valley Institute, the Appalachian Stewardship Foundation, the University Of Virginia Department of Environmental Sciences, Blandy Experimental Farm, and the Shenandoah Watershed Study (SWAS) for their financial support of my research and scholarship. I am also indebted to my advisor, Howard Epstein, for his mentorship, counsel, and support. I cannot imagine having a different advisor, nor one of which I could speak more highly. I would also like to thank my committee members, Daniel Welsch, Todd Scanlon, and Andres Clarens for their guidance and collaboration. I would also like to thank my lab mates, Stesha Dunker, JJ Frost, Qin Yu, Jenny McGarvey, Sara Brastch, and Itiya Aneece for their support through the years. I have had the fortune to work with several talented undergraduate students while here at the University, including Jerrica Frazier, Virginia Mathurin, Sang Mee Ko, Molly Siebers, Brianna Collins, Jorge Ruiz Arocho, Trevor Klein, Sarah Friedlander, and Thomas Williams. Graduate school has also been far more enjoyable and inspiring thanks to Jon Walter, Grace Wilkinson, Luke Cole, Rishi Das, Erin Swails, Alia Al-Haj, Rosemary Malfi, Stacy Lynn, Abi Bhattachan, Jennie Rheuban, Matt Long, David Seekell, Kelly Hondula and many, many others I am glad to call friends. I would also like to thank Meg Miller for lab guidance, support, and coffee; Will Tomanek and John Porter for technical assistance through the years; Hank Shugart for the chats; Danny for the field demonstrations; Todd for helping me learn to code; John and Suzie Maben for everything (where would I start?); Hellbender Burritos—not only for the food, but for the warm fire during the cold West Virginia winters; Jackie and Charlene for reminding me to slow down; the Kirbys for the friendship and the laptop that got me through UNCA; the Turpins for the opportunity and encouragement; and Eric, for doing it first and

showing it could be done. Most importantly, I want to thank my family for not thinking this was crazy to begin with and for always being there. Addison and Gus, I hope you always keep the joy of discovery you have and that you never stop asking questions. And Annie, you are beyond amazing. Your love and support has been the world.

“Besiehe! Das land Canaan!”

Henry Fansler, April, 1800

The first known European settler of the Canaan Valley
upon seeing the valley from Cabin Mountain for the first time

Chapter One: Introduction

Within complex terrain, topographic channeling and spatial heterogeneity exert controls on material flows; through the lateral redistribution of material, the temporal dynamics and spatial patterns of energy and matter (e.g. water, nutrients, etc.) are altered (Riveros-Iregui et al. 2011). The role that lateral redistribution of resources has on biogeochemical cycles, particularly terrestrial carbon cycling, is a primary research interest, as lateral fluxes within terrestrial ecosystems can be as important as vertical exchange between the land and atmosphere in determining ecosystem processes (Bormann and Likens 1967; Reiners and Driese 2001; Reiners 2005; Chapin et al. 2006). The temporal differences in carbon fluxes within and across sites (Baldocchi et al. 2006), across successional stages (Yan et al. 2006; Wang et al. 2010; Dunker and Epstein in prep.), and across environmental gradients (Pacific et al. 2008; Webster et al. 2008) have been well considered. However, there exists a gap in our understanding of how vegetation cover heterogeneity and elevation gradients interact to influence carbon and water cycling within complex terrain at the watershed and sub-watershed scales. Further understanding of the landscape controls imposed by gradients and heterogeneities within complex terrain on biogeochemical cycles is vital for both the theoretical constructs of vegetation-climate-landscape interactions and the accurate modeling and budgeting of carbon dynamics of watersheds.

COMPLEX TERRAIN

Complex or mountainous terrain refers to an area where topographic and elevation variation across a site is sufficient to affect meteorological and micrometeorological variables. The effect of complex terrain and topography on land-atmosphere exchange and ecological processes is non-trivial (Raupach and Finnigan 1997; Baldocchi et al. 2000). Further, it is

additionally important to make the theoretical and practical connection that the heterogeneity and variance of certain ecosystem variables (e.g. carbon flux rates, available soil moisture, vegetation patterns) are products of the heterogeneity of other terrain-related variables (e.g. slope, aspect, elevation) (Tague 2005; Emanuel et al. 2010). For example, convergent lowland areas exhibit higher quantities of soil moisture than divergent upland areas (McGlynn and Seibert 2003; Pacific et al. 2008), and soil temperature, soil organic matter, and nitrogen mineralization can all be influenced by aspect and elevation (Garten Jr. et al. 1999; Kang et al. 2003; Bonito et al. 2003).

LANDSCAPE CONTROLS ON SOIL CARBON FLUXES

Soil respiration (R_{SOIL}) is a significant component of the terrestrial carbon cycle with annual soil carbon emissions estimates of between 68 to 100 Pg of carbon annually (Bond-Lamberty and Thomson, 2010). In the field, R_{SOIL} can be approximated by measuring soil CO_2 efflux (F_{SOIL}) which is the instantaneous transport of soil CO_2 from below- to above-ground (Atkins et al. 2015). Soil CO_2 efflux is driven by soil temperature, soil moisture, and soil carbon availability, as well as soil chemical and physical properties (Schlesinger 1977; Raich and Schlesinger 1992; Raich and Tufekcioglu 2000). Spatial variation of soil CO_2 efflux rates has been attributed to fine root biomass, microbial biomass, mycorrhizal associations, soil moisture, as well as soil texture, soil bulk density, soil chemistry, and other edaphic properties (Xu et al. 2001; Tang and Baldocchi 2005). These factors do not drive CO_2 efflux rates monotonically or in isolation, nor are they simply additive, but rather interact with each other to create differential responses in efflux rates and magnitudes across spatial and temporal scales (Dilustro et al. 2005; Pacific et al. 2009), an effect magnified within areas of complex terrain (Riveros-Iregui and McGlynn, 2009; Kang et al. 2003, 2006).

Temperature is a well-established, primary driver of F_{SOIL} (Fang and Moncrieff, 2001). However, soil moisture plays a critical secondary role. Xu et al. (2001) showed that for a ponderosa pine plantation in northern California, F_{SOIL} was positively correlated with increasing volumetric soil moisture at values below 19%. F_{SOIL} showed a negative correlation with increasing soil moisture at values above 19% (Xu et al. 2001); F_{SOIL} is greatest during periods of intermediate soil moisture (Davidson et al. 1998). The suppression of F_{SOIL} at higher soil moisture values can be attributed to the effect soil moisture has on both CO_2 production within and transport through the soil. Decreased transport through the soil matrix is due to the lower rate of diffusivity of CO_2 through water versus that of air. When soil pore space becomes filled with water, CO_2 transport through the soil matrix is markedly decreased (Davidson and Trumbore 1995; Jassal et al. 2005). Elevated levels of soil moisture can also lead to soil anoxia and decreased aerobic respiration of soil microbes (Oberbaur et al. 1992).

The distribution of soil moisture across a landscape is driven by the drainage pattern of the system, which itself is inextricably tied to soil, bedrock type, and topography (Grayson et al. 1997). As suggested above, changes in soil moisture across a landscape can result in spatially non-monotonic changes in F_{SOIL} (Pacific et al. 2009). For systems dependent on snowmelt as a major contributor of the annual water input, the timing of snowmelt can result in major effects on the temporal dynamics and magnitude of F_{SOIL} (Riveros-Iregui et al. 2011; Pacific et al. 2009). In the Stringer Creek watershed in Montana, F_{SOIL} was found to vary in magnitude spatially as much as seven-fold and was strongly correlated to the topographically-induced lateral redistribution of soil moisture (Riveros-Iregui et al. 2011). At the catchment scale, soil moisture varies as a function of topographic channeling effects, as well as vegetation and soil

heterogeneity (Moore et al. 1986; Western et al. 1999; Emanuel et al. 2010). The vegetation of an area is also influenced strongly by terrain and topography. Vegetation in turn alters the available soil moisture—providing a crucial coupling of carbon and water cycling in terrestrial environments (Emanuel et al. 2007).

Vegetation cover and elevation partially affect F_{SOIL} through altering micrometeorological variables—soil moisture, soil temperature—as well as soil nutrient availability and soil microbial communities (Grayson et al. 1997; Raich and Tufekcioglu 2000; Emanuel et al. 2010; Pacific et al. 2011; Riveros-Iregui et al. 2011). Whereas Raich and Potter (1995) found no significant difference between broad-leaved, deciduous forests and needle-leaved, coniferous forests in the relationship between soil CO_2 efflux rates and mean monthly air temperatures, Raich and Tufekcioglu (2000) later showed coniferous forests tended to have 10% lower flux rates than broad-leaved forests occurring on similar soil types. Marked differences have been found in comparing grasslands and forests as well—with grasslands exceeding forests in F_{SOIL} rates by 20-38% (Raich and Tufekcioglu 2000; Smith and Johnson 2004). One consideration is the influence of vegetation structure and physiology on microclimates. Canopy-shaded soils within forests tend to have lower soil temperatures and retain more soil moisture due to decreased evaporation as a function of soil shading (Breshears et al. 1998; Breshears 2006). Diel variations in F_{SOIL} can also be driven by plant physiology. F_{SOIL} rises with increased inputs of plant root exudates, which are directly related to photosynthetic rates that are governed by diel solar radiation cycles (Kuzyakov 2006). Tang et al. (2005) found that diel variation of soil respiration in open areas of an oak-grass savanna was in phase with summer soil temperature regimes—i.e.

F_{SOIL} increased with higher temperatures. However, beneath canopy areas were out of phase, with maximum F_{SOIL} rates 7-12 hours later than peak temperatures.

Inter-annual effects of precipitation have strong implications for carbon cycling. Pacific et al. (2009) showed that a drier growing season (2006) led to earlier peaks in F_{SOIL} rates for both riparian and hillslope landscape positions—with cumulative F_{SOIL} increasing 33% in the riparian areas during a dry year (2006) compared to a wet year (2005), while cumulative F_{SOIL} decreased by 8% in the hillslope areas during the dry year. With forecasted changes in temperature and precipitation regimes attributable to global climate change, understanding the coupling between carbon and water cycling is crucial.

Globally, there is a strong positive correlation between R_{SOIL} and annual above-ground litter production in boreal, temperate, and tropical forests (Raich and Nadelhoffer 1989). There is also a strong linear correlation between R_{SOIL} and NPP among the world's biomes—suggesting that the controls on these above- and below-ground processes are shared and further emphasizing the importance of the link between plant production and soil respiration (Raich and Schlesinger 1992).

LANDSCAPE CONTROLS ON DECOMPOSITION

At broad spatial extents, decomposition rates are controlled by climatic variables (e.g. mean annual precipitation (MAP), mean annual temperature (MAT), etc.) (Epstein et al. 1997; Berg 2000; Epstein et al. 2002; Zhang et al. 2008). At finer extents, litter substrate quality, soil fauna community composition, and other site-level factors (e.g. pH, labile soil N, soil temperature, aeration, etc.) are influential (Berg and McClaugherty, 2008). Environmental decomposition controls are well understood at global scales (Vitousek et al. 1994; Meetenmeyer 1978; Berg and McClaugherty 2008), however, inter-site and intra-site variance of leaf litter

decomposition along environmental gradients is a topic that necessitates further exploration—especially in areas of complex, heterogeneous terrain (Zhou et al. 2008; Crutsinger et al. 2009). Understanding the controls on short-term and long-term decomposition within ecosystems is vital for properly informing ecosystem and climate models and understanding carbon cycling processes (Harmon et al. 2009).

The relationship between decomposition and net primary productivity (NPP) has profound implications for ecosystem carbon cycling (Chapin et al. 2002). Decomposition impacts soil fertility and long-term carbon storage (Berg and McClaugherty 2007). Fresh litter decomposition, through litter addition experiments, has been shown to have a priming effect on R_{SOIL} by increasing co-metabolic decomposition of recalcitrant soil organic matter, resulting in greater total F_{SOIL} rates (Chemidlin Prévost-Bouré et al. 2010). Conceptually, decomposition is the aggregation of all of the chemical, physical, and biological processes involved in the breakdown of organic matter into both mineral and "increasingly stable forms" (Berg and McClaugherty 2008). Decomposition may break organic matter down into its inorganic components (CO_2, mineral nutrients) or result in recalcitrant, complex organics (Chapin et al. 2002). Decomposition rates are controlled by climate (and the resulting soil microclimate), soil physical properties, soil and litter chemistry, soil animals, and the soil microbial community (Singh and Gupta 1977; Zhang et al. 2008). A biological view of decomposition is crucial, as decomposition is a product of soil microbial communities and exists only to meet the energetic demands of these communities (Chapin et al. 2002).

With regard to topographically complex ecosystems, Shanks and Olson (1961) showed differences in first-year decomposition rates of leaf litter from five different species of deciduous

trees along an elevation gradient in the southern Appalachians. Decomposition rates were greater at lower elevations and underneath deciduous trees. Dwyer and Merriam (1981) showed that fine-scale forest topography (< 0.5 m vertical variation) affects litter accumulation and decomposition rates by altering the temperature and moisture variability at the soil-litter interface.

VEGETATION HETEROGENITY AND THE FOREST UNDERSTORY

Within many forests, the understory can strongly impact ecosystem processes. Evergreen shrubs such as rosebay or great rhododendron (*Rhododendron maximum*) and mountain laurel (*Kalmia latifolia*) dominate the forest understory within many mountainous areas in the eastern United States, and in the case of *R. maximum*, the more dominant and prevalent of the evergreen shrub species in these forests, create dense, nearly impenetrable thickets along streams (Beier et al. 2005; Baker and Van Lear 1998). These shrubs can alter forest structure through exerting controls on overstory sapling regeneration by outcompeting tree species for available nutrients or by directly inhibiting access to available light and soil moisture (Phillips and Murdy, 1985; Clinton and Vose, 1996, Van Lear et al. 2002, Beier et al. 2005). Our understanding of the role of evergreen shrubs on ecosystem processes and their changing spatial dynamics is limited. Any approach to understanding vegetation heterogeneity within complex terrain must go further than a coarse examination of the horizontal differences in vegetation, such as a comparison of forest gaps to closed-canopy forest. In areas where there is a strong understory component, this must be considered within the analysis. Concordant with the spatial consideration of both the horizontal and vertical structure of the forest, it is also imperative to consider how these components interact to influence each other and how they change through

time. Spatial aggregation within forests is non-trivial and can result in important effects on biogeochemical processes.

WATERSHED APPROACH

Because biogeochemical cycles are intrinsically related to the hydrologic cycle in most systems, the use of the watershed approach in ecosystem studies allows for a natural method of investigation, where boundaries are well-delineated by the flow of water (Likens and Bormann 1995; Likens 2001). A further advantage to the watershed approach, from a biogeochemical perspective, is the ability to estimate air-land-water exchange of material and critical ecological processes at a scale that is both reasonable for field work and comprehensive enough for inferences (Likens 2001). Where flows occur, water acts as the primary connector across different patches of the landscape (Fisher and Welter 2003). The spatial complexity of a watershed can be examined discretely, or integratively by looking at downstream point measurements of stream chemistry (Likens 2001). Lateral flow of water leads to the movement of nutrients such as nitrogen and phosphorus, and links terrestrial and aquatic system components (Peterjohn and Correll 1984). Topography, through hydrological connectivity and subsurface flow within a catchment, can exert controls on nitrate availability and export (Welsch et al. 2001) that have direct effects on carbon dynamics, vegetation growth, and other ecosystem processes (Schlesinger and Andrews 2000; Galloway et al. 2004). The lateral movement and distribution of water within a watershed is reflexively related to the spatial arrangement of vegetation communities, as vegetation can also exert strong controls on the availability of soil moisture and its spatial distribution across the landscape (Day and Munk 1974; Muller 1982; Hwang et al. 2012).

STUDY SITE

My study site is the Weimer Run watershed, a 374 ha watershed located in West Virginia. It is an area of complex terrain located in a humid environment with no discernible seasonality in the distribution of precipitation, and with distinct vegetation and elevation gradients. The Weimer Run watershed is located within the Little Canaan Wildlife Management Area (formerly held by the Canaan Valley Institute) near Davis, West Virginia and has an elevation range of 940 m (The Blackwater River) to 1175 m (Bearden Knob) ASL (Fig. 1.1).

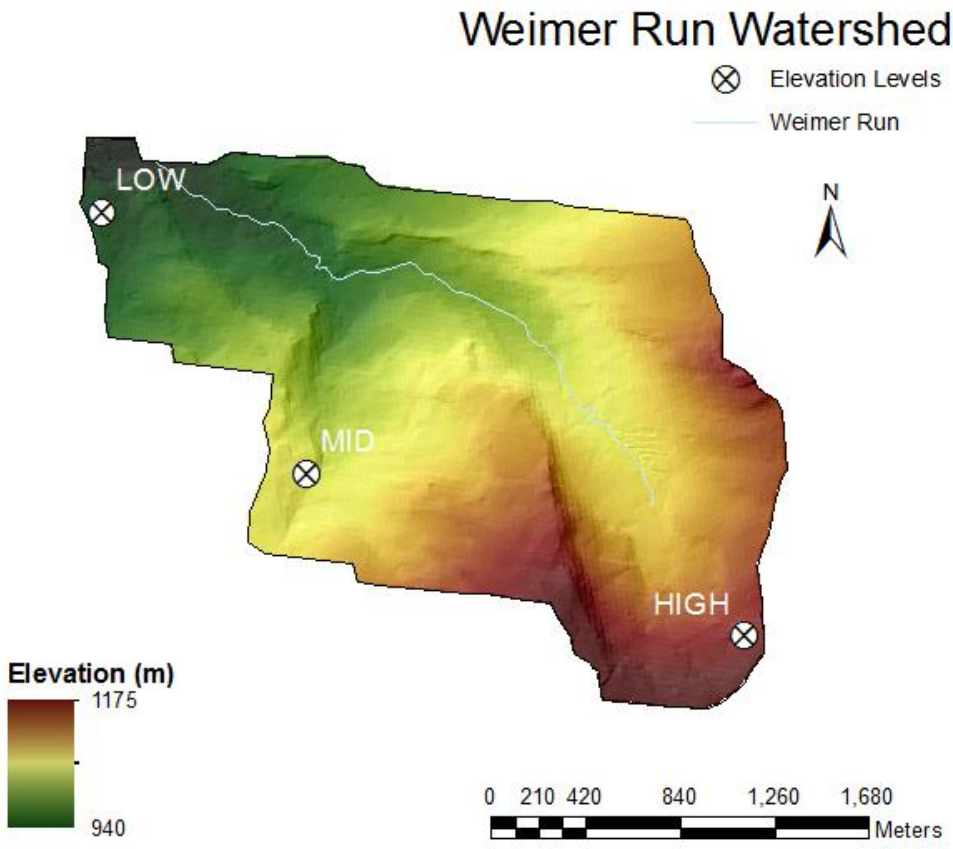

Figure 1.1. The Weimer Run watershed (374 ha).

Weimer Run is a mixed-hardwood-coniferous forest landscape, consisting of yellow birch (*Betula alleghaniensis*), red maple (Acer rubrum), red spruce (*Picea rubens*), and black cherry (*Prunus serotina*). The forest is notable for an incredibly dense understory, evergreen shrub layer consisting primarily of rhododendron (*Rhododendron spp*.) and mountain laurel (*Kalmia latifolia*).

The herbaceous understory plant community consists of various ferns, grasses, club and peat mosses. The soils are heavily acidic, with pH levels ranging from 3.8 - 4.4 (measured July 2010). Stephenson (1993) reports similar values of soil pH ranging from 3.4 – 4.1 for regionally proximate upland forest areas also located in West Virginia, with the lower values corresponding to higher elevations.

Figure 1.2. Left, looking down into the Weimer Run watershed along a powerline break; Right, Rhododendron occupying a forest gap.

SOILS AND GEOLOGY

The Weimer Run watershed is adjacent to the Canaan Valley which exists in a transitional zone between the Appalachian Valley and Ridge, and the Appalachian Plateau, known as the Folded Plateau (Matchen 2002). In the Canaan Valley area, the Folded Plateau is about 48 km in width. Pennsylvanian sandstone from the Pottsville Formation (~300 Ma) tops the ridges that surround Canaan Valley and underlie the study site. The Pottsville group consists of sandstones, shales, siltstones, mudstones, and coal (Matchen 2002).

Carter and Ciolkosz (1980) demonstrated that the mesic-frigid soil temperature boundary occurred at 1088±26 m for this area. This would imply a bimodal soil temperature regime within the watershed—with portions at or above the elevation threshold having a frigid temperature regime (where mean soil temperatures are below 8° C, and the mean summer temperature is at least 6° C warmer than the mean winter temperature), while portions below the aforementioned elevation threshold have a mesic temperature regime (where mean temperatures are greater than 8° C, but less than 15° C) (Crews and Wright 2000; Sencindiver et al. 2002). The soils of the mountains that surround the valley are primarily Spodosols and Inceptisols with some Ultisols (Sencindiver et al. 2002). Unlike many counties to the west and south, generally the hard rocks of the Allegheny and Pottsville series make the mountain ridges, while the softer sediments of the Mississippian and Devonian form the valleys and comparatively low hills or mountains (Sencindiver et al. 2002).

LAND USE AND LAND CHANGE HISTORY

The Weimer Run watershed is located in Tucker County, West Virginia. In the fall of 1746, the first European explorers arrived in the Canaan Valley (then Randolph County), the Fairfax Boundary Line Surveying Team, with the intent to find the headwaters of the Potomac (Fansler, 1962; Brown, 1959). The surveying team had set out from Charlottesville, VA earlier in the year, and included Peter Jefferson, father of President Thomas Jefferson. European exploration of Tucker County proper did not occur until 1762, during the French and Indian War (Maxwell 1884). Early explorations of Tucker County and the Canaan Valley were slow-going and fraught with danger as explorers found traversing the dense “laurel thickets” of the valley exceedingly difficult (Strother 1857).

Europeans first established settlements in Tucker County in 1774, along the Cheat River valley. Settlers found the forests of Tucker County to be unwieldy (Maxwell 1884). Many trees, some reportedly ten feet or more across at the base, were cut and burned, because they were not commercially viable (Maxwell 1884); many trees were simply too large. Infrastructure with which to manage the plentiful timber resources was lacking. Subsequently, large swaths of the forest were felled and either burned or allowed to rot where they fell (Maxwell 1884).

Commercial exploitation of the forest as a natural resource was not possible until the railroad reached Davis, WV on November 1, 1884 (Fansler 1962). Tucker County quickly became a bastion of timber production. For 38 years, from 1886 until 1924, the Babcock Sawmill in Davis produced 856,985,714 feet of lumber (Fansler 1962)—a rate of 22.5 million board feet of lumber production per year for 38 years (a total of 1.8 million ft^3). Comparatively, a large, modern mill can process between 100 and 700 million board feet annually. A 1909 report on the nation's forests indicates that forest land for the entire state of West Virginia had decreased from original estimates of 14,610,000 acres to 9,100,000 acres—a decrease from 95% total land cover to a severely diminished 59% (Kellogg 1909). Concordantly, West Virginia produced more lumber than any other state in 1909—Tucker County had 15 large sawmills operating during this period and was highly productive given the modest size of the county (Fansler 1962).

During the 1800s, ranchers and farmers in upper West Virginia, including areas surrounding Canaan Valley, would often burn large areas of forest in an attempt to make pasture and rangeland for cattle—an often futile attempt as fire would burn the area so completely that little more than mineral soil and scrub would be left, without suitable vegetation for livestock filling the void (Fansler 1962). Many lumber mills closed during the 1920s, with the final mill in

Tucker County closing in 1933. Timber production and forestry is still vital to West Virginia's economy, employing over 30,000 people and providing $3.2 billion dollars annually to the state economy (WVFA). It is the third largest manufacturing employer in the state behind fabricated metals and chemical manufacturing (West Virginia Dept. of Commerce). While 78% of West Virginia is currently forested, there have been marked changes in species composition and diversity since settlement and industrialization. Former spruce forests have been replaced with second and third growth temperate deciduous forests (Allard and Leonard 1952).

DISSERTATION FOCUS

The motivation for my dissertation is to examine the interactions between and controls of vegetation heterogeneity and landscape position on carbon cycling at the watershed scale within this West Virginia watershed. To accomplish this, my dissertation consists of multiple approaches grouped within three component chapters: 1) evaluate the landscape controls on F_{SOIL} (soil CO_2 efflux); 2) examine landscape controls on decomposition; 3) quantify the spatial and temporal dynamics of the understory evergreen shrub layer (Table 1.1).

Table 1.1. Summary of dissertation components, research questions, and approaches.

DISSERTATION COMPONENT	RESEARCH QUESTIONS	APPROACHES
I. Landscape contols on soil CO_2 efflux	1. How does soil CO_2 efflux respond to interannual variation in precipitation in a humid, complex watershed?	Plot-based measurements of soil CO_2 efflux, soil temperature, soil moisture from 2010 - 2012 using a factorial approach to consider elevation gradient and vegetation
	2. How do landscape position and vegetation heterogeneity affect soil CO_2 efflux, and how do they interact with interannual variation in precipitation?	Long term trends of precipitation were evaluated using change-point analysis to determine inter-annual variance. Statistical inferences were made from empirical data.
II. Landscape controls on decomposition, nutrient cycling, and the organic layer	1. What are the effects of vegetation cover on litter decomposition, the soil organic layer, and N dynamics across an elevation gradient within a cool, humid watershed in West Virginia?	A two year decomposition study where litterbags were deployed across the watershed from 2011 – 2013.
	2. How does N availability vary among vegetation cover across an elevation gradient within a cool, humid watershed in West Virginia during the growing season?	Cation and anion probes were used at three time intervals across the growing season to measure nitrate and ammonium availability.
III. Characterizing the evergreen shrub community	1. What are the spatial patterns and temporal dynamics of the evergreen shrub layer within the Weimer Run watershed located near the Canaan Valley in West Virginia over the period of available satellite data (1986-2011)?	Using Landsat 5 TM data from 1986 - 2011, an NDVI time-series from snow-free, winter scenes (to isolate evergreen shrubs) was generated, then compared to Tasseled Cap indices and Disturbance Index. Then both spatial linear regression and cluster analysis were used to detect temporal and spatial trends.
	2. Are the dynamics of the evergreen shrub layer related to landscape position (e.g. elevation, aspect, distance from stream)?	Each landscape variable was evaluated with respect to changes in NDVI.

REFERENCES

Allard HA, Leonard EC (1952) The Canaan and the Stony River Valleys of West Virginia, their former magnificent spruce forests, their vegetation and floristics today. Castanea 17(1): 1-60.

Atkins JW, Epstein HE, Welsch DL (2015) Vegetation and elevation influence the timing and magnitude of soil CO_2 efflux in a humid, topographically complex watershed. Biogeosciences, 12(10), 2975-2994.

Baldocchi DD, Finnigan JJ, Wilson KW, Paw U KT, Falge E (2000) On measuring net ecosystem carbon exchange in complex terrain over tall vegetation. Boundary Layer Meteorology. 96: 257-291.

Baldocchi DD, Tang JW, Xu LK (2006), How switches and lags in biophysical regulators affect spatial-temporal variation of soil respiration in an oak-grass savanna. Journal of Geophysical Research 111, G02008, doi:10.1029/ 2005JG000063.

Berg B (2000). Litter decomposition and organic matter turnover in northern forest soils. Forest Ecology and Management, 133(1-2): 13–22. doi:10.1016/S0378-1127(99)00294-7.

Berg B, McClaugherty C (2008). Plant litter: decomposition, humus formation, carbon sequestration. Springer, New York 338 p.

Bonito GM, Coleman DC, Haines BL, Cabrera ML (2003) Can nitrogen budgets explain differences in soil nitrogen mineralization rates of forest stands along an elevation gradient? Forest Ecology and Management 176(1–3): 563-574.

Bond-Lamberty, B., and Thomson, A. (2010) Temperature-associated increases in the global soil 22 respiration record, Nature, 464, 579-582, 2010.

Bormann, FH, GH Likens (1967) Nutrient Cycling. Science 155: 424-429.

Breshears DD, Nyhan JW, Heil CE, Wilcox BP (1998) Effects of woody plants on microclimate in a semiarid woodland: soil temperature and evaporation in canopy and intercanopy patches. International Journal of Plant Sciences 159(6): 1010-1017.

Breshears DD (2006)The grassland-forest continuum: trends in ecosystem properties for woody plant mosaics? Frontiers in Ecology and the Environment 4(2): 96-104.

Brown Jr S (1959) Annals of Blackwater and the Land of Canaan. Virginia Book Company. Berryville, Virginia 42 p.

Carter BJ, Ciolkosz EJ (1980) Soil temperature regimes of the central Appalachians. Soil Science Society of America Journal 44(5): 1052-1058.

Chapin III FS, Matson PA, Mooney HA (2002) Principles of Ecosystem Ecology. Springer, New York 436 p.

Chapin, FS, Woodwell GM, Randerson JT, Rastetter EB, Lovett GM,Baldocchi DD, Clark DA, Harmon ME, Schimel DS, Valentini R, Wirth C, Aber JD, Cole JJ, Goulden ML, Harden JW, Heimann M, Howarth RW, Matson PA, McGuire AD, Melillo JM, Mooney HA, Neff JC, Houghton RA, Pace ML, Ryan MG, Running SW, Sala OE, Schlesinger WH, Schulze ED (2006) Reconciling carbon-cycle concepts, terminology, and methods. Ecosystems 9(7): 1041-1050.

Chemidlin Prévost-Bouré N, Soudani K, Berveiller D, Lata JC, Dufrêne E (2010) Increase in aboveground fresh litter quantity over-stimulates soil respiration in a temperate deciduous forest. Applied Soil Ecology 46(1): 26-34.

Crews JT, Wright L (2000) Temperature and soil moisture regimes in and adjacent to the Fernow Experimental Forest. Res. Pap. NE-713. Newton Square, PA: US Department of Agriculture, Forest Service. Northeastern Research Station. 4 p.

Crutsinger GM, Sanders NJ, Classen AT (2009). Comparing intra- and inter-specific effects on litter decomposition in an old-field ecosystem. Basic and Applied Ecology 10: 535–543. doi:10.1016/j.baae.2008.10.011.

Davidson EA, Trumbore SE (1995) Gas diffusivity and production of CO_2 in deep soils of the eastern Amazon. Tellus 47B: 550-565.

Davidson EA, Belk E, Boone RD (1998) Soil water content and temperature as independent or confounded factors controlling soil respiration in a temperate mixed hardwood forest. Global Change Biology 4: 217-227.

Day FP, Monk CD (1974) Vegetation patterns on a southern Appalachian watershed. Ecology 55: 1064-1074.

Dilustro JJ, Collins B, Duncan L, Crawford C (2005) Moisture and soil texture effects on soil CO_2 efflux components in southeastern mixed pine forests. Forest Ecology and Management 204(1): 87-97.

Dunker SL, Epstein HE (in prep) Untitled manuscript based on research at Blandy Experimental Farm in Boyce, Virginia.

Dwyer LM, Merriam G (1981) Influence of topographic heterogeneity on deciduous litter decomposition. Oikos 37: 228-237.

Emanuel RE, D'Odorico P, Epstein HE (2007). A dynamic soil water threshold for vegetation water stress derived from stomatal conductance models. Water Resources Research, 43(3), W03431. doi:10.1029/2005WR004831.

Emanuel RE, Epstein HE, McGlynn BL, Welsch DL, Muth DJ, D'Odorico P (2010). Spatial and temporal controls on watershed ecohydrology in the northern Rocky Mountains. Water Resources Research, 46(11), W11553. doi:10.1029/2009WR008890.

Emanuel RE, Riveros-Iregui DA, McGlynn BL, Epstein HE (2011). On the spatial heterogeneity of net ecosystem productivity in complex landscapes. Ecosphere, 2(7), art86. doi:10.1890/ES11-00074.1.

Epstein HE, Lauenroth WK, Burke IC (1997) Effects of temperature and soil texture on ANPP in the U.S. Great Plains. Ecology 78: 2628–2631.

Epstein HE, Burke IC, Lauenroth WK (2002) Regional patterns of decomposition and primary production rates in the U.S. Great Plains. Ecology, 83(2): 320–327.

Fansler H (1962) History of Tucker County. McClain Printing Company, Parsons, West Virginia 702 p.

Farnes PE (2005) Climate Change in Montana. 73rd Western Snow Conference 45(56): 13 p.
Fioretto A, Papa S, Fuggi A (2003) Litter-fall and litter decomposition in a low Mediterranean shrubland. Biology and Fertility of Soils 39(1): 37-44.

Fisher SG, Welter JR (2003) Flowpaths as integrators of heterogeneity in streams and landscapes, pp 311-328. In Lovett GM, Jones CG, Turner MG, Weathers KC. Ecosystem function in heterogeneous landscapes. Springer-Verlag, New York. 507 p.

Galloway JN, Dentener FJ, Capone DG, Boyer EW, Howarth RW, Seitziner SP, Asner GP, Cleveland CC, Green PA, Holland EA, Karl DM, Michaels AF, Porter JH, Townsend AR, Vörösmarty CJ (2004) Nitrogen cycles: past, present, and future. Biogeochemistry 70(2): 153-226.

Garten TC, POST III WM, Hanson PJ, Cooper LW (1999) Forest soil carbon inventories and dynamics along an elevation gradient in the southern Appalachian Mountains. Biogeochemistry 45(2): 115-145.

Goulden ML, Munger JW, Fan S, Daube BC, Wofsy SC (1996) Measurements of carbon sequestration by long-term eddy covariance: Methods and a critical evaluation of accuracy. Global Change Biology 2(3): 169-182.

Grayson RB, Western AW, Chiew FHS, Blöschl G (1997). Preferred states in spatial soil moisture patterns: Local and nonlocal controls. Water Resources Research, 33(12), 2897. doi:10.1029/97WR02174.

Harmon M, Moreno A, Domingo JB (2009) Effects of partial harvest on the carbon stores in Douglas-Fir/Western Hemlock forests: a simulation study. Ecosystems 12(5): 777-791.

Hatfield RD, Grabber J, Ralph J, Brei K (1999) Using the acetyl bromide assay to determine lignin concentrations in herbaceous plants: some cautionary notes. Journal of Agricultural and Food Chemistry 47(2): 628-632.

Herman J, Moorhead D, Berg B (2008) The relationship between rates of lignin and cellulose decay in aboveground forest litter. Soil Biology and Biochemistry 40(10): 2620-2626.

HwangT, Band LE, Vose JM, Tague C (2012) Ecosystem processes at the watershed scale: Hydrologic vegetation gradient as an indicator for lateral hydrologic connectivity of headwater catchments. Water Resources Research 48(6): W06514. doi:10.1029/2011WR011301.

Jassal R, Black A, Novak M, Morgenstern K, Nesic Z, Gaumont-Guay D (2005) Relationship between soil CO_2 concentrations and forest-floor CO_2 effluxes. Agricultural and Forest Meteorology 130(3): 176-192.

Kang, S, Doh S, Lee Don., Lee Dow., Jin VL, Kimball JS (2003) Topographic and climatic controls on soil respiration in six temperate mixed-hardwood forest slopes, Korea. Global Change Biology 9(10): 1427-1437.

Kellogg RS (1909). The timber supply of the United States. US Government Printing Office.

Kuzyakov Y (2006) Sources of CO_2 efflux from soil and review of partitioning methods. Soil Biology and Biochemistry 38(3): 425-448.

Likens GE, Bormann FH. 1995. Biogeochemistry of a Forested Ecosystem. 2nd Ed. Springer-Verlag. New York 159 p.

Likens GE (2001) Biogeochemistry, the watershed approach: some uses and limitations. Frontiers of Catchment Biogeochemistry. CSIRO Land and Water, Canberra, Australia 52: 5-12.

Matchen DL (2002). The geology of Canaan Valley. The West Virginia Geologic Survey 7 p.

Maxwell H (1884) History of Tucker County, West Virginia: From the earliest exploration and settlements to the present time. Preston Publishing, Kingwood, West Virginia 574 p.

McGlynn BL, Seibert J (2003) Distributed assessment of contributing area and riparian buffering along stream networks. Water Resources Research 39(4) 1082, doi:10.1029/2002WR001521.

Moldrup P, Olesen T, Yamaguchi T, Schjonning P, Rolston DE (1999), Modeling diffusion and reaction in soils: IX. The Buckingham- Burdine-Campbell equation for gas diffusivity in undisturbed soil. Soil Science Society of America Journal 164: 542–551.

Moore AM (1986) Temperature and moisture dependence of decomposition rates of hardwood and coniferous leaf litter. Soil Biology & Biochemistry 18: 427–435.

Muller RN (1982) Vegetation patterns in the mixed mesophytic forest of eastern Kentucky. Ecology 63(6): 1901-1917.

Oberbauer SF, Gillespie CT, Cheng W, Gebauer R, Sala Serra A, Tenhunen JD (1992) Environmental effects on CO_2 efflux from riparian tundra in the northern foothills of the Brooks Range, Alaska, USA. Oecologia 92(4): 568-577.

Pacific VJ, McGlynn BL, Riveros-Iregui DA, Welsch DL, Epstein HE (2008) Variability in soil respiration across riparian-hillslope transitions. Biogeochemistry 91(1): 51-70.

Pacific VJ, McGlynn BL, Riveros-Iregui DA, Epstein HE, Welsch DL (2009). Differential soil respiration responses to changing hydrologic regimes. Water Resources Research, 45(7), W07201. doi:10.1029/2009WR007721.

Peterjohn WT, Correll DL Nutrient dynamics in an agricultural watershed: observations on the role of a riparian forest. Ecology 65(5): 1466-1475.

Raich JW, Nadelhoffer KJ (1989) Belowground carbon allocation in forest ecosystems: global trends. Ecology 70: 1346–1354.

Raich J, Schlesinger WH (1992) The global carbon dioxide flux in soil respiration and its relationship to vegetation and climate. Tellus 44: 81–99.

Raich JW, Potter CS (1995) Global patterns of carbon dioxide emissions from soils. Global Biogeochemical Cycles 9(1): 23-36.

Raich JW, Tufekcioglu A (2000) Vegetation and soil respiration: correlations and controls. Biogeochemistry 48(1): 71-90.

Raupach MR, Finnigan JJ (1997) The influence of topography on meteorological variables and surface-atmosphere interactions. Journal of Hydrology 190(3–4): 182–213.

Reiners WA, Driese KL (2001) The propagation of ecological influences through heterogeneous environmental space. Bioscience 51(11): 939-950.

Reiners WA (2005) Reciprocal cause and effect between environmental heterogeneity and transport processes. pp 67-89, In Lovett GM, Jones CG, Turner MG, Weathers KC. Ecosystem function in heterogeneous landscapes. Springer-Verlag, New York. 507 p.

Riveros-Iregui DA, McGlynn BL, Epstein HE, Welsch DL (2008). Interpretation and evaluation of combined measurement techniques for soil CO_2 efflux: Discrete surface chambers and

continuous soil CO_2 concentration probes. Journal of Geophysical Research, 113(G4), G04027. doi:10.1029/2008JG000811

Riveros-Iregui, DA and McGlynn BL (2009). Landscape structure control on soil CO_2 efflux variability in complex terrain: Scaling from point observations to watershed scale fluxes. Journal of Geophyscal Research, 114. G02010, doi:10.1029/2008JG000885, 2009

Riveros-Iregui DA, McGlynn BL, Marshall LA, Welsch DL, Emanuel RE, Epstein HE (2011). A watershed-scale assessment of a process soil CO_2 production and efflux model. Water Resources Research, 47, W00J04. doi:10.1029/2010WR009941.

Schimel, D. S.: Terrestrial ecosystems and the carbon cycle, Global Change Biology, 1, 77-91, 1 1995.

Schlesinger WH (1977) Carbon balance in terrestrial detritus. Annual Review of Ecology and Systematics 8: 51-81.

Schlesinger WH, Andrews JA (2000) Soil respiration and the global carbon cycle. Biogeochemistry 48(1): 7–20.

Sencindiver J, Thomas K, Teets J (2002) The dirt on Canaan: Soils of Canaan Valley and adjacent mountains. Paper presented at the Canaan Valley: A Heritage Landscape Celebration & Its Environs. Canaan Valley Institute.

Shanks RE, Olson JS (1961) First-year breakdown of leaf litter in southern Appalachian forests. Science 134(3473): 194-195.

Singh JS, Gupta SR (1977) Plant decomposition and soil respiration in terrestrial ecosystems. The botanical Review 43(4): 449-528.

Smith DL, Johnson L (2004) Vegetation-mediated changes in microclimate reduce soil respiration as woodlands expand into grasslands. Ecology 85(12): 3348-3361.

Stephenson S (1993). Upland Forests of West Virginia. McClain Printing Company. Parsons, West Virginia 295 p.

Strother, David Hunter (1857) Virginia Illustrated. New York: Harper & Brothers.
Tague C (2005) Heterogeneity in hydrologic processes: A terrestrial hydrologic modeling perspective pp 119-136, In Lovett GM, Jones CG, Turner MG, Weathers KC. Ecosystem function in heterogeneous landscapes. Springer-Verlag, New York. 507 p.

Tang J, Baldocchi DD (2005) Spatial–temporal variation in soil respiration in an oak–grass savanna ecosystem in California and its partitioning into autotrophic and heterotrophic components. Biogeochemistry 73(1): 183-207.

Updegraff DM (1969) Semimicro determination of cellulose inbiological materials. Analytical Biochemistry 32(3): 420-424.

USDA Tenderfoot Creek Experimental Forest (http://www.fs.fed.us/rm/tenderfoot-creek/)

Vitousek P, Turner D, Parton W, Sanford W (1994). Litter Decomposition on the Mauna Loa Environmental Matrix , Hawai ʻi : patterns , mechanisms , and models. Ecology 75(2): 418–429.

Wang J, Epstein HE, Wang L (2010) Soil CO_2 flux and its controls during secondary succession. Journal of Geophysical Research 115, G02005, doi:10.1029/2009JG001084.

Webster KL., Creed IF, Bourbonnière RA, Beall FD (2008). Controls on the heterogeneity of soil respiration in a tolerant hardwood forest. Journal of Geophysical Research, 113(G3), G03018. doi:10.1029/2008JG000706.

Welsch DL, Kroll CN, McDonnell JJ, Burns DA (2001). Topographic controls on the chemistry of subsurface stormflow. Hydrological Processes 15(10): 1925–1938. doi:10.1002/hyp.247.

Welsch DL, Hornberger GM (2004) Spatial and temporal simulation of soil CO_2 concentrations in a small forested catchment in Virginia. Biogeochemistry 71: 413-434.

West Virginia Department of Commerce (http://www.wvcommerce.org/resources/forestry/water/default.aspx)

Western AW, Grayson RB, Blöschl G, Willgoose GR, McMahon TA (1999). Observed spatial organization of soil moisture and its relation to terrain indices. Water Resources Research, 35(3), 797. doi:10.1029/1998WR900065.

WVFA (West Virginia Forestry Association) Forestry Facts. (http://www.wvfa.org/forestry-facts.html).

Xu M, DeBiase TA, Qi Y, Goldstein A, Liu Z (2001). Ecosystem respiration in a young ponderosa pine plantation in the Sierra Nevada Mountains, California. Tree physiology 21(5): 309–18.

Yan J, Yingping W, Zhou G, Zhang D (2006) Estimates of soil respiration and net primary production of three forests at different succession stages in South China. Global Change Biology 12: 810–821, doi: 10.1111/j.1365-2486.2006.01141.x.

Zhang D, Hui D, Luo Y, Zhou G (2008) Rates of litter decomposition in terrestrial ecosystems: global patterns and controlling factors. Journal of Plant Ecology, 1(2): 85–93. doi:10.1093/jpe/rtn002.

Zhou G, Guan L, Wei X, Tang X, Liu S, Liu J, Zhang D, Yan J (2008). Factors influencing leaf litter decomposition: an intersite decomposition experiment across China. Plant and Soil 311(1-2): 61–72. doi:10.1007/s11104-008-9658-5.

Chapter Two: Vegetation heterogeneity and landscape influence the timing and magnitude of soil CO_2 efflux in a humid, Appalachian watershed

ABSTRACT

In topographically complex watersheds, landscape position and vegetation heterogeneity can alter the soil water regime through both lateral and vertical redistribution, respectively. These alterations of soil moisture may have significant impacts on the spatial heterogeneity of biogeochemical cycles throughout the watershed. To evaluate how landscape position and vegetation heterogeneity affect soil CO_2 efflux ($F_{SOIL)}$ we conducted observations across the Weimer Run watershed (373 ha), located near Davis, West Virginia, for three growing seasons with varying precipitation (2010 – 1042 mm; 2011 – 1739 mm; 2012 – 1244 mm). An apparent soil temperature threshold of 11 °C at 12 cm depth on F_{SOIL} was observed in our data—where F_{SOIL} rates greatly increase in variance above this threshold. For analysis, F_{SOIL} values above this threshold were isolated and examined. Differences in F_{SOIL} among years were apparent by elevation ($F_{4, 633} = 3.17$; $p = 0.013$) and by vegetation cover ($F_{4, 633} = 2.96$; $p = 0.019$). For the Weimer Run watershed, vegetation exerts the major control on F_{SOIL}, with plots beneath shrubs at all elevations for all years showing the greatest mean rates of F_{SOIL} (6.07 µmol CO_2 m^{-2} s^{-1}) compared to plots beneath closed-forest canopy (4.69 µmol CO_2 m^{-2} s^{-1}) and plots located in open, forest gaps (4.09 µmol CO_2 m^{-2} s^{-1}) plots. During periods of high soil moisture, we find that CO_2 efflux rates are constrained and that maximum efflux rates in this system occur during periods of average to below average soil water availability. These findings offer valuable insight into processes occurring within topographically complex systems and the interactions of abiotic and biotic factors controlling biogeochemical cycles.

INTRODUCTION

Soil respiration (R_{SOIL}) is a major component of the terrestrial carbon cycle (Raich and Potter, 1995; Schimel, 1995), and is 30-60% greater than net primary productivity globally (Raich and Potter, 1995). Estimates of annual soil carbon emissions range from 68 – 100 Pg of carbon per year (Schlesinger, 1977; Raich and Schlesinger, 1992; Bond-Lamberty and Thomson, 2010). Temperate systems contribute approximately 20% of the annual global R_{SOIL} (Bond-Lamberty and Thomson, 2010), but have been shown to be recent carbon sinks, averaging 0.72 Pg of C uptake per year from 1990 – 2007 (Pan et al., 2011). R_{SOIL} can be estimated in the field by measuring soil CO_2 efflux (F_{SOIL}) — the direct rate of CO_2 crossing the soil surface over a period of time (Raich and Schlesinger, 1992). F_{SOIL} can vary spatially and temporally within and across systems as a result of the varied and complex interactions of controlling mechanisms (Drewitt et al., 2002, Trumbore, 2006; Vargas et al., 2010). The edaphic controls on F_{SOIL} at the landscape scale include soil temperature, soil moisture, root biomass, microbial biomass, soil chemistry, and soil physics (Fang et al., 1998; Davidson et al., 1998; Kang et al., 2000; Xu and Qi, 2001; Epron et al., 2004). These factors do not simply elicit additive or monotonic responses, but rather create complex responses of F_{SOIL} across spatial and temporal scales (Dilustro et al., 2005; Pacific et al., 2009).

Soil temperature is quite commonly a primary driver of F_{SOIL} (e.g. Fang and Moncrieff, 2001), and in complex terrain, temperature regimes can be mediated by elevation, slope, and aspect (Wu et al., 2013). The effects of elevation and topography on soil temperature can in turn affect carbon cycling (Schindlbacher et al., 2010) either directly or through indirect

processes (Murphy et al,. 1998). Soil water content (SWC) however often serves as an important secondary control on F_{SOIL}. At high SWC values, CO_2 transport through the soil pore space is limited (Davidson and Trumbore, 1995; Jassal et al., 2005). Production of soil CO_2 can also become limited at high SWC values due to anoxia and decreased microbial aerobic respiration (Oberbauer et al., 1992). At low SWC values, F_{SOIL} is decreased as well due to microbial desiccation and concomitantly reduced microbial activity (Van Gestel et al., 1993), resulting in decreased CO_2 production (Scanlon and Moore, 2000).

In topographically complex landscapes, precipitation gradients that exist as a function of elevation affect decomposition rates, CO_2 production, and movement of CO_2 through the soil (Schuur, 2001). The complex landscape structure and heterogeneity of mountain catchments also directly affect local soil moisture regimes through the lateral redistribution of soil water, adding to the spatial heterogeneity of these biogeochemical and physical processes. F_{SOIL} therefore varies across landscape positions as a function of this soil water redistribution (Riveros-Iregui and McGlynn, 2009). In subalpine forested systems for example, soil water content has been shown to be a strong driver of the spatial (Scott-Denton et al., 2003) and temporal (Pacific et al., 2008) variability of $F_{SOIL.}$

In addition to meteorological variables, vegetation (itself controlled by the spatial heterogeneity of micrometeorology), can influence carbon cycling within a watershed. Vegetation affects carbon cycling directly through photosynthesis (Raich and Schlesinger, 1992; Ekblad and Högberg, 2001; Högberg et al., 2001), above- and below-ground tissue allocation (Chen et al., 2013), and litter production (Prevost-Boure et al., 2010). Vegetation therefore controls the quantity and quality of soil organic matter (SOM) within systems, which in part will

determine decomposition rates and soil CO_2 production (e.g. Berg, 2000). However, the role of belowground plant and microbial processes in the dynamics of SOM has become increasingly more apparent—showing that root and rhizosphere contributions to SOM are substantive (e.g. Schmidt et al., 2011). Vegetation also exerts controls on production of CO_2 through root respiration in the soil and through complex mycorrhizal associations that can mediate the response of soil CO_2 production to rain pulse events (Vargas et al., 2010). Finally, vegetation also elicits feedbacks on the abiotic aspects of a system, including the soil moisture and soil temperature regimes, further impacting biogeochemical cycling (Wullschleger et al., 2002; Metcalfe et al., 2011; Vesterdal et al., 2012).

Inter-annual variation in R_{SOIL} within systems can be high and exceed the inter-annual variation of net ecosystem exchange (NEE) of carbon (Savage and Davidson, 2001); this inter-annual variation can be driven in large part by the dynamics of precipitation (Raich et al., 2002). Current climate models project potentially dramatic changes in precipitation in the coming years (Kirtman et al., 2013), and presently the controls on inter-annual variation of R_{SOIL} in response to changing precipitation regimes are poorly understood at spatial scales ranging from landscapes to regions. The interactions among topography, vegetation cover, and climate are therefore an important and complicated area of study.

Inter-annual climate variability in mountainous, subalpine catchments, however, has been shown to alter the spatio-temporal heterogeneity of carbon dynamics within those systems (Riveros-Iregui et al., 2011; Riveros_Iregui et al., 2012). In a subalpine watershed in Montana, Riveros-Iregui et al. (2012) found that areas with low upslope accumulated area (generally uplands and drier areas) showed F_{SOIL} increases during wet years, while poor-drainage areas

(riparian areas) showed F_{SOIL} decreases during wet years. This resulting bidirectional response is a function of the landscape heterogeneity of the system, soil biophysics, and inter-annual climate variability (Riveros-Iregui et al., 2012).

Given the possible interactions among precipitation, topography, and vegetation, we examined how F_{SOIL} varies as a function of landscape position and vegetation cover in response to inter-annual variation in precipitation within a complex, humid watershed. To do this we used a plot-based approach with repeated measures sampling to account for spatial and temporal variation of the biophysical controls on F_{SOIL} within our study watershed. The empirical nature of this study design, coupled with the use of portable infra-red gas analyzers (IRGAs) to measure soil CO_2 efflux, is a robust and proven way of quantifying the seasonal dynamics of F_{SOIL} and allows for greater consideration of the spatial variability of F_{SOIL} (Riveros-Iregui et al. 2008; Riveros-Iregui and McGlynn, 2009) at the watershed scale. We attempted to answer the following questions:

1. How does F_{SOIL} respond to inter-annual variation of precipitation in a humid, complex watershed?

2. How do landscape position and vegetation heterogeneity affect F_{SOIL}, and how do they interact with inter-annual variation in precipitation?

METHODS

SITE DESCRIPTION

The Weimer Run watershed (374 ha) is located in the Allegheny Mountain range in north-eastern West Virginia within the Little Canaan Wildlife Management Area near Davis, WV (39.1175, -79.4430) and is a sub-watershed of the Blackwater River, a tributary of the Cheat River. The watershed has an elevation range of 940 m (confluence of Weimer Run and the Blackwater River) to 1175 m (Bearden Knob) (Fig. 2.1). For the climate period 1980-2010, mean annual precipitation (MAP) for the watershed was 1450 mm yr^{-1} (PRISM Climate Group). The mean daily maximum July temperature is 18.8° C, and the mean daily maximum January temperature is -3.9° C (NCDC, Station ID DAVIS 3 SE, Davis, WV). Precipitation varied during the study period, producing a relatively dry year in 2010 (1042 mm), a wet year in 2011 (1739 mm) and a mesic year in 2012 (1244 mm) (precipitation data from BDKW2 station, MesoWest, University of Utah) (Fig. 2.5A).

The Weimer Run watershed is adjacent to the Canaan Valley in West Virginia—which exists in a transitional zone between the Appalachian Valley and Ridge and the Appalachian Folded Plateau (Matchen, 1998). The surrounding ridge tops and the study site are underlain by Pennsylvanian sandstone from the Pottsville formation (Allard and Leonard, 1952). The over-story vegetation within the watershed is a mixed northern hardwood-coniferous forest, consisting of yellow birch (*Betula alleghaniensis*), red maple (*Acer rubrum*), red spruce (*Picea rubens*), and black cherry (*Prunus serotina*) (Allard and Leonard, 1952; Fortney, 1975). The under-story is comprised of *Rhododendron maximum*, *Kalmia latifolia*, *Osmundastrum cinnamomeum*, and *Osmunda claytoniana* (Fortney, 1975).

VEGETATION AND ELEVATION CLASSES

Three elevation classes were established along the north-eastern aspect of the watershed to form an elevation gradient: LOW (975 m), MID (1050 m), and HIGH (1100 m). Site elevations were determined using a digital elevation map (DEM) derived from 1/9 arc second elevation data from the Shuttle Radar Topography Mission (SRTM) (USGS 2006) processed with ArcGIS® software (ESRI; Redlands, CA). In order to address the effects of vegetation cover on F_{SOIL}, three vegetation cover classes were established: CANOPY – closed canopy, forest interior with no shrub layer; SHRUB – closed canopy, forest interior, with dense shrub layer; OPEN – forest gap with no canopy closure, within the forest interior. Differences among vegetation classes were confirmed using plant area index (PAI) which was measured for each plot in June 2010 with a LAI-2000 Plant Canopy Analyzer (LI-COR Lincoln, Nebraska). PAI was strongly statistically significantly different among vegetation cover types (F = 13.39; p-value = 0.0003). SHRUB plots were the greatest (3.46 m^{-3} m^3) followed by CANOPY plots (2.14 m^{-3} m^3) and then OPEN plots (1.75 m^{-3} m^3) (Appendix A).

At each elevation level in the watershed, three 2 x 2 m plots of each vegetation class were established—for a total of 27 plots across the entire watershed (Fig. 2.1). One of the SHRUB replicate plots at the LOW elevation had to be removed from analysis due to inundation during the summer of 2011. Data from the remaining 26 plots were analyzed.

Soil CO_2 efflux

An EGM-4 Portable Infrared Gas Analyzer (IRGA) with an attached SRC-1 Soil Chamber (PP Systems, Amesbury, MA) was used to measure soil CO_2 efflux rates. The EGM-4 has a measurement range of 0 - 2,000 ppm (µmol mol^{-1}) with an accuracy of better than 1% and

linearity better than 1% throughout the range. The SRC-1 has a measurement range of 0 – 9.99 g CO_2 m^{-2} hr^{-1}. Plots were sampled approximately weekly (every 5 – 10 days) from the middle of May until the end of September, from 2010 to 2012. For March until mid-May, and during October and November, plots were measured approximately every two weeks (12-21 days) during times when they were snow-free. F_{SOIL} was measured 1 – 3 times at different locations within the plot at each measurement interval and averaged for a plot level estimation of F_{SOIL}. Plots were sampled between 900 and 1600 EST, and the sequence of plot measurements was varied to avoid a time-of-day bias in the results and account for diurnal variation in soil CO_2 flux over time. Our sampling followed a rotating scheduling where for one sampling period we would start at say the HIGH elevation, then proceed to work down the mountain (MID, then LOW), and the next week we would start at the MID and then work down to the LOW, then finish with the HIGH and the next would then start at the LOW, then HIGH, then MID, and so on. This method was followed through the experiment.

VOLUMETRIC WATER CONTENT

Volumetric water content (Θ_{field}) was measured using a Campbell HydroSense CD 620 (Campbell Scientific) set to water content measure mode with 12 cm probes (Campbell Scientific; +/- 3.0 % $m^{-3}m^3$, with electrical conductivity <2 dS m^{-1}; sampling volume using 12 cm rods = ~650 cm^3). A minimum of three measurements was taken in each plot per sampling event and averaged to make a plot level estimation of Θ_{field}.

Measurements taken by the Campbell HydroSense CD 620 have a known bias in soils where bulk density is outside of the 1 – 1.7 g cm^3 range, where organic matter is >10%, and where clay content is >40%. (Campbell Scientific). In order to calibrate field measurements, a

calibration procedure from Kelleners et al. (2009) was followed where *P*, the period, which is the square wave output from the probe in milliseconds, is converted to K_a, the relative soil permittivity (unitless). *P* is related to Θ_{field} as shown in Equation (1):

$$P = \left(-0.3385 * \theta_{field}^2\right) + \left(0.7971 * \theta_{field}\right) + 0.7702 \quad (1)$$

Equation (2) converts *P* to K_a.

$$\sqrt{K_a} = \frac{(P - P_{air})}{(P_{water} - P_{air}) * \left(\left(\sqrt{K_{water}} - 1\right) + 1\right)} \quad (2)$$

where P_{air} is the period in air, and P_{water} is the period in deionized water. P_{air} was calculated empirically at 0.79 ms. P_{water} was calculated at 1.37 ms following the procedure outlined in Kelleners et al. (2009) by placing the probes of the Campbell Hydrosense CD 620 in deionized water in an 18.92 L acid-washed container, with total vessel conductivity measured at 0.47 µmhos.

Soil samples were taken in conjunction with HydroSense measurements in 2012 (depth= 12 cm, volume= 56.414 cm^3, n=37), and actual VWC (Θ_{lab}) was calculated using Equation (3) from Rose (2004), where *w* is the gravimetric water content of the soil sample (g^{-3} g^3), ρ_b is the soil bulk density (g cm^{-3}), and ρ (g cm^{-3}) is the density of water:

$$\theta_{lab} = \frac{w\rho_b}{\rho} \quad (3)$$

In order to calibrate field measurements of VWC (Θ_{field}), $\sqrt{K_a}$ values were then regressed against Θ_{lab} to create an equation (4) relating $\sqrt{K_a}$ to Θ ($R^2 = 0.74$) such that field measurements of VWC (Θ_{field}) could be converted to Θ in order to account for discrepancies in organic matter, soil bulk density, and clay content:

$$\theta = 7.0341 * \left(\sqrt{K_a}\right) + 0.0806 \quad (4)$$

Θ was then converted to water-filled pore space (WFPS; m^{-3} m^3) using the soil porosity (Φ; m^{-3} m^3):

$$WFPS = \frac{\theta}{\Phi} \quad (5)$$

WFPS provides a more mechanistic variable that takes into account the bulk density and porosity of the soil, which influence the transport and storage capacity of the soil with regard to soil CO_2.

SOIL TEMPERATURE

During each field sampling session, soil temperature (T_{SOIL}; C°) was measured at 12 cm using a 12 cm REOTEMP Soil Thermometer (REOTEMP San Diego, CA) at a minimum of two

locations within the plot. These measurements were averaged to create a plot mean temperature for each sampling event.

SOILS

Soil pH was determined using a 1:1 measure of soil (from 0 – 5 cm depth) with deionized water and measured with a Fieldscout Soilstik pH Meter (Spectrum Technologies, Inc. Plainfield, IL) with an accuracy of ±0.01 pH, ±1°C.

Soil samples were taken from 0 – 5, 0 – 12, and 0 – 20 cm profiles within the soil. Soil bulk density (ρ_s), total bulk density (ρ_t), soil particle density, and soil porosity (Φ) were also calculated for each sample (Grossman and Reinsch, 2002; Flint and Flint 2002). Soil bulk density (ρ_s) is defined as the bulk density of the soil fraction, where the soil fraction consists of soil that has been sieved to less than 2 mm and all gravel and root material have been removed. Total bulk density (ρ_t) is defined as the absolute density of the sampled soil, including soil, roots, and gravel and is simply the sample dry mass over the sample volume. Total soil carbon and nitrogen were assessed using a NA 2500 Elemental Analyzer (CE instruments; Wigan, United Kingdom). Soil organic matter (SOM) content was estimated using loss-on-ignition at 500°C (Davies, 1974).

DATA ANALYSIS

We chose to parse our data at 11°C rather than strictly by growing/dormant seasons in order to develop a more functional understanding of the controls on F_{SOIL}. The 11°C threshold was chosen for multiple reasons. 1) mean measured soil temperature at 12 cm across our watershed during our three years of observations exceeded 11°C for the period May 6 to October 13. This period coincides with the growing season, and allows for slight variance with a buffer on either end. 2) Piecewise regression (using the segmented package in R) identifies an

estimated break-point of 11.58°C ±0.47 standard error when the ln(F_{SOIL}) is regressed against soil temperature. Based on our observations, we opted for the more conservative threshold of 11°C. 3) Below 11°C, the F_{SOIL} values are tightly coupled to temperature, while above 11°C there is increasing variance in F_{SOIL} that we feel warrants exploration. All analyses and means presented are for measurement periods where soil temperatures are above 11°C, unless otherwise noted.

We employed a mixed-model analysis of variance (ANOVA) with repeated measures to identify main and interactive effects of elevation and vegetation on soil CO_2 efflux, soil temperature, and water-filled pore space using the proc mixed procedure in SAS 9.3 (SAS Institute, North Carolina USA). All means presented are least-squares means calculated using a Tukey-Kramer adjustment.

To decouple the effects of soil temperature and soil moisture on F_{SOIL}, linear regressions of soil temperature against the natural-log of F_{SOIL} were done by year (2010, 2011, 2012), by vegetation cover type (OPEN, CANOPY, SHRUB), by elevation (LOW, MID, HIGH), by year and vegetation (OPEN 2010, CANOPY 2010, etc.), and by year and elevation (LOW 2010, MID 2010, etc.). The residuals from each model were then regressed against WFPS by each combination. All linear regressions use the lm function in R 3.0.1 (R Core Team 2013).

Differences in soil organic matter (SOM) were examined with a Kruskal-Wallis rank sum test using the kruskal.test() in R 3.0.1 (R Core Team, 2013). A two-way mixed-model ANOVA using the proc mixed procedure in SAS 9.3 was used to examine main and interactive effects of elevation, vegetation, and soil depth on soil bulk density and total bulk density. Soil bulk density, soil organic matter, total soil carbon, total soil nitrogen, and plant area index were individually regressed against the mean plot-level soil CO_2 efflux for each corresponding plot (e.g. High-

Canopy 1, High-Open 2, etc.). Means were calculated from all flux data above 11°C for all three years (2010-2012).

RESULTS

Exponential regression of F_{SOIL} measurements against soil temperature at 12 cm (T_{SOIL}) (Fig. 2.2A) shows a positive relationship ($R^2 = 0.316$; $y = 0.829 + e^{(0.1149x)}$) with increases in temperature resulting in increased efflux rates. The amount of variance explained by T_{SOIL} lessens above 11° C ($R^2 = 0.104$), with F_{SOIL} measurements below 11° C showing a much tighter relationship with temperature ($R^2 = 0.434$). To explore this variance, all data above 11° C were isolated and examined in order to parse out controls above this apparent temperature threshold for this system.

The natural log of flux measurements above 11° C for all years were regressed against T_{SOIL} (Fig. 2.2B) showing a significant positive relationship with soil temperature ($R^2 = 0.119$; $y = 0.096x - 0.010$). From this linear model, the residuals were then regressed against WFPS. The residuals from the $\ln(F_{SOIL})$ values above 11°C show a significant negative relationships with WFPS (Fig. 2.2C) but this explains only marginally more of the variance ($R^2 = 0.019$).

SOIL CO_2 EFFLUX (F_{SOIL})

Repeated measures ANOVA analyses show no significant differences in F_{SOIL} among years when data are pooled. Significant differences among years do occur when data are parsed by elevation ($F_{4, 633} = 3.17$; $p = 0.013$) and by vegetation ($F_{4, 633} = 2.96$; $p = 0.019$).

Across all data above 11° C, there was a significant effect of elevation ($F_{2, 633} = 3.44$; $p = 0.032$), with plots at HIGH elevation sites showing the highest F_{SOIL} rates and HIGH sites statistically differing from LOW sites, with MID elevation sites not differing from either (Fig.

2.3A). 2010 was the only year to show a statistically significant difference in F_{SOIL} among elevation classes within a year, with LOW elevation sites exhibiting significantly lower F_{SOIL} rates ($F_{2, 633} = 3.17$, $p = 0.013$).

Differences among vegetation classes were stark ($F_{2, 633} = 37.58$; $p = <.0001$). SHRUB classes across all elevation classes and all years had higher rates of F_{SOIL} (6.07 ±0.42 µmol CO_2 m^{-2} s^{-1}) than CANOPY (4.69 ±0.42 µmol CO_2 m^{-2} s^{-1}) or OPEN (4.09 ±0.42 µmol CO_2 m^{-2} s^{-1}) plots. This SHRUB effect was most notable during 2010, the driest year during the study, when SHRUB plots showed the highest rates of F_{SOIL} recorded during the study (7.48 ±0.674). Statistical differences among vegetation classes among years were complex. SHRUB 2010 and OPEN 2011 were uniquely different among all combinations (Fig. 2.3B).

WATER-FILLED PORE SPACE (WFPS)

WFPS tracked well with precipitation across years, with 2010 having the lowest values of WFPS and 2011 having the highest rates of WFPS. WFPS in 2011 was significantly greater than either 2010 or 2012 ($F_{2, 633} = 16.06$; $p = <.0001$) (Table 2). During 2010, when precipitation was lower than average, an apparent elevation effect on WFPS is observed, with HIGH elevation plots exhibiting significantly lower WFPS measurements than either LOW elevation or MID elevation plots (Fig. 2.3E). During 2011 and 2012, under extreme and moderate moisture regimes, this elevation effect is not evident. During 2010, vegetation treatment types are not significantly different, but in 2011, when there is more moisture in the system, statistical differences among vegetation classes are apparent, as SHRUB and CANOPY plots exhibit higher WFPS values than OPEN plots (Fig. 2.3F).

SOIL TEMPERATURE (T_{SOIL})

Data for all years showed a significant effect of elevation on T_{SOIL} across elevation classes for all data above 11°C ($F_{2, 633} = 170.76$; $p = <.0001$). LOW elevation sites were warmer (15.99 ±0.35 °C), than MID sites (14.71 ±0.35 °C) and HIGH (14.94 ±0.35 °C) elevation sites. There was no statistical difference in soil temperature by elevation within years (Fig. 2.3C).

Vegetation (Fig. 2.3D) had a statistically significant effect on T_{SOIL} (F = 52.79; $p = <.0001$). SHRUB plots were the coolest (14.93 ±0.35 °C), OPEN plots the warmest (15.62 ±0.35 °C), and CANOPY plots were in between (15.10 ±0.35 °C). No within year comparisons were statistically significant. There were also no differences in temperature among years, when data were pooled and compared by year alone.

SOIL PHYSICAL AND CHEMICAL CHARACTERISTICS

Soils within the Weimer Run watershed are heavily acidic, with pH ranging from 3.87 – 4.32 across the sampling area (Appendix A). Soil bulk density (ρ_s) from 0 – 12 cm ranges from 0.49 – 1.11 g cm^{-3} (Fig. 2.4A and 2.4B), with lower values occurring beneath the shrub understory at lower elevations and higher values found in open, forest gap areas. There is an effect of elevation ($F_{2, 56} = 5.77$; $p = 0.005$) and vegetation ($F_{2, 56} = 10.55$; $p = 0.0001$) on ρ_s for all soil profiles (0 – 5, 0 – 12, and 0 – 20 cm). Elevation effects on ρ_s by soil depth are mixed, with statistical differences at 5 cm depth ($F_{2, 12} = 4.11$; $p = 0.044$) and at 20 cm depth ($F_{2, 18} = 4.15$; $p = 0.003$). By elevation classes across all vegetation types, ρ_s from 0 – 12 cm is lowest at LOW elevations (0.0.65 ±0.08 g cm^{-3}), highest at MID elevations (0.95 ±0.08 g cm^{-3}), and in between at HIGH elevations (0.73 ±0.08 g cm^{-3}). Vegetation shows significant differences at 12 cm ($F_{2, 18} = 3.60$; $p = 0.048$) and 20 cm ($F_{2, 18} = 5.15$; $p = 0.002$). By vegetation classes across all elevations, ρ_s

from 0 – 12 cm is lowest in SHRUB plot (0.58 ±0.08 g cm^{-3}), highest in OPEN plots (0.92 ±0.08 g cm^{-3}), and in between at CANOPY plots (0.83 ±0.08 g cm^{-3}). No interactive effects of elevation and vegetation were evident (Appendix B).

Soil porosity from 0 – 12 cm ranges from 0.58 - 0.82 m^{-3} m^3 and is correlated with vegetation cover—with higher values beneath the SHRUB plots (0.77 ±0.03 m^3 m^{-3}), medial values in CANOPY plots (0.68 ±0.03 m^3 m^{-3}), and lower values in OPEN plots (0.65 ±0.03 m^3 m^{-3}). (Appendix E). SHRUB plots also show the highest concentrations of total soil carbon (9.35 %) significantly greater than other vegetation types (F = 9.79; p = 0.0002). Vegetation also influences total soil nitrogen, with SHRUB plots exhibiting higher proportions of total soil N than other plots (Appendix E) (F = 6.36; p = 0.0029). Total soil carbon also differed by elevation, with LOW and HIGH classes showing greater proportions of total soil carbon in samples than MID elevation sites (Appendix D) (F = 6.28; p = 0.0031). MID level plots also showed lower proportions of total soil nitrogen than other elevation levels (Appendix D) (F = 6.45; p = 0.0027).

Kruskal-Wallis tests show that soil organic matter (SOM) for all soil depths (0 - 5, 0 - 12, and 0 - 20 cm) varied significantly by vegetation (χ^2 = 8.21; p = 0.016) and by soil depth (χ^2 = 36.18; p = <.0001), but not by elevation (χ^2 = 1.82; p = 0.401). Differences in SOM by vegetation treatment through the soil column were significant for the 0 – 5 and the 0 – 20 cm soil profiles (Appendix D). The highest rates of SOM were found at the HIGH elevation plots (40.14%) compared to the MID (21.73%) and LOW elevation plots (33.03%) (Fig. 2.4C). SHRUB plots (33.54%) and CANOPY plots (33.14%) had similar SOM values. OPEN plots were lower (27.76%) (Fig. 2.4D).

Regressions of mean plot-level soil CO_2 efflux against soil bulk density, soil organic matter, total soil carbon, total soil nitrogen, and plant area index yielded a statistically significant relationship only between soil bulk density (R^2 = 0.302; p = 0.003; Fig.2. 5).

DISCUSSION

For data above 11°C across the three study years with varying precipitation regimes, it becomes apparent that there is an intrinsic link between the movement of carbon and water in this system in response to landscape heterogeneities and inter-annual climate dynamics. During 2010, our comparatively dry year, we see increased rates of F_{SOIL} across the watershed, but more pronounced increases in fluxes from SHRUB plots. While SHRUB plots do exhibit greater rates of fluxes than other classes in this watershed during the course of this study, the magnitude of these fluxes is enhanced when the watershed is drier. Conversely, during 2011, the relatively wet year, vegetation-level differences in F_{SOIL} are statistically unapparent. When changing precipitation regimes are considered, along with future projections of warming and carbon dynamics, the importance of this coupling among water, carbon, and vegetation within humid watersheds cannot be understated. Changes in the distribution, variability, and amount of rainfall, as a result of climate change, are expected to have a major effect on carbon cycling (Borken et al., 2002). The magnitude of this effect, however, remains uncertain (Wu et al., 2011; Ahlström et al., 2012; Reichstein et al., 2013).

During 2010 (driest year), we see a strong effect of elevation on WFPS, with each elevation level statistically different from each other. During 2011 and 2012, however, only the MID elevation differs. When precipitation decreases across the watershed, as is the case during 2010, a different soil moisture regime manifests at higher elevations, with lower values of WFPS

that contribute, in the case of this watershed, to increased rates of F_{SOIL}. During periods of increased precipitation, the watershed exhibits a more uniform soil moisture regime. The difference in the magnitude of carbon fluxes across elevation levels decreases during years with higher precipitation. During periods of higher precipitation and increased soil moisture, air space within the soil remains filled and transportation of CO_2 through the soil is limited, resulting in decreased rates of F_{SOIL}. Production of CO_2 in the soil is also decreased due to the increased incidence of anoxic conditions as a function of increased WFPS. The LOW elevation plots were the warmest for each year of the study, yet exhibited the lowest rates of F_{SOIL} for the entire study period. One consideration not explicitly detailed in our study is the effect of topographic aspect on soil water redistribution as plots in our study all had an east-northeasterly aspect. Landscape positions with varying aspect can have differing soil water contents while having similar soil temperature regimes (Kang et al., 2003) that still result in varied soil carbon fluxes. Another contributor to the magnitude of carbon fluxes can be the amount of upslope accumulated area or the connectivity of varying landscape positions to flow paths within watersheds (McGlynn and Seibert, 2003; Pacific et al., 2012). During our wet year, however, we see a diminished effect of these topographic heterogeneities.

Enhanced fluxes during years of decreased precipitation suggest that soil respiration in humid mountain watersheds is strongly controlled by soil water, and to a lesser extent, soil temperature. During average and above-average precipitation years, soil respiration values are lower due to limited CO_2 production and/or diffusion through the soil. During years where precipitation is below average, soil respiration values increase. However, what is not considered here are the cumulative effects of inter-annual variability in precipitation. Would consecutive dry

or consecutive wet years result in increases or decreases following the second year? Data from the National Climate Data Center's (NCDC) station in Canaan Valley, WV (Station ID 461393) show that precipitation in this region of WV is increasing, notably so since 1993 (Fig. 2.6B). This increase in precipitation appears to be driven by a notable increase in the number of extreme precipitation days (EPDs), defined here as days where precipitation exceeds 25.4 mm (Fig. 2.6C). While precipitation is generally increasing in the Weimer Run watershed, and similar areas across West Virginia, the year-to-year variance is increasing as well. A Breusch-Pagan test, which tests for the presence of heteroscedasticity in linear regression models, shows that NCDC precipitation data from Canaan Valley since 1970 exhibit a statistically significant increase in inter-annual variance (BP = 8.58; p = 0.003). Meaning, the low precipitation years are trending much lower than the mean, while the high precipitation years are trending much higher than the mean, with fewer overall "average" precipitation years. This increased variance appears to again be driven by the increased variance in EPDs from year-to-year (Fig. 2.6B and 2.6C) and has been attributed to changes in the North Atlantic Subtropical High and anthropogenic climate change (Li et al., 2011). As soils are subject to year-to-year wet/dry cycles, cumulative effects on carbon cycling and carbon fluxes are likely. It is beyond the scope of this study to answer the question posed above; however, with the observed dynamics in precipitation for the region, this may be an important line of future research. These relative extremes in rainfall amounts that occurred during this study resulted in significant differences in soil moisture regimes (measured as WFPS) across the entire watershed and among both our elevation and vegetation cover classes (Section 3.2; Tables 1 and 2). During 2011, there were 34 EPDs, whereas in 2010 there were only 11 and in 2012 only 9. Precipitation also affected the variance of WFPS within the watersheds by year,

as measured by the coefficient of variation (CV) with 2011 showing decreased variance of WFPS (CV = 25.5) compared to either 2010 (CV = 40.6) or 2012 (CV = 32.4). Increased precipitation and increased numbers of EPDs changes the soil moisture regime within the watershed that in turn affects CO_2 fluxes.

A noticeable increase in CO_2 fluxes from plots with shrub cover is apparent in our data, despite consistently lower soil temperatures in these plots. The magnitude of these increases rises during drier years. We propose that increases in soil CO_2 efflux from beneath shrubs is related to the observed differences in soils beneath plots with shrub cover in this watershed. Soil bulk density, soil porosity, soil carbon, and other soil properties have been shown to drive the spatial variability of carbon fluxes (Jassal et al., 2004; Fiener et al., 2012; Luan et al., 2011). The effect of the soil microbial community on the temperature sensitivity of soil respiration can also be enhanced in soils with high soil C:N ratios (Karhu et al., 2014). Here we see shrubs decrease soil bulk density (Fig. 2.4B; Appendix E) and increase soil porosity (soil porosity (Φ) for SHRUB plots averaged 0.77 m^3m^{-3} from 0 – 12 cm depth, compared to 0.65 m^3m^{-3} for OPEN plots and 0.68 m^3m^{-3} for CANOPY plots; Appendix E), allowing for greater diffusivity within the soil matrix, and increased transportation potential of soil CO_2 through the soil. While soils under SHRUB plots have higher concentrations of SOM and soil C, soil bulk density is lower, which results in overall lower values of SOM and comparable values of soil C by volume. The increased soil porosity in soils beneath shrub cover is likely resulting in increased oxidation of labile soil C. It should be considered that SHRUB plots, to 20 cm soil depth, had the highest mean values of SOM (18.13%), higher soil C (9.35 %), higher soil N (0.47%), higher C:N ratios (19.36), and lower ρ_s (0.39 g cm^{-3}) compared to CANOPY (SOM = 12.48%; soil C = 6.35%; soil N = 0.37%; soil C:N =

16.30) and OPEN plots (SOM = 12.48%; soil C = 5.14%; soil N = 0.31; soil C:N = 15.76) (Appendix D). The high C:N ratios for SHRUB plots indicate possibly lower amounts of available, labile carbon and possibly lower rates of decomposition than other areas of the watershed. This is corroborated by early results from a two-year litterbag experiment conducted in this watershed (Atkins et al., in prep). This indicates that root respiration contributions from shrubs may be substantive and may also be influenced by varying soil moisture and precipitation regimes.

There was slight, but not statistically significant, indication of intra-growing season variability in flux data, where peak fluxes occurred during August for all elevation and vegetation classes for 2010 and 2012, and late July for 2011 (data not shown). However, this difference in peak flux appears to be tied more to moisture in the system rather than soil temperature and/or phenology.

The most dominant shrub species in this watershed is *Rhododendron maximum*, an ericaceous understory shrub that has been shown to increase SOM and soil N in forests where it is present (Boettcher and Kalisz, 1990; Wurzberger and Hendrick, 2007). *R. maximum* occurs most commonly in forest coves and on north-facing slopes with mesic to moist soil water regimes (Lipscomb and Abrams, 1990). Ericaceous litter also contributes to declines in soil fertility, lower N mineralization rates, and lower decomposition rates due to higher concentrations of foliar polyphenols (Hättenschwiler and Vitousek, 2000; DeLuca et al., 2002; Côté, 2000; Wurzberger and Hendrick, 2007). Ericaceous plants have ericoid mycorrhizae that provide a competitive advantage to breaking down organic N over ectomycorrhizae associated with many deciduous and coniferous species (Bending and Read, 1997) which leads to the inhibition of over-story species regeneration (Nilsen et al., 2001).

The areal extent of *R. maximum* has increased in some areas of southern and central Appalachia (Phillips and Murdy, 1985; Rollins et al., 2010; Brantley et al., 2013; Elliott et al., 2014). Shrub cover in the region is expected to continue to increase given fire suppression, lack of grazing, and forest canopy die-off from infestations (Nowacki and Abrams, 2008; Ford et al., 2011). If precipitation increases in this area in accordance with climate projections, the accompanying increase in soil moisture availability may further the expansion of *R. maxiumum*. The loss of previously dominant foundational species in these systems (e.g. *Picea rubens* in West Virginia due to logging and fire in the late 1800s and early 1900s; *Tsuga canadensis* die-off from hemlock woolly adelgid across the Appalachians and eastern US) may result in possible, multiple stable-states (Ellison et al., 2005). Increase in shrub cover has the potential to further impact ecosystem fluxes and biogeochemical cycling and may contribute strongly to future forest community dynamics. However, conversely, if the variance of inter-annual precipitation continues to increase, drought years may serve as a possible control on shrub expansion. Future precipitation dynamics will be a strong determinant of the biogeochemical fluxes and cycling for this watershed, and possibly, for the region.

Our findings indicate that for this consistently wet, humid watershed, increases in precipitation may result in decreased soil water heterogeneity and decreased fluxes of carbon from the soil surface, while decreased precipitation may result in increased soil water heterogeneity and increased carbon fluxes—especially from areas with high shrub coverage. Similar studies in drier watersheds have found that increases in soil water availability largely result in increases in soil carbon fluxes. Pacific et al. (2008) showed that for the Stringer Creek watershed, a sub-alpine, montane watershed in Montana, the spatial variability of soil CO_2 efflux

was controlled by the input of soil water driven by seasonal snowmelt. For riparian areas lower in the study watershed, soil carbon fluxes increased during the growing season in phase with increases in soil water content driven by seasonal snowmelt. Fluxes were suppressed at high levels of soil water early in the growing season, but as soil water decreased, fluxes increased. Pacific et al. (2009) further compared a wet and a dry year in the same watershed, finding that cumulative fluxes were 33% higher in riparian areas during the dry year, but 8% lower at landscape positions higher in the watershed. Decreased moisture inputs resulted in significant responses in fluxes across landscape positions, but the riparian areas respond similarly to the entirety of the Weimer Run watershed, with dry years resulting in empirically validated increases in carbon fluxes. It has been shown in previous studies and research (Clark and Gilmour, 1983; Davidson et al., 2000; Sjogersten et al., 2006; Pacific et al., 2008) that a production optimality of surface CO_2 efflux exists in response to soil water content such that peak rates of surface CO_2 efflux coincide with medial values of soil water content along a temporal transition within an elevation gradient. Our study adds the dimension of vegetation to this model, demonstrating that vegetation heterogeneity can have significant effects on surface CO_2 efflux within humid watersheds during periods of below-average soil water availability.

There are other possible avenues of carbon loss not considered here that may be affected by inter-annual climatic variability. It is possible that dissolved organic carbon (DOC) and dissolved inorganic carbon (DIC) fluxes from the watershed are increased during wet years due to increased flow in the system. Fluxes from these pools may be significant, but are difficult to measure and often carry a high-degree of uncertainty. DIC and DOC fluxes are highly variable spatially, coinciding with preferential flow paths within watersheds as a function of run-off

(McGlynn and McDonnell, 2003; Kindler et al., 2011). Manipulative experiments have shown that simulated drought decreases DOC leaching across an elevation gradient by as much as 80 – 100% (Hagedorn and Joos, 2014), indicating that these fluxes are also responsive to inter-annual climate variability.

The threshold approach employed in this paper allows for a quantification of the controls on soil CO_2 efflux during periods when fluxes are not temperature limited. This threshold was chosen empirically after analyzing the data. While the exact threshold of 11°C may not be applicable to all watersheds, if similar or related methods for threshold determination (e.g. piece-wise regression, or Bayesian change-point analysis) are used, this approach offers potential for comparisons and insights into controls on fluxes. If varying thresholds are found, it would be of research interest to examine the variance.

CONCLUSIONS

We completed a three-year plot-based study focusing on evaluating the effects of vegetation cover and elevation on soil carbon cycling in response to inter-annual variability in precipitation. By looking at data above 11° C for soil temperature measured at 12 cm depth, we were able to focus on the effects of soil moisture on carbon cycling without having to control for temperature limitation. We found that during a relatively dry year (2010; 1042mm) the magnitude of soil carbon flux was enhanced across the watershed, but the increase was differential due to statistically greater fluxes from plots with high shrub coverage. Greater fluxes of carbon from plots with high shrub cover were due in part to decreased soil bulk density, high quantities of soil organic matter, and possible increased root respiration present beneath shrubs as compared to either closed-canopy or open-area plots. For 2011 and 2012, relatively wetter

years, fluxes were decreased, and the effects of vegetation cover on the magnitude and variability of fluxes were statistically insignificant. Elevation had an effect on carbon cycling in the system by exacerbating vegetation effects during dry periods through increased effects on soil water distribution in the system. While soil water was correlated with elevation for all of our data, the effect was more pronounced during our driest year (2010) where areas higher in the watershed were much drier than lower positions. With the expected increase in precipitation as forecast by climate models and the empirical basis of increased inter-annual variance in precipitation, these findings offer important insights on the relations among landscape, vegetation, soil, and the associated biogeochemical effects for complex, humid watersheds. Given the increased likelihood of greater inter-annual variance in precipitation in the future, the coupling between carbon movement and vegetation cover is potentially quite crucial and under-considered. Further, the role of ericaceous shrubs and their future in this system are quite complex and may have profound influence on biogeochemical cycles.

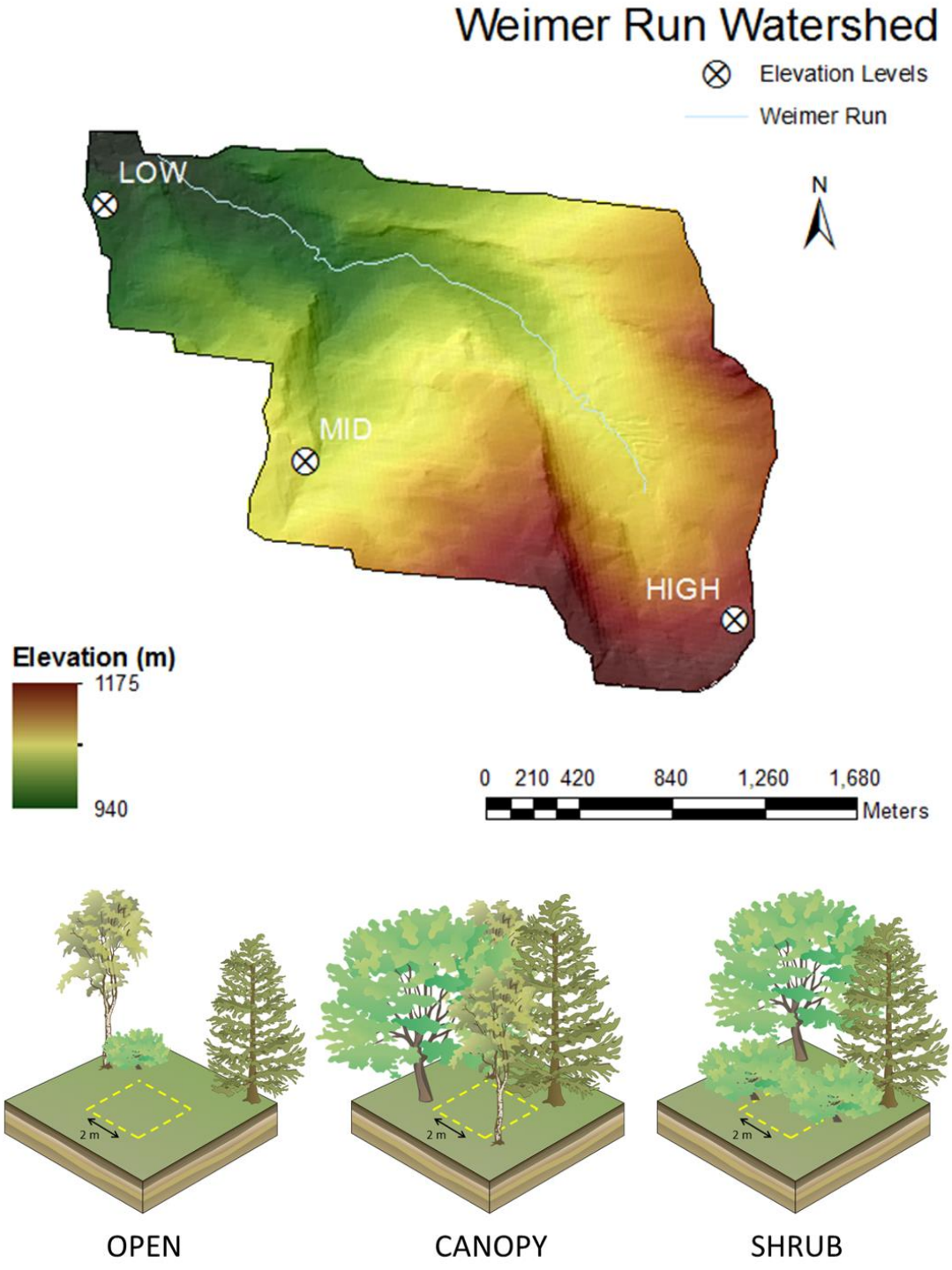

Figure 2.1. Weimer Run watershed (374 ha) (top); Conceptual diagram showing vegetation classes. Images courtesy of the Integration and Application Network, University of Maryland Center for Environmental Science (ian.umces.edu/symbols/) (bottom).

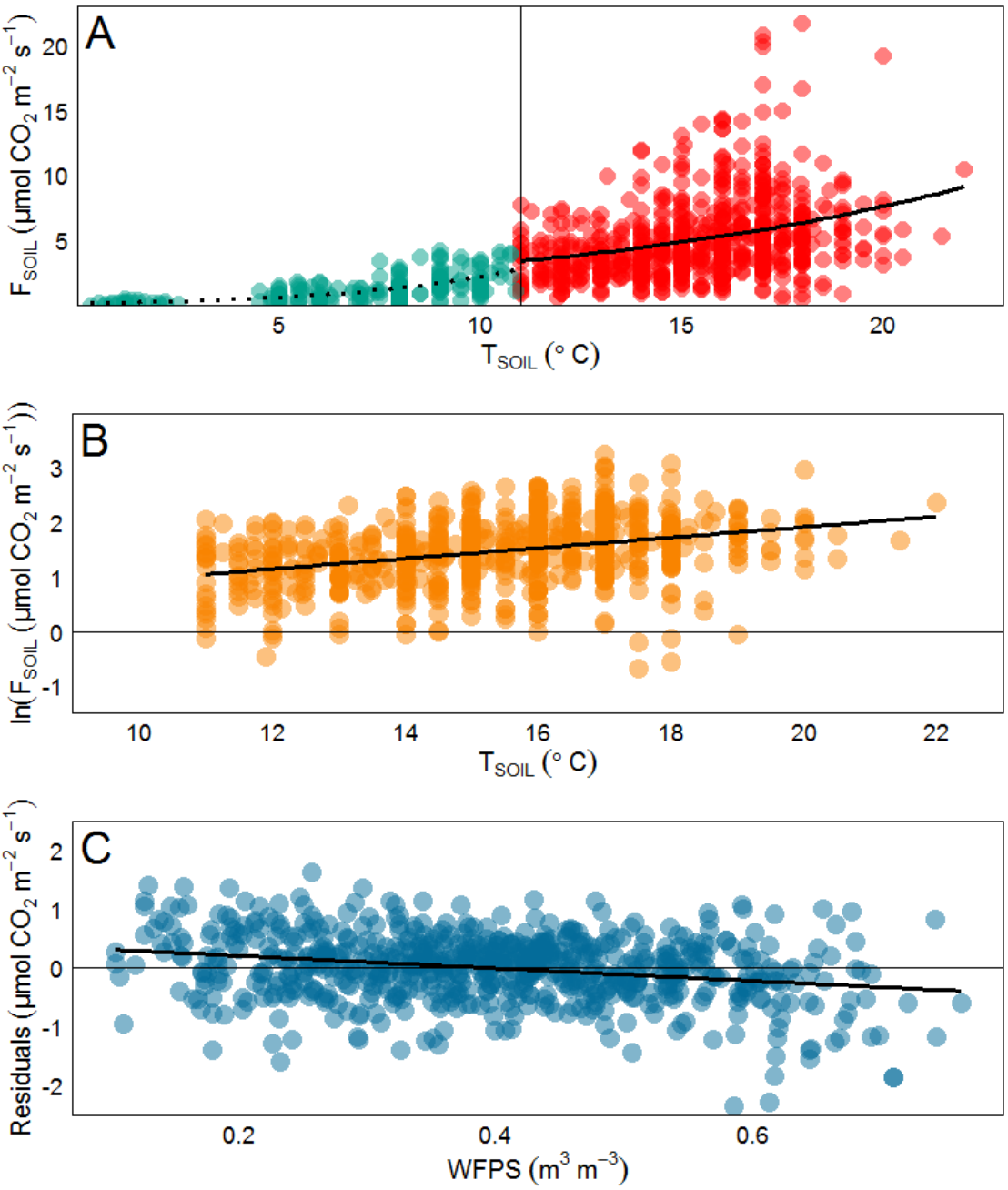

Figure 2.2. (A) Soil CO_2 efflux (µmol CO_2 m^{-2} s^{-1}) against soil temperature (°C) at 12 cm with data split at 11° C. For all data, exponential regression shows an R^2 = 0.3163. For flux rate values below 11° C, R^2 = 0.434, for flux rate values above 11° C, R^2 = 0.104. (B) Natural log of soil CO_2 efflux (µmol CO_2 m^{-2} s^{-1}) against soil temperature (°C) at 12 cm for all data above 11° C. For flux rate values below 11° C, linear regression gives an R^2 = 0.1188, p=<<0.0001. (C) Residuals of the natural log of soil CO_2 efflux (µmol CO_2 m^{-2} s^{-1}) against water-filled pore space (0 – 12 cm) for all data above 11° C. R^2 = 0.06, p = <<0.0001.

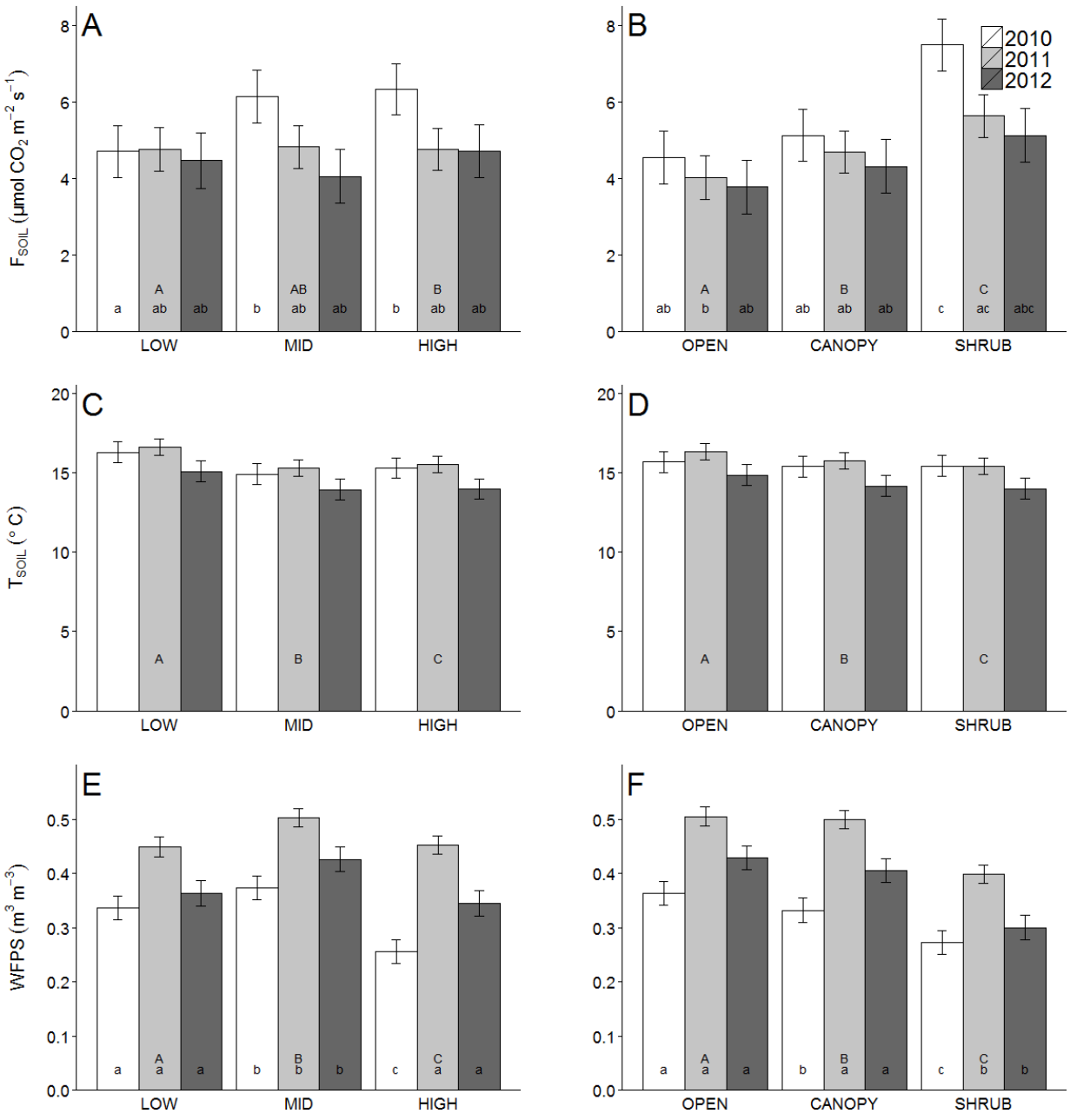

Figure 2.3. (A, C, E) Least-squares means of soil CO_2 efflux (µmol CO_2 m^{-2} s^{-1}); WFPS (m^3 m^{-3}); and soil temperature at 12 cm (C°) by elevation. (B, D, E) Least-squares means of soil CO_2 efflux (µmol CO_2 m^{-2} s^{-1}); WFPS (m^3m^{-3}); and soil temperature at 12 cm (C°) by vegetation. Capital letters indicate difference between elevation classes and lower case letters indicate differences among class levels within years. Bars indicate standard error. Colors indicate sampling year.

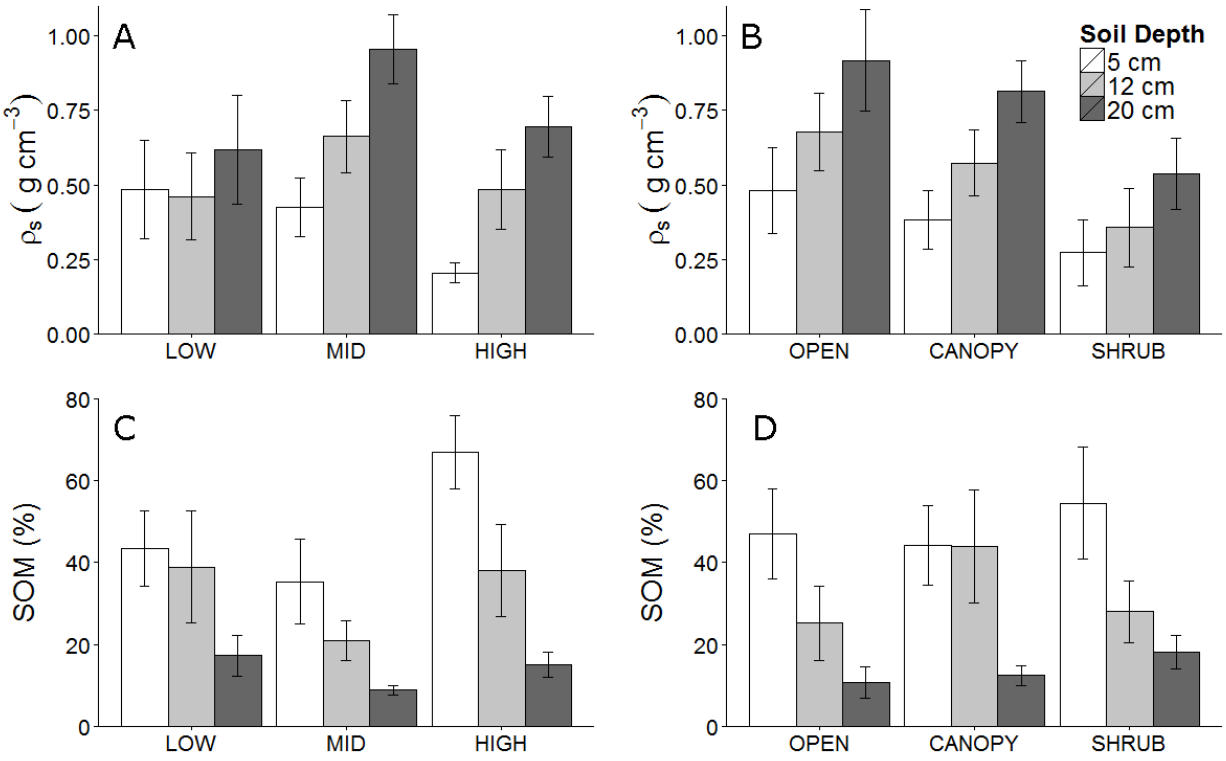

Figure 2.4. (A, C) Means of soil bulk density (g cm^{-3}) and soil organic matter (%) by elevation treatment. (B, D) Means of soil bulk density (g cm^{-3}) and soil organic matter (%) by vegetation treatment. Bars indicate standard error. Colors indicate soil depth profiles.

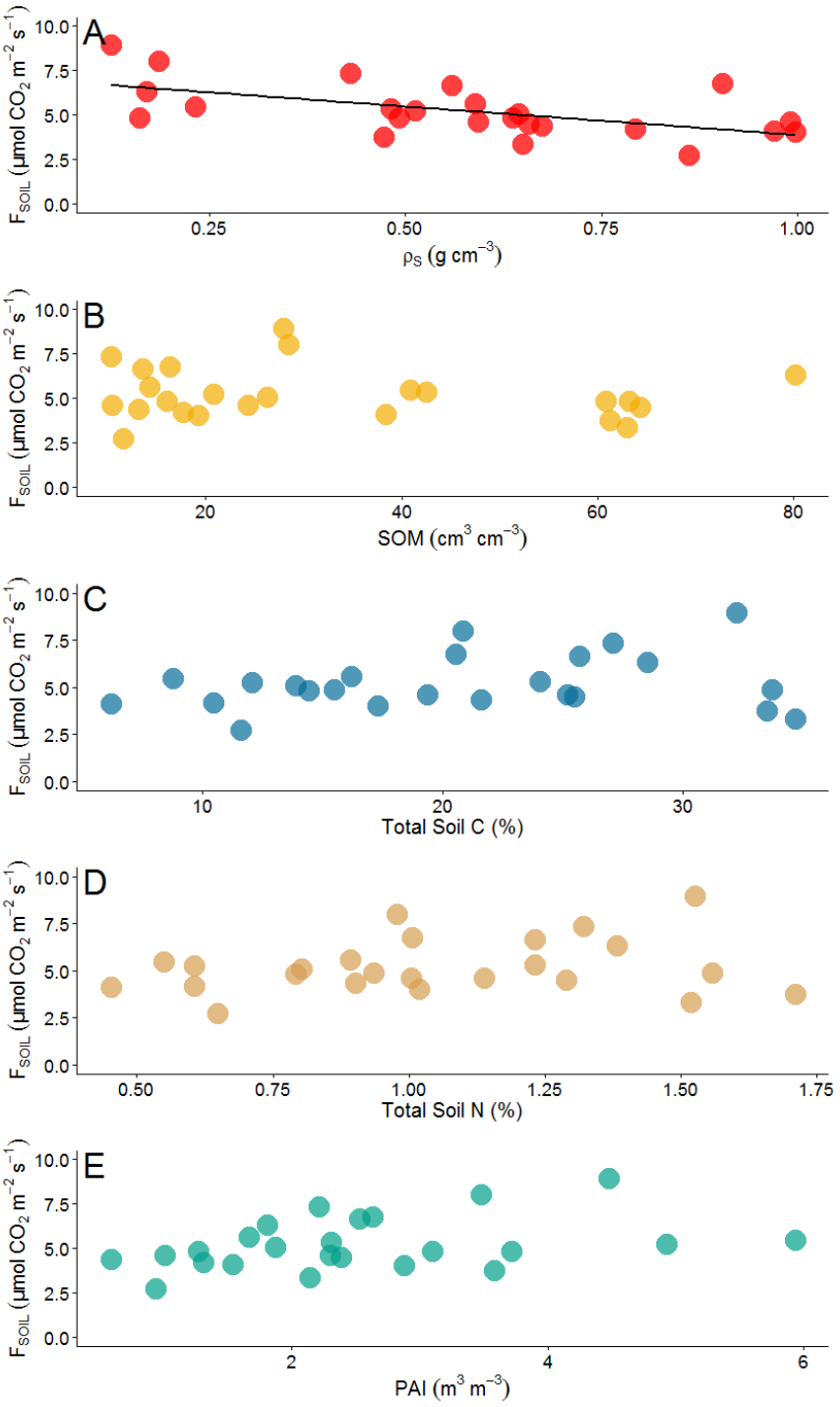

Figure 2.5. (A) Soil bulk density (g cm^{-3}), (B) soil organic matter (%), (C) total soil carbon (%), (D) total soil nitrogen (%), and (E) plant area index (m^{-3} m^3) against mean plot-level soil CO_2 efflux by plot for all measurements across all three years where soil temperature (°C) was above 11 °C. Only soil bulk density (A) shows a significant relationship (R^2 = 0.302; p = 0.003) with mean plot-level soil CO_2 efflux.

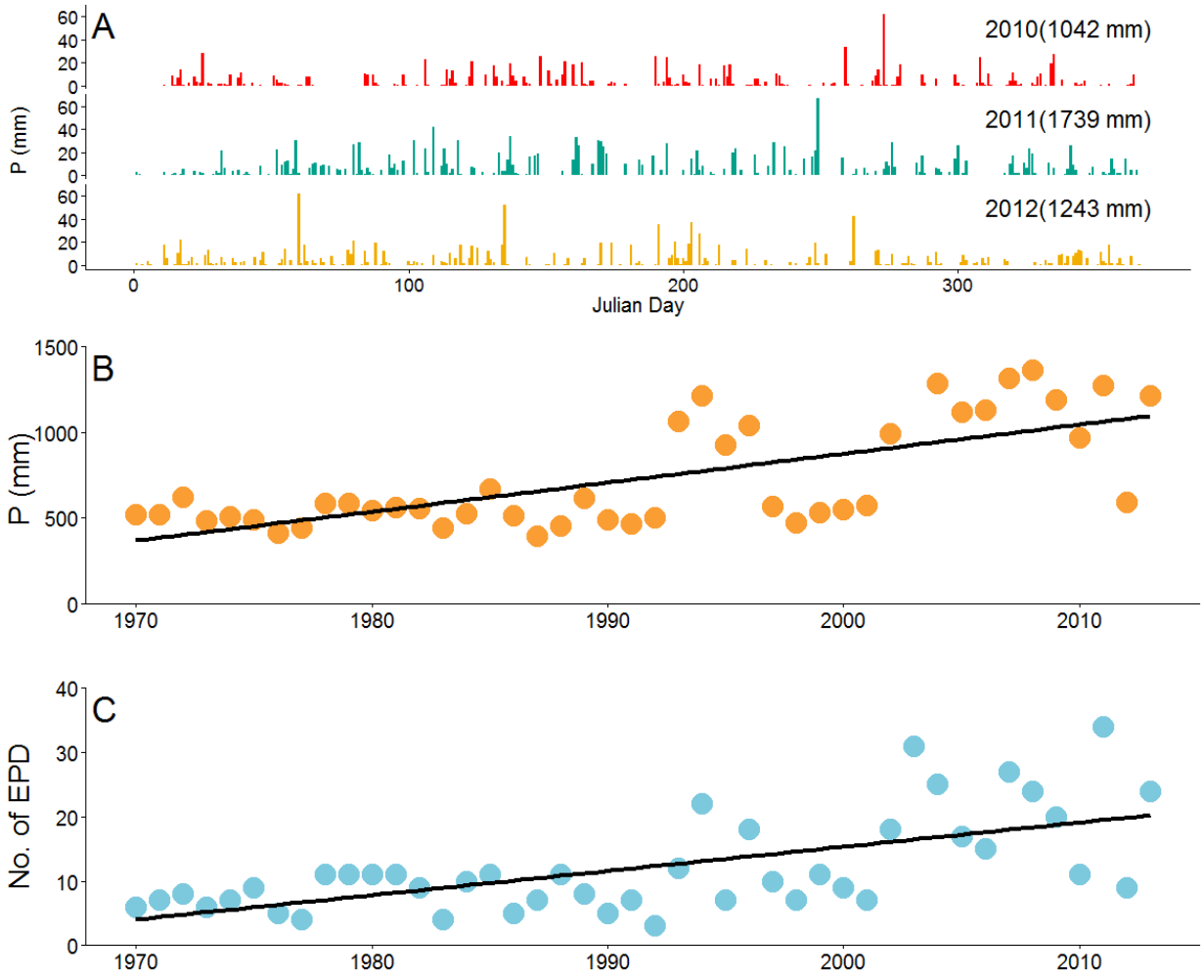

Figure 2.6. (A) Hyetographs for 2010, 2011, and 2012 from the Bearden Knob weather station located within the Weimer Run watershed (BDKW2 MesoWest; University of Utah). Precipitation totals by year are indicated within each graph and are in mm yr^{-1}. (B) Precipitation for the years 1970 – 2013 (mm yr^{-1}) from NCDC station Canaan Valley, WV (461393). Linear regression shows that mean annual precipitation is increasing by 17.88 mm yr^{-1} (r = 0.697; $F_{1,42}$ = 39.74; r^2 = 0.474; p = <.0001). The year to year variance in precipitation is also increasing (BP = 8.58; p = 0.003). (C) Number of extreme precipitation days (EPD) per year (defined as days where total precipitation exceeded 25.4 mm per day). The number of EPDs are increasing by 0.38 days per year (r = 0.637; $F_{1,42}$ = 28.69; r^2 = 0.392; p = <.0001). The variance is also increasing (BP = 11.12; p = <.0001).

Table 2.1. Least-squares means of dynamic environmental variables. Error terms indicate standard error.

YEAR	CLASS	F_{SOIL} (μmol CO_2 m^{-2} s^{-1})	WFPS (m^3 m^{-3})	T_{SOIL} (C°)
2010	LOW	4.69 ±0.687	0.337 ±0.022	16.29 ±0.656
2010	MID	6.13 ±0.691	0.373 ±0.022	14.90 ±0.656
2010	HIGH	6.32 ±0.668	0.256 ±0.022	15.30 ±0.654
2011	LOW	4.75 ±0.571	0.449 ±0.018	16.61 ±0.520
2011	MID	4.82 ±0.561	0.503 ±0.017	15.31 ±0.519
2011	HIGH	4.76 ±0.551	0.452 ±0.017	15.54 ±0.518
2012	LOW	4.45 ±0.722	0.363 ±0.023	15.08 ±0.659
2012	MID	4.04 ±0.702	0.426 ±0.023	13.93 ±0.658
2012	HIGH	4.71 ±0.681	0.345 ±0.022	13.98 ±0.656
2010	OPEN	4.54 ±0.685	0.363 ±0.022	15.67 ±0.656
2010	SHRUB	7.48 ±0.674	0.272 ±0.022	15.42 ±0.655
2010	CANOPY	5.11 ±0.674	0.332 ±0.022	15.39 ±0.655
2011	OPEN	4.02 ±0.562	0.505 ±0.017	16.31 ±0.519
2011	SHRUB	5.63 ±0.559	0.399 ±0.017	15.38 ±0.518
2011	CANOPY	4.68 ±0.557	0.499 ±0.017	15.76 ±0.518
2012	OPEN	3.77 ±0.698	0.429 ±0.022	14.86 ±0.656
2012	SHRUB	5.12 ±0.705	0.300 ±0.023	13.98 ±0.658
2012	CANOPY	4.31 ±0.697	0.405 ±0.022	14.15 ±0.657
	LOW	4.61 ±0.431	0.383 ±0.012	15.99 ±0.356
	MID	4.99 ±0.427	0.434 ±0.012	14.71 ±0.356
	HIGH	5.25 ±0.418	0.351 ±0.012	14.94 ±0.355
	OPEN	4.09 ±0.425	0.432 ±0.012	15.61 ±0.355
	SHRUB	6.07 ±0.424	0.324 ±0.012	14.93 ±0.355
	CANOPY	4.69 ±0.423	0.412 ±0.012	15.10 ±0.355
2010		5.71 ±0.634	0.322 ±0.021	15.50 ±0.652
2011		4.78 ±0.525	0.468 ±0.016	15.82 ±0.516
2012		4.36 ±0.647	0.378 ±0.021	14.36 ±0.653

Table 2.2. Statistical table from repeated measures mixed-model ANOVA. For all comparisons by ELEVATION, VEGETATION and YEAR, *n* = 633; *df* = 2, 633. For ELEVATION BY YEAR and VEGETATION BY YEAR comparisons, *n* = 633; *df* = 4, 633.

ELEVATION	F	*p*
F_{soil}	3.44	0.0326*
WFPS (0 - 12 cm)	57.94	<.0001*
Soil Temp (12 cm)	170.76	<.0001*
VEGETATION		
F_{soil}	37.58	<.0001*
WFPS (0 - 12 cm)	108.01	<.0001*
Soil Temp (12 cm)	52.79	<.0001*
ELEVATION BY VEGETATION		
F_{soil}	2.47	0.0436*
WFPS (0 - 12 cm)	19.50	<.0001*
Soil Temp (12 cm)	9.55	<.0001*
YEAR		
F_{soil}	1.40	0.2464
WFPS (0 - 12 cm)	16.06	<.0001*
Soil Temp (12 cm)	1.66	0.1918
ELEVATION BY YEAR		
F_{soil}	3.17	0.0134*
WFPS (0 - 12 cm)	5.92	0.0001*
Soil Temp (12 cm)	1.02	0.3945
VEGETATION BY YEAR		
F_{soil}	2.96	0.0192*
WFPS (0 - 12 cm)	2.04	0.0878
Soil Temp (12 cm)	5.46	0.0003*

APPENDIX

Appendix 2.A. Least-squares means of vegetation variables and soil chemical and physical properties. Error terms indicate standard error.

ELEVATION	VEGETATION	PAI (m^3 m^{-3})	MI (lux)	SOIL pH
LOW	OPEN	1.06 ±0.42	46856.33 ±2697.8	3.99 ±0.14
LOW	SHRUB	2.01 ±0.42	72819.75 ±3672.5	4.26 ±0.14
LOW	CANOPY	1.82 ±0.42	29966.01 ±1589.6	3.99 ±0.14
MID	OPEN	1.49 ±0.42	42500.11 ±3796.2	4.32 ±0.14
MID	SHRUB	3.68 ±0.42	19923.95 ±1194.9	4.11 ±0.14
MID	CANOPY	1.54 ±0.42	25855.61 ±1465.3	4.13 ±0.14
HIGH	OPEN	2.70 ±0.42	26230.93 ±1556.2	4.11 ±0.14
HIGH	SHRUB	4.71 ±0.42	12060.48 ±931.0	3.87 ±0.14
HIGH	CANOPY	3.05 ±0.51	20273.25 ±1174.5	4.17 ±0.14
LOW		1.63 ±0.24	49879.7 ±1932.9	4.08 ±0.08
MID		2.23 ±0.24	29138.82 ±1486.5	4.18 ±0.08
HIGH		3.49 ±0.26	19521.56 ±801.0	4.05 ±0.08
	OPEN	1.75 ±0.24	47346.97 ±2179.5	4.14 ±0.08
	SHRUB	3.46 ±0.24	26375.92 ±1389.7	4.08 ±0.08
	CANOPY	2.14 ±0.26	25361.26 ±852.7	4.10 ±0.08

Appendix 2.B. Mixed-model ANOVA results for the main and interactive effects of elevation, vegetation, and soil depth on soil bulk density (ρ_s) and total bulk density (ρ_t).

		Soil Bulk Density (ρ_s)		Total Bulk Density (ρ_t)	
Class	Depth (cm)	*F*	*p*	*F*	*p*
Elevation		5.77	0.0053	4.79	0.0120
Vegetation		10.55	0.0001	9.93	0.0002
Soil Depth		15.70	<.0001	17.80	<.0001
Elevation*Vegetation		0.40	0.8089	0.29	0.8851
Elevation*Depth		1.70	0.1619	1.57	0.1951
Vegetation*Depth		0.31	0.8719	0.18	0.9501
Elevation	5	4.11	0.0436	4.67	0.0316
Vegetation	5	2.72	0.1059	3.10	0.0822
Elevation*Vegetation	5	1.28	0.3300	1.27	0.3342
Elevation	12	1.63	0.2228	1.17	0.3333
Vegetation	12	3.60	0.0483	3.47	0.0533
Elevation*Vegetation	12	0.73	0.5856	0.66	0.6286
Elevation	20	4.15	0.0330	3.35	0.0582
Vegetation	20	5.15	0.0170	4.19	0.0321
Elevation*Vegetation	20	0.30	0.8733	0.16	0.9551

Appendix 2.C. Kruskal-Wallis rank sum test results for the effects of elevation, vegetation, and soil depth on soil organic matter (SOM %), soil C (%), soil N (%), and soil C:N (%).

		SOM (%)		SOIL C (%)		SOIL N (%)		SOIL C:N	
TREATMENT	DEPTH (cm)	χ^2	*p*-value	χ^2	*p*-value	χ^2	*p*-value	χ^2	*p*-value
Elevation		1.82	0.401	4.59	0.101	5.08	0.078	1.4	0.496
Vegetation		8.21	0.016	10.64	0.004	6.83	0.032	30.08	<.0001
Depth		36.18	<.0001	98.61	<.0001	111.28	<.0001	13.52	0.004
Elevation	5	0.39	0.822	10.63	0.004	11.05	0.004	6.47	0.039
Vegetation	5	8.99	0.011	5.60	0.061	4.19	0.123	12.09	0.002
Elevation	12	2.03	0.361	4.72	0.094	6.35	0.042	0.47	0.812
Vegetation	12	2.55	0.278	3.05	0.216	2.72	0.257	4.21	0.122
Elevation	20	5.72	0.057	9.29	0.009	11.68	0.002	0.64	0.724
Vegetation	20	6.14	0.046	15.28	<.0001	11.30	0.004	23.66	<.0001

Appendix 2.D. Total soil carbon (%), total soil nitrogen (%), total soil C:N ratio and soil organic matter (SOM) (%) by all combinations of elevation, vegetation, depth levels and classes.

ELEV	VEG	DEPTH	SOIL C (%)	SOIL N (%)	SOIL C:N	SOM (%)
LOW	OPEN	5	14.11 ±1.14	0.87 ±0.069	16.12 ±0.33	42.06 ±7.88
LOW	OPEN	12	13.89 ±2.47	0.67 ±0.065	18.69 ±1.84	25.79 ±8.92
LOW	OPEN	20	7.43 ±0.87	0.42 ±0.042	15.42 ±0.45	15.26 ±4.71
LOW	SHRUB	5	29.62 ±1.37	1.53 ±0.063	19.02 ±0.22	53.44 ±8.21
LOW	SHRUB	12	26.13 ±1.20	1.23 ±0.060	21.42 ±0.78	18.20 ±2.38
LOW	SHRUB	20	10.92 ±0.55	0.54 ±0.027	20.19 ±0.18	22.46 ±3.31
LOW	CANOPY	5	19.41 ±1.07	0.96 ±0.041	20.19 ±0.51	34.83 ±2.46
LOW	CANOPY	12	20.47 ±2.39	1.05 ±0.112	18.64 ±0.30	68.45 ±3.42
LOW	CANOPY	20	5.96 ±0.49	0.36 ±0.023	14.85 ±0.42	14.32 ±2.90
MID	OPEN	5	11.11 ±0.85	0.66 ±0.044	15.57 ±0.35	33.13 ±6.91
MID	OPEN	12	14.47 ±0.63	0.81 ±0.034	17.89 ±0.30	17.41 ±2.61
MID	OPEN	20	3.71 ±0.06	0.23 ±0.002	15.99 ±0.12	7.06 ±0.44
MID	SHRUB	5	15.62 ±1.51	0.75 ±0.060	19.97 ±0.42	29.17 ±7.44
MID	SHRUB	12	18.79 ±1.06	0.90 ±0.041	20.00 ±0.40	21.86 ±2.03
MID	SHRUB	20	4.42 ±0.13	0.25 ±0.005	17.37 ±0.20	10.26 ±0.94
MID	CANOPY	5	17.32 ±2.60	0.92 ±0.125	17.90 ±0.50	43.67 ±9.03
MID	CANOPY	12	19.47 ±1.05	1.02 ±0.041	18.51 ±0.43	23.57 ±5.61
MID	CANOPY	20	6.59 ±0.35	0.37 ±0.019	17.81 ±0.16	9.43 ±0.56
HIGH	OPEN	5	27.22 ±2.86	1.30 ±0.120	19.14 ±1.21	65.76 ±4.91
HIGH	OPEN	12	23.51 ±2.44	1.18 ±0.093	18.75 ±0.79	32.76 ±8.74
HIGH	OPEN	20	4.63 ±0.26	0.28 ±0.006	15.80 ±0.54	9.95 ±1.01
HIGH	SHRUB	5	48.12 ±1.17	2.12 ±0.007	22.65 ±0.48	80.80 ±3.38
HIGH	SHRUB	12	28.13 ±3.15	1.34 ±0.117	19.88 ±0.65	44.01 ±5.95
HIGH	SHRUB	20	11.76 ±0.39	0.60 ±0.019	19.55 ±0.13	21.67 ±2.28
HIGH	CANOPY	5	24.27 ±3.25	1.22 ±0.166	20.16 ±0.45	54.29 ±7.70
HIGH	CANOPY	12	29.59 ±3.40	1.47 ±0.128	19.22 ±1.01	37.40 ±16.8
HIGH	CANOPY	20	6.52 ±0.19	0.39 ±0.009	16.42 ±0.12	13.69 ±0.38
LOW		5	21.61 ±0.55	1.15 ±0.026	18.38 ±0.14	43.44 ±9.26
LOW		12	20.21 ±0.81	0.99 ±0.035	19.45 ±0.30	38.94 ±13.5
LOW		20	8.13 ±0.22	0.44 ±0.010	16.87 ±0.15	17.35 ±5.01
MID		5	14.17 ±0.49	0.76 ±0.022	17.57 ±0.16	35.33 ±10.2
MID		12	17.70 ±0.32	0.91 ±0.013	18.84 ±0.13	20.95 ±4.88
MID		20	4.80 ±0.07	0.88 ±0.003	16.99 ±0.06	8.91 ±1.10
HIGH		5	31.46 ±1.25	1.48 ±0.053	20.36 ±0.34	66.95 ±8.95
HIGH		12	26.90 ±0.93	1.32 ±0.035	19.29 ±0.24	38.14 ±11.2
HIGH		20	7.90 ±0.15	0.44 ±0.006	17.40 ±0.11	15.10 ±3.09
	OPEN	5	16.30 ±0.58	0.89 ±0.026	16.68 ±0.20	46.98 ±10.91
	OPEN	12	16.99 ±0.54	0.89 ±0.022	18.33 ±0.24	25.26 ±9.05
	OPEN	20	5.144 ±0.16	0.31 ±0.007	15.76 ±0.11	10.76 ±3.9
	SHRUB	5	27.84 ±0.90	1.35 ±0.039	20.06 ±0.14	54.47 ±13.6
	SHRUB	12	23.02 ±0.62	1.10 ±0.024	20.28 ±0.18	28.03 ±7.57
	SHRUB	20	9.134 ±0.17	0.47 ±0.008	19.06 ±0.07	18.13 ±4.12
	CANOPY	5	20.05 ±0.74	1.02 ±0.035	19.36 ±0.17	44.27 ±9.64
	CANOPY	12	21.92 ±0.63	1.12 ±0.027	18.70 ±0.17	43.86 ±13.7
	CANOPY	20	6.353 ±0.11	0.37 ±0.005	16.30 ±0.10	12.48 ±2.42
LOW			17.01 ±0.19	0.88 ±0.009	18.10 ±0.05	33.03 ±22.0
MID			14.09 ±0.13	0.74 ±0.006	18.06 ±0.03	21.73 ±17.1
HIGH			19.52 ±0.24	0.97 ±0.010	18.55 ±0.05	40.14 ±27.2
	OPEN		13.36 ±0.15	0.73 ±0.007	16.94 ±0.05	27.76 ±22.6
	SHRUB		20.16 ±0.19	0.99 ±0.009	19.68 ±0.03	33.54 ±24.3
	CANOPY		16.33 ±0.18	0.84 ±0.008	18.03 ±0.04	33.14 ±23.9
		5	21.14 ±0.26	1.07 ±0.011	18.55 ±0.06	48.58 ±23.4
		12	20.73 ±0.20	1.04 ±0.008	19.11 ±0.06	32.21 ±21.2
		20	6.93 ±0.05	0.38 ±0.002	17.09 ±0.03	13.79 ±7.80

Appendix 2.E. Least-squares means of soil porosity (Φ) and soil bulk density (ρ) for the 0 – 12 cm soil depth used in calculating WFPS.

ELEVATION	VEGETATION	Φ (m^3 m^{-3})	ρ (g cm^{-3})
LOW	OPEN	0.68 ±0.05	0.83 ±0.14
LOW	SHRUB	0.81 ±0.05	0.49 ±0.14
LOW	CANOPY	0.75 ±0.05	0.64 ±0.14
MID	OPEN	0.58 ±0.05	1.11 ±0.14
MID	SHRUB	0.72 ±0.05	0.72 ±0.14
MID	CANOPY	0.61 ±0.05	1.01 ±0.14
HIGH	OPEN	0.69 ±0.05	0.81 ±0.14
HIGH	SHRUB	0.79 ±0.05	0.55 ±0.14
HIGH	CANOPY	0.68 ±0.05	0.83 ±0.14
LOW		0.75 ±0.03	0.65 ±0.08
MID		0.64 ±0.03	0.95 ±0.08
HIGH		0.72 ±0.03	0.73 ±0.08
	OPEN	0.65 ±0.03	0.92 ±0.08
	SHRUB	0.77 ±0.03	0.58 ±0.08
	CANOPY	0.68 ±0.03	0.83 ±0.08

REFERENCES

Ahlström, A., Schurgers, G., Arneth, A., & Smith, B.: Robustness and uncertainty in terrestrial ecosystem carbon response to CMIP5 climate change projections, Environmental Research Letters, 7, 4, 044008, 2012.

Allard, H. A. and E. C. L.: The Canaan and Stony River Valleys of West Virginia, their former magnificent spruce forests, Castanea, 17, 1, 1–60, 1952.

Atkins, J., Epstein, H. E., and Welsch, D. L.: Leaf-litter decomposition differs by vegetation cover along an elevation gradient in a West Virginia watershed, In preparation.

Bending, G. D., and Read, D. J.: Lignin and soluble phenolic degradation by ectomycorrhizal and ericoid mycorrhizal fungi. Mycological Research, 101, 11, 1348-1354, 1997.

Berg, B.: Litter decomposition and organic matter turnover in northern forest soils, Forest Ecology and Management, 133(1-2), 13–22, doi:10.1016/S0378-1127(99)00294-7, 2000.
Boettcher, S. E., and Kalisz, P. J.: Single-tree influence on soil properties in the mountains of eastern Kentucky, Ecology, 1365-1372, 1990.

Bond-Lamberty, B., and Thomson, A.: Temperature-associated increases in the global soil respiration record, Nature, 464, 579-582, 2010.

Borken, W., XU, Y. J., Davidson, E. A., and Beese, F.: Site and temporal variation of soil respiration in European beech, Norway spruce, and Scots pine forests, Global Change Biology, 8, 12, 1205-1216, 2002.

Brantley, S., Ford, C. R., and Vose, J. M.: Future species composition will affect forest water use after loss of eastern hemlock from southern Appalachian forests, Ecological Applications, 23, 4, 777-790, 2013.

Brito, P., Trujillo, J. L., Morales, D., Jimenenz, M.S., and Wieser, G.: Soil moisture overshadows temperature control over soil CO_2 efflux in a Pinus caneriensis forest at treeline in Tenerife, Canary Islands, Acta Oecologica, 48, 1-6, 2013.

Clark, M. D., & Gilmour, J. T.: The effect of temperature on decomposition at optimum and saturated soil water contents, Soil Science Society of America Journal, 47. 5, 927-929, 1985
Côté, L., Brown, S., Paré, D., Fyles, J., and Bauhus, J.: Dynamics of carbon and nitrogen mineralization in relation to stand type, stand age and soil texture in the boreal mixedwood, Soil Biology and Biochemistry, 32, 8, 1079-1090, 2000.

Davidson, E. A., Verchot, L. V., Cattânio, J. H., Ackerman, I. L., and Carvalho, J. E. M.: Effects of soil water content on soil respiration in forests and cattle pastures of eastern Amazonia, Biogeochemistry, 48, 1, 53-69, 2000.

Davidson, E. A., and Trumbore, S. E.: Gas diffusivity and production of CO2 in deep soils of the eastern Amazon, Tellus B, 47, 5, 550-565, 1995

Davidson, E. A., Belk, E. and Boone, R. D.: Soil water content and temperature as independent or confounded factors controlling soil respiration in a temperate mixed hardwood forest, Global Change Biology, 4, 2, 217-227, 1998.

DeLuca, T., Nilsson, M. C., amd Zackrisson, O.: Nitrogen mineralization and phenol accumulation along a fire chronosequence in northern Sweden, Oecologia, 133, 2, 206-214, 2002

Dilustro, J. J., Collins, B., Duncan, L. and Crawford, C.: Moisture and soil texture effects on soil CO_2 efflux components in southeastern mixed pine forests, Forest Ecology and Management, 204, 87-97, 2005.

Drewitt, G. B., Black, T. A., Nesic, Z., Humphreys, E. R., Jork, E. M., Swanson, R., Ethier, G. J., Griffis, T. and Morgenstern, K.: Measuring forest floor CO_2 fluxes in a Douglas-fir forest, Ag. and For. Meteorology, 110, 299–317, 2002.

Ekblad, A., & Högberg, P.: Natural abundance of ^{13}C in CO_2 respired from forest soils reveals speed of link between tree photosynthesis and root respiration, Oecologia, 127, 3, 305-308, 2001.

Ellison, A. M., Bank, M. S., Clinton, B. D., Colburn, E. A., Elliott, K., Ford, C. R., Foster, D. R., Kloeppel, B. D., Knoepp, J. D., Lovett, G. M., Mohan, J., Orwig, D. A., Rodenhouse, N. L., Sobczak, W. V., Stinson, K. A., Stone, J. K., Swan, C. M, Thompson, J., Von Holle, B., and Webster, J. R.: Loss of foundation species: consequences for the structure and dynamics of forested ecosystems, Frontiers in Ecology and the Environment, 3, 9, 479-486, 2005.

Elliott, K. J., Vose, J. M., and Rankin, D.: Herbaceous species composition and richness of mesophytic cove forests in the southern Appalachians: synthesis and knowledge gaps, Journal of the Torrey Botanical Society, 141, 1, 39-71, 2014.

Epron, D., Nouvellon, Y., Roupsard, O., Mouvondy, W., Mabiala, A., Saint-André, L., Joffre, R., Jourdan, C., Bonnefond, J., Bergibier, P. and Hamel, O.: Spatial and temporal variations of soil respiration in a *Eucalyptus* plantation in Congo, Forest Ecology and Management, 202, 149-160, 2004.

Fang, C., Moncrieff, J. B., Gholz, H. L. and Clark, K. L.: Soil CO_2 efflux and its spatial variation in a Florida slash pine plantation, Plant and Soil, 205, 135-146, 1998.

Fang, C. and Moncrieff, J. B.: The dependence of soil CO_2 efflux on temperature, Soil Biology and Biochemistry, 33, 155–165, 2001.

Fiener, P., Dlugoß, V., Korres, W., & Schneider, K.: Spatial variability of soil respiration in a small agricultural watershed—Are patterns of soil redistribution important?, Catena, 94, 3-16, 2001
Flint, A. L., & Flint, L. E.: 2.2 Particle Density, Methods of Soil Analysis: Physical Methods, 4, 229-240, 2002.

Ford, C. R., Elliott, K. J., Clinton, B. D., Kloeppel, B. D., and Vose, J. M.: Forest dynamics following eastern hemlock mortality in the southern Appalachians, Oikos, 121, 523-536, 2012.
Fortney, R. H.: The vegetation of Canaan Valley, West Virginia: a taxonomic and ecological study, Doctoral dissertation, West Virginia University, 1975.

Fortney, R. H., and Rentch, J. S.: Post logging era plant successional trends and geospatial vegetation patterns in Canaan Valley, West Virginia, 1945 to 2000, Castanea, 317-334, 2003.
Grossman, R. B., Reinsch, T. G., Dane, J. H., & Topp, C.: Methods of Soil Analysis: Physical methods, 4, 2002.

Hagedorn, F., and Joos, O.: Experimental summer drought reduces soil CO_2 effluxes and DOC leaching in Swiss grassland soils along an elevational gradient, Biogeochemistry, 117, 2-3, 395-412, 2014.

Hättenschwiler, S., and Vitousek, P. M.: The role of polyphenols in terrestrial ecosystem nutrient cycling, Trends in Ecology & Evolution, 15, 6, 238-243, 2000.

Högberg, P., Nordgren, A., Buchmann, N., Taylor, A. F., Ekblad, A., Högberg, M. N., Nyberg, G., Ottosson-Löfvenius, M., and Read, D. J.: Large-scale forest girdling shows that current photosynthesis drives soil respiration, Nature, 411, 6839, 789-792, 2001.

Kirtman, B., Power, S.B., Adedoyin, J.A., Boer, G.J., Bojariu, R., Camilloni, I., Doblas-Reyes, F.J., Fiore, A.M., Kimoto, M., Meehl, G.A., Prather, M., Sarr, A., Schär, C., Sutton, R., van Oldenborgh, G.J., Vecchi, G., and Wang, H. J.: Near-term Climate Change: Projections and Predictability. In: Climate Change 2013: The Physical Science Basis. Contribution of Working Group I to the Fifth Assessment Report of the Intergovernmental Panel on Climate Change [Stocker, T.F., Qin, D.. Plattner, G.-K., Tignor, M., Allen, S.K., Boschung, J., Nauels, A., Xia, Y., Bex , V., and Midgley, P. M. (eds.)], Cambridge University Press, Cambridge, United Kingdom and New York, NY, USA, 2013.
Jassal, R. S., Black, T. A., Drewitt, G. B., Novak, M. D., Gaumont-Guay, D., and Nesic, Z.: A model of the production and transport of CO_2 in soil: predicting soil CO_2 concentrations and CO_2 efflux from a forest floor, Agricultural and Forest Meteorology, 124, 3, 219-236, 2004.

Jassal, R., Black, A., Novak, M., Morgenstern, K., Nesic, Z., and Gaumont-Guay, D.: Relationship between soil CO_2 concentrations and forest-floor CO_2 effluxes, Agricultural and Forest Meteorology, 130, 3, 176-192, 2005.

Jongen, M., Pereira, J. S., Aires, L. M. I., & Pio, C. A. (2011). The effects of drought and timing of precipitation on the inter-annual variation in ecosystem-atmosphere exchange in a Mediterranean grassland. *Agricultural and forest meteorology*, *151*(5), 595-606.

Kang, S., Kim, S., Oh, S., and Lee, D.: Predicting spatial and temporal patterns of soil temperature based on topography, surface covered and air temperature, Forest Ecology and Management, 136, 1-3, 173-184, 2000.

Kang, S., Doh, S., Lee, D., Lee, D., Jin, V. L. and Kimball, J. S.: Topographic and climatic controls on soil respiration in six temperate mixed-hardwood forest slopes, Korea, Global Change Biology, 9, 1427-1437, 2003.

Karhu, K., Auffret, M. D., Dungait, J. A., Hopkins, D. W., Prosser, J. I., Singh, B. K., Subke, J-A., Wookey, P. A., Ågren, G. I., Sebastià, M-T., Gouriveau, F., Bergkvist, G., Meir, P., Nottingham, A. T., Salinas, N., and Hartley, I. P.: Temperature sensitivity of soil respiration rates enhanced by microbial community response, Nature, 513, 7516, 81-84, 2014.

Kelleners, T.J., Paige, G. B. and Gray, S. T.: Measurement of the ielectric properties of Wyoming soils using electromagnetic sensors,Soil Science Society of America Journal, 73, 1626-1637, 2009.
Kindler, R., Siemens, J. A. N., Kaiser, K., Walmsley, D. C., Bernhofer, C., Buchmann, N., Cellier, P., Eugster, W., Gleixner, G., Grũnwald, T., Heim, A., Ibrom, A., Jones, S. K., Jones, M., Klumpp, K., Kutsch, W., Larsen, K. S., Lehuger, S., Loubet, B., McKenzie, R., Moors, E., Osborne, B., Pilegaard, K., Rebmann, C., Saunders, M., Schmidt, M. W. I., Schrumpf, M., Seyfferth, J., Skiba, U., Soussana, J-F., Sutton, M. A., Tefs, C., Vowincke, B., Zeeman, M. J., and Kaupenjohann, M.: Dissolved carbon leaching from soil is a crucial component of the net ecosystem carbon balance, Global Change Biology, 17, 2, 1167-1185, 2011.

Li, W., Li, L., Fu, R., Deng, Y., and Wang, H.: Changes to the North Atlantic subtropical high and its role in the intensification of summer rainfall variability in the southeastern United States, Journal of Climate, 24, 5, 1499-1506, 2011.

Luan, J., Liu, S., Wang, J., Zhu, X., and Shi, Z.: Rhizospheric and heterotrophic respiration of a warm-temperate oak chronosequence in China, Soil Biology and Biochemistry, *43*, 3, 503-512, 2011.

Matchen, D. L.: Geology of the Canaan Valley region, Geological Society of America, Southeastern Section, 47th annual meeting Charleston, West Virginia, 50, 1998.

McGlynn, B. L., and McDonnell, J. J.: Role of discrete landscape units in controlling catchment dissolved organic carbon dynamics, Water Resources Research, 39, 4, 2003.

McGlynn, B. L., and Seibert, J.: Distributed assessment of contributing area and riparian buffering along stream networks, Water resources research, 39, 4, 2003.

Metcalfe, D. B., Fisher, R. A., & Wardle, D. A.: Plant communities as drivers of soil respiration: pathways, mechanisms, and significance for global change, Biogeosciences, 8,8, 2047-2061, 2011.

Murphy, K. L., Klopatek, J. M., and Klopatek, C. C.: The effects of litter quality and climate on decomposition along an elevational gradient. Ecological Applications, 8, 4, 1061-1071, 1998.

Nilsen, E. T., Clinton, B. D., Lei, T. T., Miller, O. K., Semones, S. W., and Walker, J. F.: Does Rhododendron maximum L.(Ericaceae) reduce the availability of resources above and belowground for canopy tree seedlings?. The American Midland Naturalist, 145, 2, 325-343, 2001.

Noormets, A., Gavaz, M. J., Mcnulty, S. G., Domec, J., Sun, G., King, J. S. and Chen, J.: Response of carbon fluxes to drought in a coastal plain loblolly pine forest, Global Change Biology, 16, 272–287, doi: 10.1111/j.1365-2486.2009.01928.x, 2010.

Nowacki, G. J., and Abrams, M. D.: The demise of fire and "Mesophication" of forests in the eastern United States, BioScience, 58, 2, 123-138, 2008.

Oberbauer, S. F., Gillespie, C. T., Cheng, W., Gebauer, R., Serra, A. S., and Tenhunen, J. D.: Environmental effects on CO_2 efflux from riparian tundra in the northern foothills of the Brooks Range, Alaska, USA, Oecologia, 92, 4, 568-577, 1992.

Pacific, V. J., McGlynn, B. L., Riveros-Iregui, D., Welsch, D. L. and Epstein, H. E.: Variability in soil respiration across riparian-hillslope transitions, Biogeochemistry, 91(1), 51–70, doi:10.1007/s10533-008-9258-8, 2008.

Pacific, V. J., McGlynn, B. L., Riveros-Iregui, D. a., Epstein, H. E. and Welsch, D. L.: Differential soil respiration responses to changing hydrologic regimes, Water Resources Research, 45, 7, W07201, doi:10.1029/2009WR007721, 2009.

Riveros-Iregui, D. A., McGlynn, B. L., Emanuel, R. E., and Epstein, H. E.: Complex terrain leads to bidirectional responses of soil respiration to inter-annual water availability, Global Change Biology, 18, 2, 749-756, 2012.

Pan, Y., Birdsey, R. A., Fang, J., Houghton, R., Kauppi, P. E., Kurz, W. A., Phillips, O. L., Shvidenko, A., Lewis, S. L., Canadell, J. G., Ciais, P., Jackson, R. B., Pacala, S. W., McGuire, A. D., Piao, S., Rautianinen, A., Sitch, S. and Hayes, D.: A large and persistent carbon sink in the world's forests. Science, 333, 988-993, 2011.

Phillips, D. L., and Murdy, W. H.: Notes: Effects of Rhododendron (Rhododendron maximum L.) on regeneration of Southern Appalachian Hardwoods, Forest Science, 31, 1, 226-233, 1985.
Chemidlin Prévost-Bouré, N., Soudani, K., Damesin, C., Berveiller, D., Lata, J. C., and Dufrêne, E.: Increase in aboveground fresh litter quantity over-stimulates soil respiration in a temperate deciduous forest, Applied Soil Ecology, 46, 1 , 26-34, 2010.

PRISM Climate Group, Oregon State University, http://prism.oregonstate.edu, created 4 Feb 2004

R Core Team (2013). R: A language and environment for statistical computing. R Foundation for Statistical Computing, Vienna, Austria, http://www.R-project.org/.

Raich, J. W. and Potter, C. S.: Global patterns of carbon dioxide emissions from soils, Global Biogeochemical Cycles, 9, 23-36, 1995.

Raich, J. W. and Schlesinger, W. H.: The global carbon dioxide flux in soil respiration and its relationship to vegetation and climate, Tellus B, 44, 81-99, 1992.

Raich, J. W., Potter, C. S., and Bhagawati, D.:Interannual variability in global soil respiration, 1980–94, Global Change Biology, 8, 8, 800-812, 2002.

Reichstein, M., Bahn, M., Ciais, P., Frank, D., Mahecha, M. D., Seneviratne, S. I., Zscheischler, J., Beer, C., Buchmann, N., Frank, D. C., Paple, D., Rammig, A., Smith, P., Thonicke, K., van der Velde, M., Vicca, S., Walz, A., and Wattenbach, M.: Climate extremes and the carbon cycle, Nature, 500, 7462, 287-295, 2013.

Riveros-Iregui, D. A., McGlynn, B. L., Epstein, H. E., and Welsch, D. L.: Interpretation and evaluation of combined measurement techniques for soil CO_2 efflux: Discrete surface and continuous soil CO_2 concentration probes, Journal of Geophysical Research, 113, G04027, doi: 10.1029/2008JG000811, 2008.

Riveros-Iregui, D. A., and McGlynn, B. L.: Landscape structure control on soil CO_2 efflux variability in complex terrain: Scaling from point observations to watershed scale fluxes. Journal of Geophysical Research: Biogeosciences, 114, G2, 2005–2012, 2009.

Riveros-Iregui, D., McGlynn, B. L., Marshall, L., Welsch, D. L., Emanuel, R. E., and Epstein, H. E.: A watershed-scale assessment of a process soil CO_2 production and efflux model, Wat. Res. Research, 47, W00J04, doi:10.1029/2010WR009941, 2011.

Riveros-Iregui, D. A., McGlynn, B. L., Emanuel, R. E., and Epstein, H. E.: Complex terrain leads to bidirectional responses of soil respiration to inter-annual water availability, Global Change Biology, 18, 2, 749-756, 2012.

Rollins, A. W., Adams, H. S., and Stephenson, S. L.: Changes in forest composition and structures across the red spruce-hardwood ecotone in the central Applachains, Castanea, 75, 3, 303-314, 2010.

Rose, C (2004) An Introduction to the Environmental Physics of Soil, Water and Watersheds. University of Cambridge Press. p.442.

Savage, K. E., and Davidson, E. A.: Interannual variation of soil respiration in two New England forests, Global Biogeochemical Cycles, 15, 2, 337-350, 2001.

Scanlon, D. and Moore, T.: Carbon dioxide production from peatland soil profiles: the influence of temperature, oxic/anoxic conditions and substrate, Soil Science, 165, 153-160, 2000.

Schimel, D. S.: Terrestrial ecosystems and the carbon cycle, Global Change Biology, 1, 77-91, 1995.

Schaufler, G., Kitzler, B., Schindlbacher, A., Skiba, U., Sutton, M. A., & Zechmeister-Boltenstern, S.: Greenhouse gas emissions from European soils under different land use: effects of soil moisture and temperature, European Journal of Soil Science, 61, 5, 683-696, 2010.

Schlesinger, W. H.: Carbon balance in terrestrial detritus, annual Review of Ecology and Systematics, 8, 51-81, 1977.

Schmidt, M. W., Torn, M. S., Abiven, S., Dittmar, T., Guggenberger, G., Janssens, I. A., Kleber, M., Kögel-Knabner, I., Lehmann, J., Manning, D. A. C., Nannipieri, P., Rasse, D. P., Weiner, S., and Trumbore, S. E.: Persistence of soil organic matter as an ecosystem property. Nature, 478, 7367, 49-56, 2011.

Schuur, E. A., and Matson, P. A.: Net primary productivity and nutrient cycling across a mesic to wet precipitation gradient in Hawaiian montane forest, Oecologia, 128, 3, 431-442, 2001.
Scott-Denton, L. E., Sparks, K. L., and Monson, R. K.: Spatial and temporal controls of soil respiration rate in a high-elevation, subalpine forest, Soil Biology and Biochemistry, 35, 4, 525-534, 2003.

Sjögersten, S., van der Wal, R., and Woodin, S. J.: Small-scale hydrological variation determines landscape CO_2 fluxes in the high Arctic, Biogeochemistry, 80, 3, 205-216, 2006.

Trumbore, S.: Carbon respired by terrestrial ecosystems–recent progress and challenges, Global Change Biology, 12, 141-153, 2006.

University of Utah, National Weather Service Forecast Office in Salt Lake City, Dataset Title: Utah MesoWest Weather Data from the University of Utah and the National Weather Service Forecast Office in Salt Lake City. <http://www.met.utah.edu/mesowest>.

Van Gestel, M., Merckx, R., and Vlassak, K.: Microbial biomass responses to soil drying and rewetting: the fate of fast-and slow-growing microorganisms in soils from different climates, Soil Biology and Biochemistry, 25, 1, 109-123, 1993.

Vargas, R., Hasselquist, N., Allen, E. B. and Allen, M. F.: Effects of a hurricane disturbance on aboveground forest structure, arbuscular mycorrhizae and belowground carbon in a restored tropical forest, Ecosystems, 13, 118–128, doi:10.1007/s10021-009-9305-x, 2010.

Vesterdal, L., Elberling, B., Christiansen, J. R., Callesen, I., and Schmidt, I. K.: Soil respiration and rates of soil carbon turnover differ among six common European tree species, Forest Ecology and Management, 264, 185-196, 2012.

Wu, Z., Dijkstra, P., Koch, G. W., Penuelas, J., & Hungate, B. A.: Responses of terrestrial ecosystems to temperature and precipitation change: a meta-analysis of experimental manipulation, Global Change Biology, 17(2), 927-942, 2011.

Wu, W., Tang, X. P., Guo, N. J., Yang, C., Liu, H. B., and Shang, Y. F.: Spatiotemporal modeling of monthly soil temperature using artificial neural networks, Theoretical and applied climatology, 113, 3-4 481-494, 2013.

Wullschleger, S. D., Tschaplinski, T. J., and Norby, R. J.: Plant water relations at elevated CO_2–implications for water-limited environments, Plant, Cell & Environment, 25, 2, 319-331, 2002.

Wurzburger, N., and Hendrick, R. L.: Rhododendron thickets alter N cycling and soil extracellular enzyme activities in southern Appalachian hardwood forests, Pedobiologia, 50, 6, 563-576, 2007.

Xu, M. and Qi, Y.: Spatial and seasonal variations of Q_{10} determined by soil respiration measurements at a Sierra Nevadan forest, Global Biogeochemical Cycles, 15, 687-696, 2001.

Chapter Three: Nutrient cycling, litter decomposition, and the organic layer among varying vegetation cover classes along an elevation gradient in a West Virginia watershed

ABSTRACT

Though decomposition is controlled by climate and substrate quality at coarse spatial scales, at the watershed scale, microclimates mediated by forest structure and landscape position can influence decomposition rates and in turn affect nutrient cycling and the soil organic layer. To evaluate the effects of landscape position and vegetation heterogeneity on decomposition and soil nitrogen availability, a two-year litterbag study using yellow birch leaf litter was employed across the Weimer Run watershed from 2011 to 2013. Plots for litterbag placement were established among three elevation classes: LOW (975 m), MID (1050 m), and HIGH (1100 m). Within each elevation level, three different vegetation cover classes were also established: CANOPY, closed canopy forest; SHRUB, closed canopy with shrub cover; and OPEN, interior forest gap, for a total of 27 plots (3 elevation classes x 3 vegetation classes x 3 replicates each) across the watershed. Following collection, litter samples were analyzed for C, N, and lignin concentrations. Nitrogen availability within plot soils was measured using anion and cation exchange resin membrane probes. Initial litter decomposition varied by elevation, with greater rates of decomposition at locations lower in the watershed. Organic layer depth increased with increasing elevation. Soil nitrogen availability differed by vegetation cover, with differences in nitrogen more pronounced during the early growing season and largely driven by differences in nitrate (NO_3^-) beneath areas of canopy closure in the forest. Controls on decomposition and nitrogen cycling within the Weimer Run watershed varied spatially and were subject to complex interactions. This work suggests that landscape position and vegetation influence nitrogen

cycling, decomposition, and organic layer development within this watershed, but are not conclusive. Further efforts may be necessary to establish a better understanding.

INTRODUCTION

Decomposition is the integration of the chemical, physical, and biological processes involved in the breakdown of organic matter into stable, inorganic component forms (Berg and McClaugherty 2008) and recalcitrant, complex organics (Chapin et al. 2002). Decomposition is a key aspect of nutrient cycling (Vitousek, 2004) and global element cycles, particularly carbon and nitrogen (Olson, 1963; Raich and Schlesinger, 1992). At regional and global scales, decomposition is controlled by climate, and litter chemistry or substrate quality (Meetenmeyer, 1978; Aerts, 1997; Zhang et al. 2008; Silver and Miya, 2000), and at finer scales, influenced by soil fauna composition and abundance (Singh and Gupta, 1977), interactions among varying types of leaf litter (Hattenschwiler and Gasser, 2005) as well as forest structure and microclimate.

Forest microclimates are influenced by forest structure, heterogeneity, and fragmentation (Hastwell and Morris, 2013). The physical structure of plant communities can affect moisture and temperature regimes (Hastwell and Morris, 2013; Atkins et al. 2015) through effects of canopy-gap dynamics on wind, solar radiation, and rainfall interception and redirection (Belsky and Canham, 1994; Breshears, 2006). Increased fragmentation results in a large edge to core ratio, leading to greater edge effects on the forest—often resulting in higher temperatures and decreased soil moisture due to wind and solar exposure. The effects of forest structure and fragmentation on litter decomposition rates can be significant (Hastwell and Morris, 2012). Constraining the high uncertainties that result from the spatial and temporal variation in decomposition rates, particularly in eastern North American forests, could improve

understanding of the interactions in the relationships among decomposition dynamics, nutrient cycling, and environmental heterogeneities.

While litterfall amounts may decrease with increasing elevation, forest floor litter mass may increase due to slower turnover rates (Zhou et al. 2014). Elevation gradients often result in coniferous tree supplantation of deciduous trees at higher elevations (Reiners and Lang, 1987). The additive effects of the more recalcitrant nature of coniferous litter combined with decreased temperatures (Zhou et al. 2014) and precipitation at altitude may account for increased forest floor mass as a function of lowered decomposition rates. Shanks and Olson (1961) showed differences in first-year decomposition rates of leaf litter from five different species of deciduous trees along an elevation gradient in the southern Appalachians. Decomposition rates were faster at lower elevations and faster underneath deciduous trees. Dwyer and Merriam (1981) showed that fine-scale forest topography (< 0.5 m vertical variation) affects leaf litter decomposition, which is positively correlated with soil temperature along elevation gradients in sub-alpine forests.

There is varying evidence in the literature for what has been termed the "home-field advantage" (HFA)—an observation where litter of a certain plant species decomposes more rapidly beneath that plant species than others (Gholz et al. 2000; Ayres et al. 2009). The hypothesized mechanism for this is the adaptation and specialization of the decomposer community beneath that plant. However, this is not a uniform empirical observation (Prescott et al. 2000; Chapman and Koch, 2007). Generally, areas where HFA is more prevalent are those where one species is dominant. While the interactions of the contrasting substrate qualities of individual species across leaf litter matrices have been investigated, these interactions have only

been shown to have a pronounced effect on decomposition when the individual species substrate qualities and litter matrix quality are highly contrasting (Freschet et al. 2012). More plainly, if the quality of one species litter is significantly divergent from the average litter quality of the other species in an ecosystem, then species matrix interactions are seen (Veen et al. 2015).

Litterbag approaches are a popular method used to quantify decomposition rates and can be augmented by additional treatments. Landscape controls on decomposition may be examined by the use of common lignin and cellulose sources, allowing for quantification of the effects of site specific conditions within and across environmental heterogeneities. While the lignin:N ratio is a sound predictor of decomposition rates (Melillo et al. 1982; Chapin et al. 2002; Fioretto et al. 2003), it has also been hypothesized that lignin to cellulose ratios may be strongly indicative of litter decomposition rates (Herman et al. 2008).

Nitrogen cycling is an intrinsic component of litter decomposition influenced by vegetation cover and forest structure (Reich et al. 2001). Deciduous and evergreen overstory trees diverge in their nutrient and element cycling capacities and timescales (Day and Monk, 1977; Chastain et al. 2006), with deciduous trees exerting more influence on short and long time scales, and evergreen species at intermediate timescales—with marked intra-specific variance (Day and Monk, 1977). The heterogeneity and structure of a forest can exert landscape controls on nitrogen cycling. Nitrogen mineralization rates were found to be greater in closed canopy areas of mature, conifer forests than in open, forest gaps in the Upper Peninsula of Michigan (Schliemann and Bockheim, 2014). N mineralization can also vary seasonally, peaking during the growing season (Knoepp and Swank, 1998). There is also inter-annual variance in N

mineralization rates. Watersheds located in the Coweeta Hydrologic Laboratory, in the southern Appalachians, show evidence of inter-annual variance in N mineralization that has been attributed to differences in rainfall rather than temperature, with increases in N mineralization rates during years of higher rainfall (Knoepp and Swank, 1998). N mineralization rates also increase with elevation in the mountains of the southern Appalachians (Garten and Ven Miegroet, 1994), but above 700 m, there is high variance among areas of differing vegetation, with significantly higher N mineralization occurring in areas with no evergreen shrubs—indication that vegetation, specifically evergreen shrubs, can differentially affect N mineralization (Knoepp and Swank, 1998). The evergreen shrub layer of the southern and mid-Appalachians increases retention of N and slows N cycling in areas where shrubs are present—an effect estimated to peak at 30 years post-shrub stand establishment (Chastain et al. 2006).

Differences in N mineralization along elevation and vegetation gradients can be a function of the variance of soil temperature, substrate quality, and soil moisture (Powers, 1990). While the forests and watersheds of the southern Appalachians share many similarities with the mid-Appalachians, there are important, ecologically relevant differences. Mid-Appalachian forests are often far less botanically diverse. Due to their more northerly latitude, mid-Appalachian forests are subject to colder winter temperatures, contracted growing seasons, increased snowfall, and more persistent snow coverage. These ecosystem differences would be expected to impact nitrogen cycling.

Our understanding of the influence of the interactions between forest vegetation heterogeneity and elevation gradients on litter decomposition within cool, humid temperate watersheds is lacking. By discretizing the landscape within a watershed into both elevation and

vegetation cover classes, we can attempt to parse out the controls exerted on decomposition and N availability by environmental heterogeneities. By employing a combined approach using litterbags in a factorial design across elevation and vegetation gradients coupled with measures of nitrogen availability and a characterization of the organic layer, we seek to answer the following questions:

1) What are the effects of vegetation cover on litter decomposition, the soil organic layer, and N dynamics across an elevation gradient within a cool, humid watershed in West Virginia?

2) How does N availability vary among vegetation cover across an elevation gradient within a cool, humid watershed in West Virginia during the growing season?

METHODS

SITE DESCRIPTION

The study was conducted in the Weimer Run watershed (374 ha), located in the Little Canaan Wildlife Management Area near Davis, WV (39.1175, –79.4430). The watershed has an elevation gradient of 940 – 1175 m with mixed northern hardwood-coniferous forest cover (Fortney, 1975; Atkins et al. 2014). A prominent under-story vegetation layer exists in the watershed, populated by *Rhododendron maximum, Kalmia latifolia, Osmundastrum cinnamomeum*, and *Osmunda claytoniana* (Fortney, 1975). Mean annual rainfall is 1450 mm yr^{-1} (PRISM Climate Group). The mean daily maximum July temperature is 18.8 °C, and the mean daily maximum January temperature is -3.9 °C (NCDC, Station ID DAVIS 3 SE, Davis, WV).

VEGETATION AND ELEVATION CLASSES

Three elevation classes were established along the north-eastern aspect of the watershed to form an elevation gradient: LOW (975 m), MID (1050 m), and HIGH (1100 m). At each elevation level, three 2 x 2 m plots of three different vegetation classes were established—for a total of 27 plots across the entire watershed. The vegetation cover classes were defined as follows: CANOPY – closed canopy, forest interior with no shrub layer; SHRUB – closed canopy, forest interior, with dense shrub layer; OPEN – forest gap with no canopy closure, within the forest interior. Differences among vegetation classes were confirmed by measuring plant area index (PAI) for each plot in June 2010 with a LAI-2000 Plant Canopy Analyzer (LI-COR Lincoln, Nebraska). PAI was strongly significantly different among vegetation cover types, with SHRUB plots exhibiting the greatest values, followed by CANOPY and OPEN plots respectively (Atkins et al. 2015).

LITTERBAG EXPERIMENT

To assess relative decomposition rates, five litterbags were placed within each plot. The litterbags were constructed using a fine mesh nylon with mesh openings of 0.92 mm^2 (0.96 mm x 0.96 mm; thickness of nylon = 0.1 mm). The edges of each bag were sealed using a ULINE H-163 Poly bag impulse heat sealer (U-Line; Pleasant Prairie, Wisconsin). The impulse sealer allows for a non-reactive, weatherproof seal. The finished size of each bag was approximately 15 cm x 15 cm.

Each litter bag was filled with a common, senescent litter (*B. alleghaniensis*). Litter for each elevation level was collected at that level (i.e. litter used in litterbags at the LOW elevation level came from trees located near those plots, etc.) Litter was collected during September, 2011, in litter traps suspended beneath trees. All senescent litter used was <7 days old, as traps were placed during the second week of September, 2011, and all litter was collected the

following week. Senescent litter was taken to the lab and sorted to ensure that only intact *B. alleghaniensis* leaves were used. Leaves were oven-dried for 72 hours at 60 °C. Each litterbag was filled with 2 ±0.05 g of oven-dried litter, then individually weighed and tagged with a 1" x 3-1/2" (2.54 x 8.89 cm) all-weather, aluminum PermaTag (Forestry Suppliers; Jackson, Mississippi). Each tag was marked with a unique identifying number corresponding to plot elevation level and vegetation cover class.

Litterbags were attached to an aluminum wire via openings in the PermaTags on each bag. The aluminum wire was then staked to the ground using landscape pins (Forestry Suppliers; Jackson, Mississippi). Litterbags were arranged in a circle to make sure that no bag was touching another and were placed on the soil surface, fully inside the assigned plot. Five litterbags were placed at each plot on October 1, 2011. The retrieval schedule was as follows: 1) November, 2011 (1 month); 2) June, 2012 (6 months); 3) October, 2012 (12 months); 4) June, 2013 (18 months); 5) October, 2013 (24 months).

LEAF LIGNIN, CARBON, AND NITROGEN

Lignin concentrations for leaf litter following retrieval were determined using an acetyl-bromide based multi-step lignin digestion assay with spectrophotometry (Foster et al. 2010a; Foster et al. 2010b). Total leaf carbon and nitrogen were assessed using a NA 2500 Elemental Analyzer (CE Instruments; Wigan, United Kingdom).

NITROGEN AVAILABILITY

Nitrogen supply rates were estimated in the field using plant root simulator probes (PRS probes; Western Ag. Innovations, Canada) incubated in the soils from 0 – 10 cm depth for three deployments in 2010: 1) between June 14 and July 14 (30 days); 2) August 1 – September 1 (30 days); 3) September 1 to October 6 (36 days). PRS probes were placed in the corner of each plot

per the manufacturer's specifications. Following incubations, they were collected, refrigerated, rinsed with deionized water and shipped to Western Ag Innovations for analyses of NH_4^+ and NO_3^-.

SOILS AND THE ORGANIC LAYER

Organic layer depth for each plot was determined by measurement with a ruler at three points within the plot and then averaged for a plot mean organic layer depth. Soil samples of the organic layer were then taken and analyzed for total soil carbon and nitrogen using a NA 2500 elemental analyzer (CE instruments; Wigan, United Kingdom), after being oven-dried and sieved to less than 2 mm with gravel and roots removed.

DATA ANALYSIS

Relative decomposition rates were calculated using the single-pool negative exponential model:

$$M_t = M_0 \, e^{-kt}$$

Where M_t is the mass of litter at time t, M_0 is the initial mass of litter, e is the base of the natural logarithm, and k is the decomposition constant. Decomposition rates were not normally distributed and were compared using a Kruskal-Wallis test to compare by elevation and vegetation in R 3.2.2 (R Core Team, 2015).

Soil nutrient availability was compared across elevation, vegetation, and elevation by vegetation within each time period using Analysis of Variance (ANOVA) in R 3.2.2. Differences among time periods were not reasonably comparable based on the method used to calculate NH_4^+ and NO_3^- by Western Ag.

Differences in organic layer depth (cm), organic layer C (%), organic layer N (%), and organic layer C:N were evaluated using ANOVA in R 3.2.2. Additionally, organic layer C, organic

layer N, and organic layer C:N were further evaluated using Analysis of Covariance (ANCOVA) in R 3.2.2 with organic layer depth as a dependent variable.

RESULTS

LITTER BAG EXPERIMENT

Measurements of mass remaining following decomposition from litter bags were consistent with expectations with greater rates of decomposition at landscape positions lower in the watershed and total mass remaining values after two years increasing with elevation (LOW 41.1%, MID 44.4%, and HIGH 47.8%). Results from beneath vegetation cover classes after two years were also as expected, with OPEN sites having the least total mass remaining (41.7%), followed by CANOPY sites (44.2%), and SHRUB sites (47.7%) (Figs. 3.1 and 3.2).

Relative decomposition rates (*k*) and total mass remaining (%) among elevations were influenced strongly by season as represented by collection period (Table 1), with significant differences among elevation classes after the first collection (November, 2011; $p = 0.02$) and the third collection (October, 2012; $p = 0.02$). Both mass loss and *k* show nearly significant differences for both collection period 4 (June, 2013; $p = 0.05$) and period 5 (October, 2013; $p = 0.05$). Period 2 (June, 2012) had the highest *p*-values with regard to elevation. This is of note because the winter of 2011-2012 had below-average snow fall, with much of the watershed free of snow for the entire winter and soil temperatures well below the average. In comparison, the winter of 2012-2013, which corresponds with collection periods 4 and 5, was a year of average to above-average snow fall for the region and therefore warmer soil temperatures.

No statistically significant differences in either mass loss or *k* on a per collection basis for vegetation cover are present for the entire length of the experiment, with *k* calculated by the traditional, single-pool, negative exponential model (Table 3.1). Overall decomposition rates are

negatively correlated with final leaf N content (r = -0.36; Fig. 3.3). Lignin to N ratio (Lignin:N) was a poor predictor of decomposition rates.

NITROGEN AVAILABILITY

Total soil nitrogen availability during 2010, measured as NO_3^- and NH_4^+, was greater in plots beneath the forest canopy than other plots, an effect more pronounced at positions lower in the watershed. Total soil nitrogen is generally lower in August than either June/July or September. While some plots show greater N in September, accurate comparisons between September and other months cannot be made due to the discrepancy in incubation time. However, by comparing plots within months, inferences can be made. Two-way ANOVA results comparing total N, NO_3^-, and NH_4^+ with respect to elevation, vegetation, and elevation x vegetation for June show differences in total inorganic N by vegetation cover (F = 3.618 p = 0.047), a pattern likely driven by statistically significant differences in NO_3^- with greater NO_3^- availability in plots beneath the forest canopy (F = 4.293; p = 0.029) than other plots. No other significant relationships or differences were found in any other month.

ORGANIC LAYER

Two-way ANOVA results of organic layer depth show no differences among elevation and vegetation cover classes. Organic layer C (%) does differ by vegetation (F = 3.883; p = 0.043), with shrub plots having significantly greater organic soil C (%). This in turn drives up the C:N ratios in shrub plot soils (F = 7.029; p = 0.007).

DISCUSSION

Initial decomposition of birch litter is most impacted by elevation, with the greatest rates of decomposition found in open areas at lower elevations in the watershed. Open forest gaps, particularly at points lower in this watershed, tend to have greater light exposure, higher soil

temperatures, and lower soil moisture (Atkins et al. 2015). Given these environmental conditions, these results are expected. After one year of decomposition, similar significant results are seen (Table 3.1).

Collection two, taken eight months after deployment, following the winter of 2011-12, is an interesting anomaly in the findings. Decomposition rates following every other collection period show significant or nearly-significant differences by elevation, yet the differences were less clear during this period (November 2011 – June 2012). Snowfall during this winter totaled 2984 mm compared to the following winter (2012-2013) where snowfall totaled 5684 mm. Decreased snowfall results in a spotty, underdeveloped snow pack that can result in more prevalent and deeper soil freezing. Soils beneath a well-developed snow pack remain at or above freezing during the course of the winter, while soils without snow pack are exposed to freezing temperatures that retard decomposition. During the winter of 2011-2012, 65.9% of the time between October 1 to May 31, snow depth was recorded at 0, but only 43.2% of the time during the winter of 2012-2013 was snow depth recorded at 0. Decreased snow fall results in an absent or undeveloped snow pack and could slow decomposition and minimize altitudinal effects otherwise seen across this watershed. It is necessary to consider the carbon cycling and climate implications of altered snow regimes as changing patterns in snowfall and inter-annual climatic variability are affect water cycling. The movement of carbon and nutrients such as nitrogen are coupled to the water cycle, with potential ecosystem cascades, if fundamental changes occur to the system.

Differences in decomposition rates by vegetation cover classes may not be evident for several reasons. There may be fine-scale, localized differences in the microbial communities to

which the lack of differences could be attributed. There is perhaps variation in microbial composition and biomass among vegetation cover classes, with communities beneath shrubs diverging from those in open areas or beneath the forest canopy. By using yellow birch as a common litter type among all plots, "home-field advantage" (HFA), the concept that litter decomposes more rapidly beneath the plant from which it comes, rather than a different species (Gholz et al. 2000; Ayres et al. 2009) may be another possible explanation. HFA could also explain possible differences in microbial community composition, if in fact there is wide variation. However, HFA should be more pronounced in lower quality litter or litter containing difficult to decompose, more highly recalcitrant or even toxic compounds (Ayres et al. 2009). There is also the possibility that the relative high quality of yellow birch litter (initial senescent yellow birch litter: N% = 2.4; C% = 52.1; C:N = 21.7) acts as a top-down control on decomposition whereby yellow birch litter decomposes readily despite bottom-up controls from differences in the microbial communities and microclimates facilitated by the varying vegetation classes with in this study.

Elevated N may be observed in leaf litter over the course of decomposition, if this is a primarily fungal dominated system, as soil fungi have lower nutrient demands and typically higher C:N ratios than soil bacteria that leads to slower immobilization of N over the course of decomposition (Strickland and Rousk, 2010). However, the C:N ratio of our leaf litter remains rather low as well, below the threshold for mineralization (~25:1). The ratio of fungal to bacterial dominance is expected to decrease in areas of high N deposition or across increasing depositional gradients as increased N deposition decreases fungal abundance (Lilleskov et al. 2001; Strickland and Rousk, 2010). The Weimer Run watershed is located in an area of West

Virginia that receives high rates of both nitrate (12.09 kg ha^{-1} 2010-2012 mean) and ammonium deposition (3.11 kg ha^{-1} 2010-2012 mean) (NADP; Station WV18, Parsons, WV). However, the soils within the Weimer Run watershed are very acidic (below pH 4.3) and very wet (Atkins et al. 2015), conditions that do favor fungal rather bacterial abundance (Rousk et al. 2009). However, given these caveats, it is possible that much of the effects of soil pH and nutrient addition examined in studies writ large are masked by methodologies that cannot accurately and conclusively determine fungal abundance (Strickland and Rousk, 2010). Further study, both broadly and within this watershed, would be needed to examine soil fungal and bacterial groups explicitly in order to tease out both their differences in composition and abundance along with their controls on decomposition.

Nutrient availability, as assessed by Western Ag PRS probes, varies with vegetation, with more available soil N in areas beneath the forest canopy, early in the growing season (June). This pattern is driven by greater availability of NO_3^- which implies greater rates of nitrification in those areas or low NO_3^- losses, or lower NO_3^- uptake by vegetation. A comparison of the NH_4^+ to NO_3^- ratio by vegetation shows that more NO_3^- beneath shrubs and forest canopy areas is available relative to NH_4^+, implying greater rates of nitrification (Fig. 3.5). However, the caveat should be made that direct rates of nitrification were not measured during this study. The environments beneath shrubs and canopy areas could be more conducive to nitrification, due to lower soil bulk density and higher soil porosity, than open areas of the forest, despite being cooler and wetter than open areas.

Organic layer depth is notably deeper beneath shrubs and at higher elevations. Deeper organic soils at elevation implies lower rates of decomposition, which is in line with our findings.

Higher organic layer C:N ratios beneath shrubs, given their ericoid mycorrhizal associations, could lend credence to the idea of greater fungal dominance within the watershed. Conversely, nitrogen availability data coupled with implied spatial dynamics of nitrification might contradict these assertions. However, this is a very wet watershed, and lateral transfers and flows that distribute inorganic N and other nutrients more evenly are likely to be important, yet were not specifically assessed.

Moving forward, examining the spatial distribution of fungal and bacterial functional groups in relation to landscape position and vegetation could further elucidate the controls on decomposition, organic layer dynamics, and nutrient cycling in this watershed. Landscape position should be considered not only as elevation, but along determined flow paths within the watershed that could be defined via geospatial techniques (Seibert and McGlynn, 2007).

CONCLUSIONS

By employing a litterbag study using a common leaf litter (yellow birch), this study was able to show that initial decomposition of leaf litter varies with elevation, with greater rates of decomposition at locations lower in the watershed. Organic layer depth also increases with increasing elevation, which agrees with observed lower rates of decomposition at higher elevations. Organic layer C:N ratios are higher in plots beneath shrubs, at higher points in the watershed. Nitrogen availability, as measured using WesternAg PRS probes, differs seasonally and by vegetation cover. However, there are no observed differences in decomposition rates by vegetation cover class either within or among elevation classes considered in this study. Both landscape position and vegetation influence decomposition, nutrient cycling, and organic layer development within this watershed, yet these relationships and controls are complex and further work is necessary to understand the interactions within this system.

TABLES AND FIGURES

Table 3.1. Kruskal-Wallis table of significance values (*p* – values) for mass loss (%) and decomposition rate (*k)* per collection period. (*) indicates statistically significant results.

	Mass Loss (%)	
COLLECTION	VEGETATION	ELEVATION
1 Month	0.40	0.02*
8 Months	0.67	0.32
12 Months	0.68	0.02*
18 Months	0.20	0.05
24 Months	0.41	0.05

Table 3.2. Analysis of Covariance (ANCOVA) results of organic layer C, N, and C:N. Organic layer depth (cm) was used as the covariate. (*) indicates statistically significant results.

ANCOVA Results		
Organic Layer C	F	*p*
Organic Layer Depth	0.49	0.491
ELEV	0.56	0.584
VEG	4.57	0.029*
ELEV:VEG	0.30	0.869
Organic Layer N		
Organic Layer Depth	2.16	0.162
ELEV	0.56	0.581
VEG	3.36	0.064
ELEV:VEG	0.74	0.579
Organic Layer C:N		
Organic Layer Depth	0.04	0.841
ELEV	0.93	0.415
VEG	6.87	0.008*
ELEV:VEG	0.86	0.507

Table 3.3. Analysis of Variance (ANOVA) results of nitrogen availability from Western Ag PRS probes. Collected during the summer of 2010. (*) indicates statistically significant results.

	Jun. (30 days)		Aug. (30 days)		Sept. (30 days)	
	F	*p*	*F*	*p*	*F*	*p*
Total N						
ELEV	13.57	0.286	0.193	0.827	0.789	0.475
VEG	36.18	0.047*	1.447	0.271	1.609	0.237
ELEV:VEG	0.953	0.953	0.938	0.472	1.195	0.359
NO_3^-						
ELEV	0.271	0.765	2.006	0.174	0.467	0.637
VEG	4.293	0.029*	2.586	0.113	1.444	0.271
ELEV:VEG	0.742	0.576	1.643	0.223	1.401	0.288
NH_4^+						
ELEV	2.467	0.113	0.208	0.815	0.818	0.463
VEG	2.008	0.163	0.869	0.442	1.729	0.216
ELEV:VEG	0.109	0.978	0.962	0.461	1.449	0.274

Table 3.4 Western Ag PRS-Probe data by elevation and vegetation class combination with collection time and incubation period indicated. Units are in μg 10 cm^{-2} period of $incubation^{-1}$.

ELEVATION	VEGETATION	INCUBATION PERIOD	†Total N	†NH_4^+	†NO_3^-
HIGH	CANOPY	JUNE (30 days)	60.1	38.3	21.8
HIGH	OPEN	JUNE (30 days)	30.3	25.1	5.2
HIGH	SHRUB	JUNE (30 days)	40.5	30.8	9.7
LOW	CANOPY	JUNE (30 days)	83.9	68.4	15.5
LOW	OPEN	JUNE (30 days)	48.4	42.4	6.0
LOW	SHRUB	JUNE (30 days)	54.1	47.3	6.8
MID	CANOPY	JUNE (30 days)	59.5	40.7	18.9
MID	OPEN	JUNE (30 days)	32.7	25.1	7.5
MID	SHRUB	JUNE (30 days)	35.4	25.5	9.9
HIGH	CANOPY	AUGUST (30 days)	31.3	17.1	14.2
HIGH	OPEN	AUGUST (30 days)	45.6	35.1	10.5
HIGH	SHRUB	AUGUST (30 days)	26.0	17.3	8.7
LOW	CANOPY	AUGUST (30 days)	48.6	40.5	8.1
LOW	OPEN	AUGUST (30 days)	21.9	19.9	2.0
LOW	SHRUB	AUGUST (30 days)	29.1	24.2	4.9
MID	CANOPY	AUGUST (30 days)	52.7	46.0	6.7
MID	OPEN	AUGUST (30 days)	29.1	24.7	4.4
MID	SHRUB	AUGUST (30 days)	26.8	17.3	9.5
HIGH	CANOPY	SEPTEMBER (36 days)	45.5	34.5	11.0
HIGH	OPEN	SEPTEMBER (36 days)	46.9	39.4	7.5
HIGH	SHRUB	SEPTEMBER (36 days)	26.3	20.7	5.7
LOW	CANOPY	SEPTEMBER (36 days)	86.3	74.0	12.3
LOW	OPEN	SEPTEMBER (36 days)	34.3	29.2	5.1
LOW	SHRUB	SEPTEMBER (36 days)	34.6	26.3	8.3
MID	CANOPY	SEPTEMBER (36 days)	24.9	21.2	3.7
MID	OPEN	SEPTEMBER (36 days)	30.3	25.5	4.8
MID	SHRUB	SEPTEMBER (36 days)	30.9	26.9	4.0

†Units are in μg 10 cm^{-2} period of $incubation^{-1}$

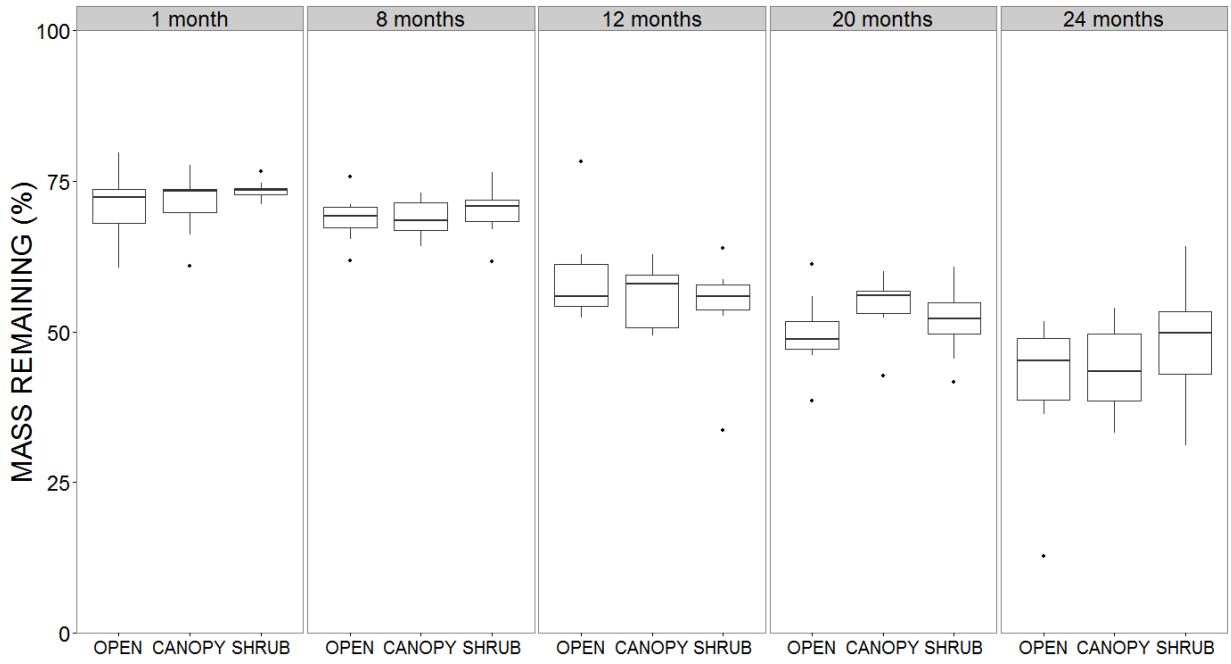

Figure 3.1. Leaf litter mass remaining by collection period for each vegetation class (OPEN, CANOPY, SHRUB).

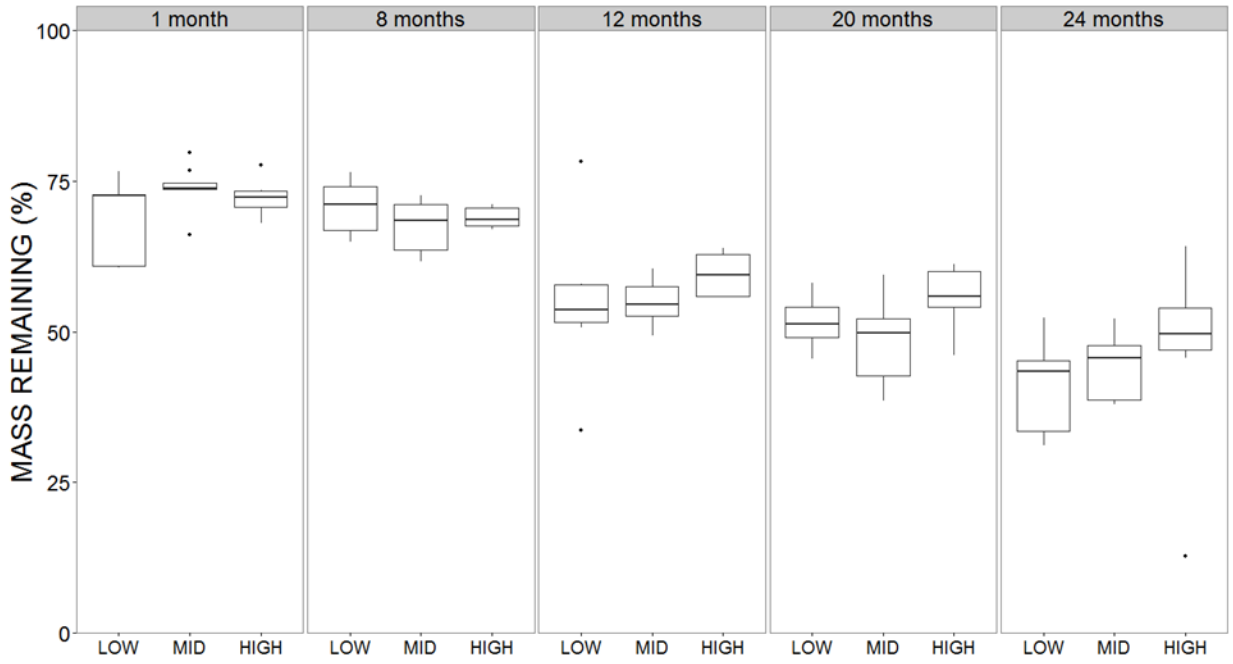

Figure 3.2. Leaf litter mass remaining by collection period for each elevation class (LOW, MID, HIGH).

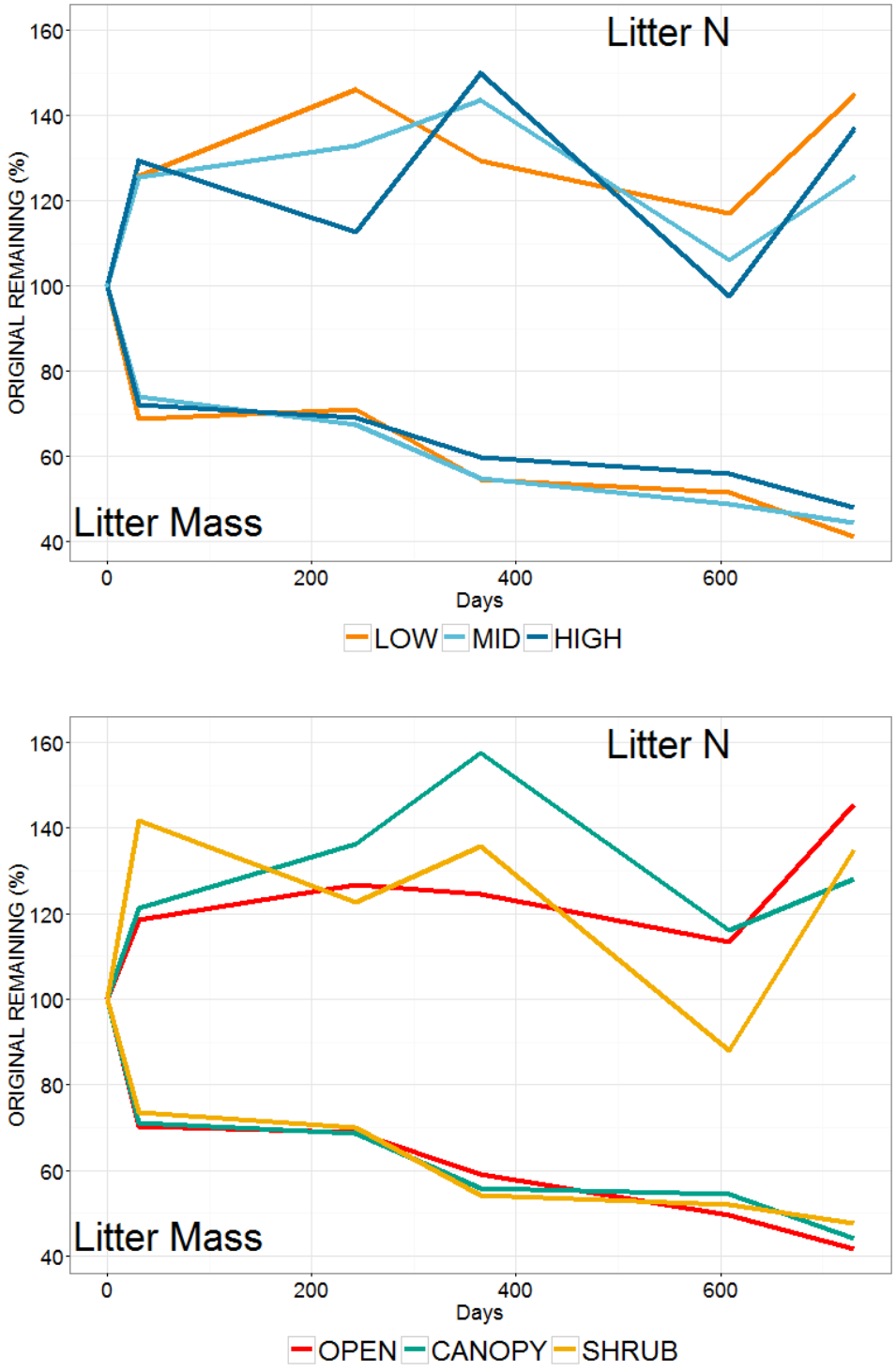

Figure 3.3. Litter mass remaining (%) and litter nitrogen (as % of initial) by elevation class (top) and vegetation class (bottom).

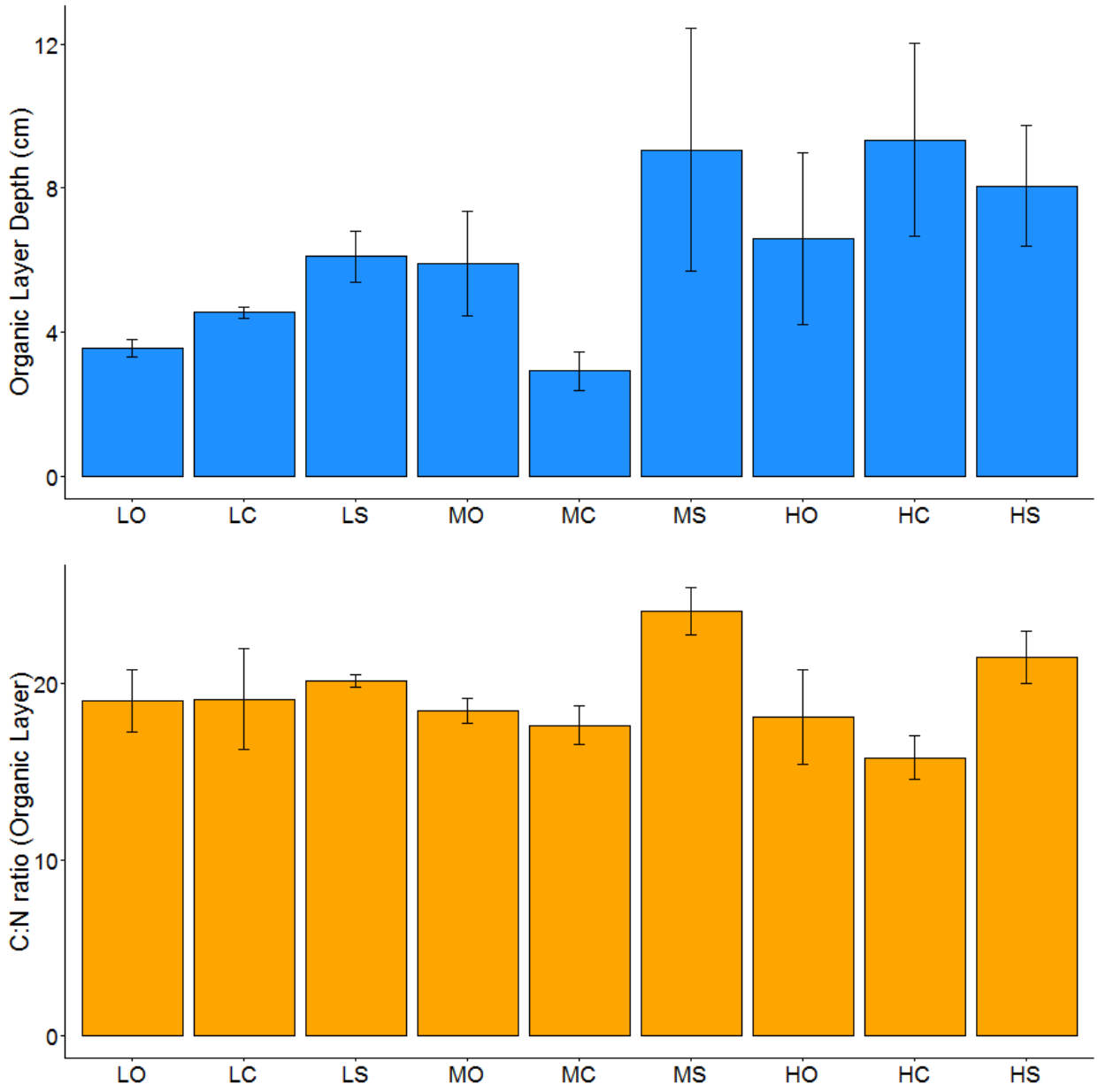

Figure 3.5. Organic layer depth (top) and organic layer C:N (bottom) by elevation and vegetation plot combination (H = High, M = Mid, L = Low, C = Canopy, S = Shrub, O = Open)

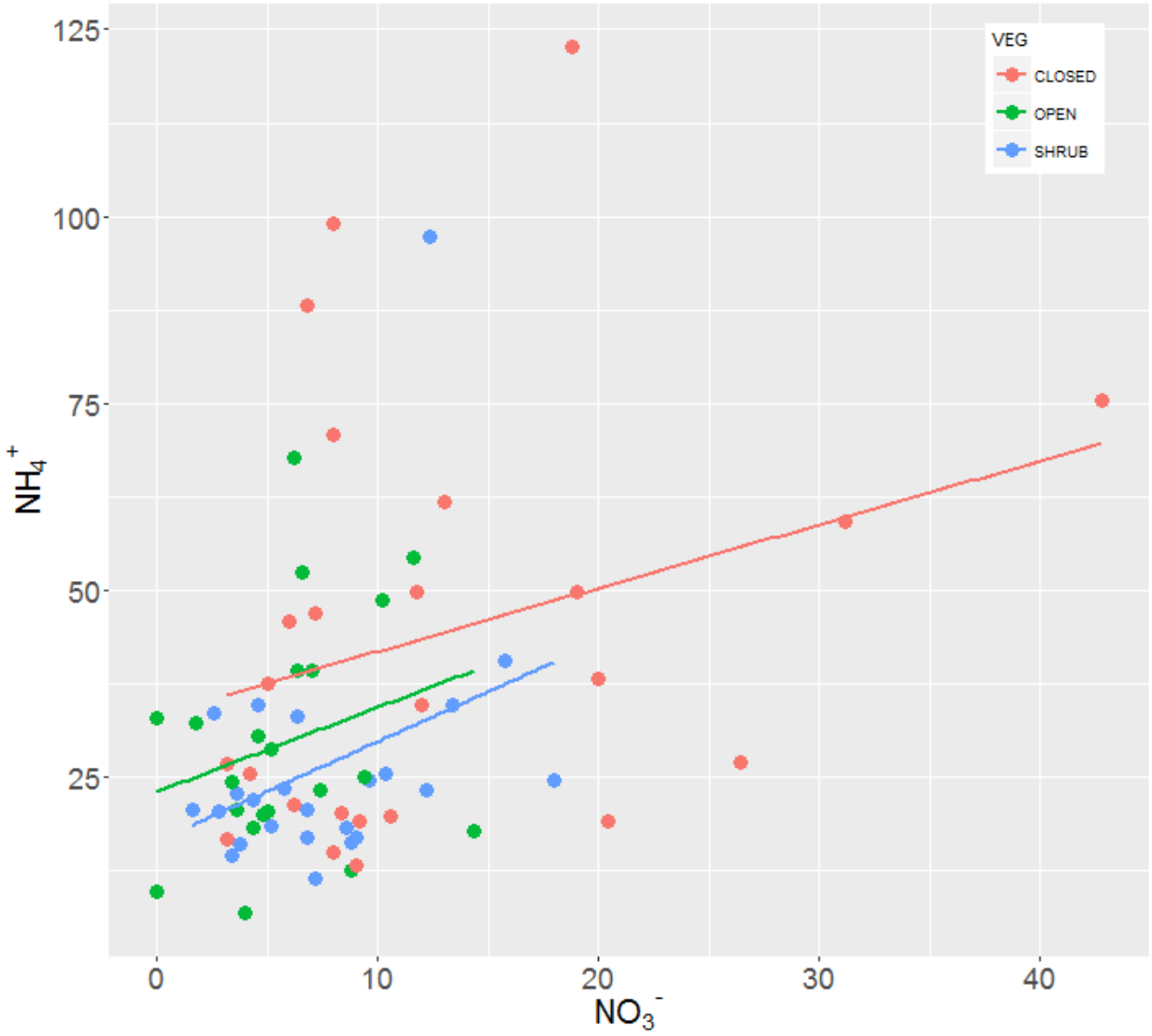

Figure 3.6 Ammonium (NH_4^+) against nitrate (NO_3^-) taken from Western Ag PRS probe data by vegetation class. Lines indicate correlations within vegetation class.

REFERENCES

Aerts, R. (1997). Nitrogen partitioning between resorption and decomposition pathways: a trade-off between nitrogen use efficiency and litter decomposibility?. Oikos, 603-606.

Atkins, J. W., Epstein, H. E., & Welsch, D. L. (2015). Vegetation and elevation influence the timing and magnitude of soil CO2 efflux in a humid, topographically complex watershed. Biogeosciences, 12(10), 2975-2994.

Austin, A. T., & Ballaré, C. L. (2010). Dual role of lignin in plant litter decomposition in terrestrial ecosystems. Proceedings of the National Academy of Sciences, 107(10), 4618-4622.

Ayres, E., Steltzer, H., Simmons, B. L., Simpson, R. T., Steinweg, J. M., Wallenstein, M. D., ... & Wall, D. H. (2009). Home-field advantage accelerates leaf litter decomposition in forests. Soil Biology and Biochemistry, 41(3), 606-610.

Belsky, A. J., & Canham, C. D. (1994). Forest gaps and isolated savanna trees. BioScience, 77-84.

Berg, B., & McClaugherty, C. (2008). Plant litter. Decomposition, humus formation, carbon sequestration. 2nd Ed Springer.

Bothwell L, Selmants PC, Giardina CP, Litton CM. 2014. Leaf litter decomposition rates increase with rising mean annual temperature in Hawaiian tropical montane wet forests. PeerJ

Breshears, D. D. (2006). The grassland-forest continuum: trends in ecosystem properties for woody plant mosaics?. Frontiers in Ecology and the Environment, 4(2), 96-104.

Chapin, F. S., Matson PA, Mooney H A. (2002). Principles of terrestrial ecosystem ecology.

Chapman, S. K., & Koch, G. W. (2007). What type of diversity yields synergy during mixed litter decomposition in a natural forest ecosystem?. Plant and Soil, 299(1-2), 153-162.

Chastain Jr., R.A., Currie, W.S., Townsend, P.A. (2006). Carbon sequestration and nutrient-cycling implications of the evergreen understory layer in Appalachian forests. Forest Ecology and Management, 231, 63-77.

Day Jr, F. P., & Monk, C. D. (1977). Seasonal nutrient dynamics in the vegetation on a southern Appalachian watershed. American Journal of Botany, 1126-1139.

Dwyer, L. M., & Merriam, G. (1981). Influence of topographic heterogeneity on deciduous litter decomposition. Oikos, 228-237.

Fioretto, A., Papa, S., & Fuggi, A. (2003). Litter-fall and litter decomposition in a low Mediterranean shrubland. Biology and Fertility of Soils, 39(1), 37-44.

Fortney, R. H.: (1975). The vegetation of Canaan Valley, West Virginia: a taxonomic and ecological study, Doctoral dissertation, West Virginia University, 235 pp.

Foster, C. E., Martin, T. M., Pauly, M. Comprehensive Compositional Analysis of Plant Cell Walls (Lignocellulosic biomass) Part I: Lignin. J. Vis. Exp. (37), e1745, doi:10.3791/1745 (2010).

Foster, C. E., Martin, T. M., Pauly, M. Comprehensive Compositional Analysis of Plant Cell Walls (Lignocellulosic biomass) Part II: Carbohydrates. J. Vis. Exp. (37), e1837, doi:10.3791/1837 (2010).

Freschet, G. T., Aerts, R., & Cornelissen, J. H. (2012). A plant economics spectrum of litter decomposability. Functional Ecology, 26(1), 56-65.

Garten Jr, C. T., & Miegroet, H. V. (1994). Relationships between soil nitrogen dynamics and natural 15N abundance in plant foliage from Great Smoky Mountains National Park. Canadian Journal of Forest Research, 24(8), 1636-1645.

Gholz, H. L., Wedin, D. A., Smitherman, S. M., Harmon, M. E., & Parton, W. J. (2000). Long-term dynamics of pine and hardwood litter in contrasting environments: toward a global model of decomposition. Global Change Biology, 6(7), 751-765.

Hättenschwiler, S., & Gasser, P. (2005). Soil animals alter plant litter diversity effects on decomposition. Proceedings of the National Academy of Sciences of the United States of America, 102(5), 1519-1524.

Hastwell, G. T., & Morris, E. C. (2013). Structural features of fragmented woodland communities affect leaf litter decomposition rates. Basic and Applied Ecology, 14(4), 298-308.

Herman, J., Moorhead, D., & Berg, B. (2008). The relationship between rates of lignin and cellulose decay in aboveground forest litter. Soil Biology and Biochemistry, 40(10), 2620-2626.

Knoepp, J. D., & Swank, W. T. (1998). Rates of nitrogen mineralization across an elevation and vegetation gradient in the southern Appalachians. Plant and Soil, 204(2), 235-241.

Lilleskov, E. A., Fahey, T. J., Horton, T. R., & Lovett, G. M. (2002). Belowground ectomycorrhizal fungal community change over a nitrogen deposition gradient in Alaska. *Ecology*, *83*(1), 104-115.

Martin Köchy and Scott D. Wilson 1997. Litter decomposition and nitrogen dynamics in aspent forest and a mixed-grass prairie. Ecology 78:732–739. http://dx.doi.org/10.1890/0012-9658(1997)078[0732:LDANDI]2.0.CO;2

Meentemeyer, V. (1978). Macroclimate and lignin control of litter decomposition rates. Ecology, 59(3), 465-472.

Melillo, J. M., Aber, J. D., Muratore, J. F. (1982) Nitrogen and Lignin Control of Hardwood Leaf Litter Decomposition Dynamics. Ecology 63:621–626. http://dx.doi.org/10.2307/1936780

Olson, J. S. (1963). Energy storage and the balance of producers and decomposers in ecological systems. Ecology, 44(2), 322-331.

Prescott, C. E., Zabek, L. M., Staley, C. L., & Kabzems, R. (2000). Decomposition of broadleaf and needle litter in forests of British Columbia: influences of litter type, forest type, and litter mixtures. Canadian Journal of Forest Research, 30(11), 1742-1750.

Powers, R. F. (1990). Nitrogen mineralization along an altitudinal gradient: interactions of soil temperature, moisture, and substrate quality. Forest Ecology and Management, 30(1), 19-29.
Raich, J. W., & Schlesinger, W. H. (1992). The global carbon dioxide flux in soil respiration and its relationship to vegetation and climate. Tellus B, 44(2), 81-99.

Reiners, WA, and Lang, GE (1987). Changes in Litterfall along a gradient in altitude. Journal of Ecology, 75, 629-638.

Rousk, J., Brookes, P. C., & Bååth, E. (2009). Contrasting soil pH effects on fungal and bacterial growth suggest functional redundancy in carbon mineralization. Applied and Environmental Microbiology, 75(6), 1589-1596.

Schliemann, S. A., & Bockheim, J. G. (2014). Influence of gap size on carbon and nitrogen biogeochemical cycling in Northern hardwood forests of the Upper Peninsula, Michigan. Plant and soil, 377(1-2), 323-335.

Shanks, R. E., & Olson, J. S. (1961). First-year breakdown of leaf litter in southern Appalachian forests. Science, 134(3473), 194-195.

Seibert, J., & McGlynn, B. L. (2007). A new triangular multiple flow direction algorithm for computing upslope areas from gridded digital elevation models. Water Resources Research, 43(4).

Silver, W. L., & Miya, R. K. (2001). Global patterns in root decomposition: comparisons of climate and litter quality effects. Oecologia, 129(3), 407-419. http://www.jstor.org/stable/3546886

Singh, J. S., & Gupta, S. R. (1977). Plant decomposition and soil respiration in terrestrial ecosystems. The botanical review, 43(4), 449-528.

Strickland, M. S., & Rousk, J. (2010). Considering fungal: bacterial dominance in soils–methods, controls, and ecosystem implications. Soil Biology and Biochemistry, 42(9), 1385-1395.

Veen, G. F., Freschet, G. T., Ordonez, A., & Wardle, D. A. (2015). Litter quality and environmental controls of home-field advantage effects on litter decomposition. Oikos, 124(2), 187-195.

Vitousek, P. M. (2004). Nutrient cycling and limitation: Hawai'i as a model system. Princeton University Press.

Zhang, D., Hui, D., Luo, Y., & Zhou, G. (2008). Rates of litter decomposition in terrestrial ecosystems: global patterns and controlling factors. Journal of Plant Ecology, 1(2), 85-93.

Zhou, Y., Su, J., Janssens, I. A., Zhou, G., & Xiao, C. (2014). Fine root and litterfall dynamics of three Korean pine (Pinus koraiensis) forests along an altitudinal gradient. Plant and soil, 374(1-2), 19-32.

Chapter Four: Characterization of Understory Shrub Expansion in a West Virginia watershed from 1986 - 2011 using Landsat Derived Vegetation Indices

ABSTRACT

Understory, evergreen shrubs are a strong presence in Appalachian forests in the eastern United States. Rhododendron (*Rhododendron maximum*) is the most prevalent species constituent of this community. *R. maximum* is a clonal, evergreen shrub that can affect the diversity and structure of these forests by altering light and moisture regimes and changing soil chemical and physical properties. Our understanding of the spatial and temporal dynamics of *R. maximum* within the secondary, mesic forest that occupies this region, particularly in the upland forests of West Virginia, is lacking. By using a combination of remotely sensed vegetation indices (NDVI; Tasseled cap Greenness, Wetness, and Brightness; and Disturbance Index) on snow-free, leaf-off Landsat 5 TM scenes from 1986 to 2011 for the Weimer Run watershed near Canaan Valley, West Virginia, we show extensive greening attributed to expansion of the evergreen shrub community. From 1986 to 2011, there is a 0.07-0.09 increase in winter NDVI, with 95.2% of the 374 ha watershed exhibiting greening. Greening is most notable at lower elevations, along streams, and on southerly oriented slopes. Contrasting models of shrub expansions informed by vegetation indices indicate a relative increase in shrub coverage of between 33.6 and 54.7% for the watershed.

INTRODUCTION

Rhododendron maximum is an abundant evergreen shrub component of the forest understory in the mid and southern Appalachian mountains of the United States, ranging from northern Georgia to Pennsylvania. *R. maximum* grows in dense thickets that can inhibit the regeneration of certain canopy tree species, such as *Picea rubens, Quercus alba, Acer rubrum,*

and *Quercus prinus* (Phillips and Murdy, 1985; Clinton and Vose, 1996, Van Lear et al. 2002, Beier et al. 2005), and thereby alter forest community structure. Presence of *R. maximum* increases stocks of soil organic matter, soil nitrogen, leaf litter biomass, and fine root biomass, while decreasing soil bulk density, lowering decomposition rates and soil moisture, and reducing light availability (Clinton and Vose, 1996; Atkins et al. 2015; Atkins et al. in prep; Wurzberger and Hendrick, 2007; Nilsen et al. 2001). From both an ecological and management perspective, it is therefore important to understand the spatial and temporal dynamics of *R. maximum* within Appalachian forests.

The temporal trajectories of forests throughout the mid and southern Appalachians have been consistently shaped by human intervention and influence since initial settlement by Native Americans around 1300 BCE. Pre-Columbian use of fire in this region was isolated to clearing of vegetation and intentional burning for agriculture or hunting (Flatley et al. 2013; Fowler and Konopik, 2007). Naturally occurring fires are believed to be of minor importance given the relatively high precipitation in a majority of this region. Since European colonization, much of this area has been logged—often multiple times—and subsequently affected by severe forest fires attributed in part to former timber harvesting practices (Allard and Leonard, 1952). Forest fires decimate understory and shrub biomass and basal area, but can lead to increased post-fire stem densities (Elliott et al. 1999). Fire suppression and cessation has been indicated as a potential driver in *R. maximum* establishment and expansion. Over the last century, fire suppression as a management practice has been a potentially influential driver of vegetation dynamics throughout the region (McGee and Smith, 1967; Phillips and Murdy, 1985).

Human impacts on these forests are not solely restricted to timber harvest and direct settlement, as these forests have been differentially impacted by inadvertently human-introduced pathogens and threats such as chestnut blight, which wiped out the american chestnut (*Castanea dentata)* throughout the southern Appalachians, as well as the hemlock wooly adelgid, and the gypsy moth (Anagnostakis, 1987; McClure et al. 2001; Knapp et al. 1986). In the Great Smoky Mountains of the southern Appalachians, *R. maximum* and *Kalmia latifolia* responded positively to release events following hestnut blight damage in former american chestnut stands (Woods and Shanks, 1959; Day and Monk, 1974; Monk et al. 1985), expanding and establishing dense thickets.

There are however, noticeable differences between the present and historical forests of the mid and southern Appalachians. Given the close proximity in time between when mid Appalachian forests were first explored and settled, and when they were heavily logged, there is often a disconnect in our understanding of what the state and function of these forests are, were, and "ought" to be. Resource exploitation of these forests has been relatively recent compared to other areas of the eastern United States. Formerly, forests in the higher, more remote regions of the mid Appalachians were populated by large stands of *P. rubens* and contained a notable and dominant understory populated by *K. latifolia* and *R. maximum* (Maxwell, 1884). The earliest reports of the dense *P. rubens* forests near Canaan Valley, West Virginia come from attempts to locate the headwaters of the Potomac River (Kennedy, 1853; Strother, 1857) and speak of the dense "laurel-brakes" within the forest, often in rather hyperbolic terms.

Present-day forests in the mid Appalachians are markedly different than pre-settlement times. Large stands of *P. rubens* have been replaced by secondary growth forests often consisting of *Betula alleghaniensis* and *Acer rubrum* with *P. rubens*, *Tsuga canadensis*, and other species playing a less prominent role in the forest, or relegated to isolated mountain tops or sheltered fragments (Allard, 1956; Abrams and McCay, 1996). Recent efforts have been undertaken to restore *P. rubens* in potentially suitable areas within the mid and southern Appalachians in an attempt to preserve and expand the fragile ecosystems (Koo et al. 2014a; Koo et al. 2014b; Koo et al. 2015; Walter et al. in prep).

Currently, our understanding of the spatial and temporal dynamics of the evergreen shrub understory community within these forests is lacking. To better estimate the future of these forests and to inform both management and restoration activities, it is necessary to gain a better understanding of this community. *R. maximum* is the most dominant and prevalent species within the evergreen shrub community in the mid Appalachians and is most closely associated with mesic sites and close proximity to streams (Day and Monk, 1974), but may be present in more xeric sites as well (Whittaker, 1956). Elevation and aspect influence the distribution of *R. maximum* as well, with increased presence on northern facing slopes and a negative correlation with increasing elevation (Day and Monk, 1974). *R. maximum* often grows in dense thickets, reaching up to 80% coverage with average heights of 3 to 7 m and stem densities ranging from 5,000 to 17,000 per ha (Beier et al. 2005; Baker & Van Lear 1998). These thickets have characteristically low-branching woody growth that can greatly inhibit extensive ground-sampling.

Remote sensing techniques, including derived vegetation indices, are useful tools for quantifying the spatial and temporal dynamics of vegetation. The Normalized Vegetation Difference Index (NDVI) is a commonly employed remotely sensed vegetation index that uses the red and near-infrared wavelengths and has a strong correlation with plant biomass and leaf area index (Tucker, 1979; Lillesand et al. 2008). NDVI has performed well in tracking shrub expansion and greening in other ecosystems, such as the arctic tundra (Walker et al. 2012; Frost et al. 2014) and in semi-arid landscapes (Weiss et al. 2004; Fensholt et al. 2012). NDVI can be derived from Landsat 5 Thematic Mapper (TM) data. Landsat 5 TM data consists of seven spectral bands, including one thermal band. Bands 1, 2, and 3 are in the visible range (between 0.45 and 0.69 μm), bands 4 and 5 are in the near-infrared (0.76 – 0.90 and 1.55 – 1.75 μm), and band 7 is in the mid-infrared (2.08 – 2.35 μm). The spatial resolution for bands 1-5 and 7 is 30 meters, potentially sufficiently fine enough resolution to detect dense, evergreen shrub thickets.

Tasseled Cap transformations combine the six non-thermal bands of the Landsat 5 TM sensor, allowing for the inclusion of more available information into land surface classification (Dymond et al. 2002). Tasseled Cap transformations result in orthogonal Brightness, Greenness, and Wetness values (Crist and Cicone, 1984) and have been shown to improve vegetation classifications due to their sensitivity to phenological changes (Dymond et al. 2002). Brightness is a weighted sum of each of the six reflectance bands of the Landsat TM imagery. Greenness contrasts the near-infrared with the first three visible bands. Wetness contrasts the mid-infrared band with the other bands (Crist et al. 1985; Cohen and Spies, 1992).

The Disturbance Index algorithm (DI) was derived to combine the information from each Tasseled Cap transformation to identify areas of disturbance within mature forests (Healey et al. 2005). By recombining Tasseled Cap transformations, spectral variation along these axes (Brightness, Greenness, and Wetness) within the Tasseled Cap data space can be mapped, resulting in differences among areas of vegetative and non-vegetative cover.

To examine the recent spatio-temporal dynamics of the evergreen understory (*R. maximum*) in a watershed within the mid-Appalachians, we answer the following questions:

1) What are the spatial patterns and temporal dynamics of the evergreen shrub layer within the Weimer Run watershed located near the Canaan Valley in West Virginia over the period of available satellite data (1986-2011)?

2) Are the dynamics of the evergreen shrub layer related to landscape position (e.g. elevation, aspect, distance from stream)?

METHODS

STUDY AREA

Our study area for this project is the Weimer Run watershed, a 374 ha watershed located in the Little Canaan Wildlife Management Area near Davis, West Virginia (39.1175, -79.4430). Weimer Run has an elevation range of 940 – 1175 m and is a sub-watershed of the Blackwater River watershed, a tributary of the Cheat River. For the climate period 1980 – 2010, the mean annual precipitation was 1450 mm yr^{-1} , and the mean daily July maximum temperature was 18.8

°C, while the mean daily maximum January temperature was -3.9 °C (Atkins et al. 2015; National Climate Data Center, Station ID DAVIS 3 SE, Davis, WV).

LANDSAT DATA

Six scenes of deciduous leaf-off, snow-free data from the Landsat 4-5 TM archive were used in our analysis (Table 4.1), from 1986 to 2011. Landsat 5 TM data were converted to Landsat 7 ETM+ DN data equivalent (Vogelmann et al. 2001) and then converted to radiance data using band-specific gain and bias numbers for the Landsat 7 ETM+ sensors (Chander et al. 2009). Radiance data were then converted to TOA ("top of the atmosphere") reflectance values (Chander et al. 2009) to account for differences in sun angle and day of year, and to allow for more accurate scene-to-scene comparisons. Tasseled cap transformations (Brightness, Wetness, and Greenness), NDVI, and DI were calculated from TOA reflectance values (Huang et al. 2002).

VEGETATION INDICES

NDVI was calculated as follows:

$$NDVI = \frac{NIR - Red}{NIR + Red} \quad (1)$$

where *NIR* is the near infrared band (band 4) and *RED* is the red band (band 3), each corrected to TOA reflectance, from each Landsat ETM+ scene. Each Tasseled Cap index was calculated as

$$TC_i = (coeff_1 \times band_1) + (coeff_2 \times band_2) + (coeff_3 \times band_3) + (coeff_4 \times band_4) + (coeff_5 \times band_5) + (coeff_7 \times band_7) \quad (2)$$

where TC_i represents each Tasseled Cap index (Brightness, Greenness, and Wetness), $coeff_1$ through $coeff_7$ are the band and index specific coefficients used in the transformation (Table 4.2), and $band_1$ through $band_7$ are the Landsat ETM+ bands, corrected to TOA reflectance.

DI is an algebraic combination of rescaled, or normalized, Tasseled Cap bands, derived with the following equation (Healey et al. 2005):

$$DI = B_r - (G_r + W_r) \quad (3)$$

where B_r, G_r, *and* W_r are the rescaled Tasseled Cap bands for Brightness, Greenness, and Wetness respectively. Each band is rescaled using the mean (μ) and standard deviation (σ) as follows (Healey et al. 2005):

$$X_r = \left(X - X_\mu\right)/X_\sigma \quad (4)$$

where *X* represents each Tasseled Cap band to be rescaled. The DI transformation is typically used to detect forest disturbance, developed with the intention of spotlighting areas within contiguous forests that lack vegetation and represent disturbance associated change (Healey et al. 2005). A high DI value for a pixel is correlated with a disturbance, as disturbed areas will be brighter (higher B_r values) and less green and less wet (lower negative G_r and B_r values). In forest disturbance studies, the means and standard deviations for each band normalization are derived from pixels within the scene known to represent intact forest (Healey et al. 2005; Masek et al. 2008). For our analysis, since we are using winter, leaf-off Landsat scenes, and our intentions are to detect the differences among evergreen shrub cover and non-evergreen cover, the means and standard deviations used to normalize each Tasseled Cap transformation are derived from all of the pixels of the scene within our watershed, allowing for the inclusion of the maximum amount of scene information. The higher the DI value in our analysis, the more likely that area can be characterized as lacking evergreen shrub coverage, and conversely, areas of lower DI values are more likely to be characterized as exhibiting evergreen shrub coverage.

MODEL SELECTION AND IMAGE CLASSIFICATIONS

Without extensive ground-truthing and historical records, it is difficult to conclusively determine *R. maximum* cover and expansion within the Weimer Run watershed. There is minor obfuscation within scenes from other evergreen vegetation. However, *P. rubens, K. latifolia,* and *T. canadensis* are only minor constituents of the Weimer Run watershed. In 2011, we sampled the forest over-story (all species above 5 cm diameter-at-breast-height) within 40 m x 40 m plots at approximately 1075 m asl and found species composition to be 37.7 % or 303 stems ha^{-1} yellow birch (*Betula alleghaniensis*), 35.8% or 287 stems ha^{-1} red maple (*Acer rubrum*), 7.3% or 59 stems ha^{-1} black cherry (*Prunus serotina*), 6.6 % or 53 stems ha^{-1} red spruce (*Picea rubens*), and 5.8% or 46 stems ha^{-1} eastern hemlock (*Tsuga canadensis*) with american beech, winterberry, and mountain holly comprising the remainder. Given the low density of evergreen species, which decreases with elevation, we have a relatively high degree of certainty that the majority of what is appearing as green vegetation in these winter scenes is in fact *R. maximum*. However, these other species are still present at low numbers and distributions, and this caveat must be included.

In order to most accurately classify the expansion of evergreen cover within the Weimer Run watershed, our analysis compares six models: 1) NDVI – Normalized Difference Vegetation Index; 2) Greenness – the Greenness index values in isolation; 3) Brightness – the Brightness index values in isolation; 4) Wetness – the Wetness index values in isolation; 5) DI – the Disturbance Index algorithm that recombines all three Tasseled Cap transformation indices following normalization; 6) Greenness + Wetness (G+W) – created by adding the Greenness and Wetness values from Tasseled Cap transformations for each pixel. Using G+W allows for the inclusion of more information regarding the canopy closure and forest shadow included in the

Wetness term with information about 'greening' included within the Greenness term. It is our opinion that the additive index of G+W offers a possible viable mathematical means by which to quantify shrub expansion.

SPATIAL ANALYSIS

For each derived vegetation index for our earliest (1986) and most recent (2011) scenes, shrub (evergreen) and non-shrub cover was determined using Iso Cluster Unsupervised Classification in ArcGIS 10.2 (ESRI; Redlands, CA) with two classes and a minimum class size of 20 pixels. Four models, (NDVI, Greenness, G+W, and DI) were selected for comparison. Brightness and Wetness indices were excluded because two classes were not consistently generated. For each pixel, at each x, y coordinate in the watershed, if a model classified the pixel as SHRUB, it was given a 1, if the pixel was classified as NON-SHRUB, it was given a 0. These classifications were then composited additively in R 3.2.2 (R Core Team, 2015). For example, if a given pixel was classified as SHRUB by each model, it would have a total score of 4, whereby if no model classified it as SHRUB, it would have a 0. The composite data layer was then projected spatially using ArcGis 10.2 (ESRI; Redlands, CA) to create a map of model agreement on SHRUB versus NON-SHRUB classification for 1986 and 2011.

NDVI values for 1986 and 2011 where then evaluated pixel by pixel in R 3.2.2 (R Core Team, 2015) to determine pixel trajectories, with four possible outcomes from 1986 to 2011: 1) a pixel classified as NON-SHRUB in 1986 remains NON-SHRUB in 2011; 2) a pixel classified as NON-SHRUB changes to SHRUB; 3) a pixel classified as SHRUB changes to NON-SHRUB; and 4) a pixel classified as SHRUB remains SHRUB.

TREND ANALYSIS

Trends in NDVI were calculated using linear regression for each pixel through time for each Landsat TM scene using R 3.2.2. Linear regression analysis was restricted to NDVI, as it is a normalized ratio that allows for a high degree of confidence for both inter- and intra-scene comparisons. Since NDVI is widely used in ecological and agricultural studies, it is more likely well-known, is more mathematically intuitive, and tracks well both spatially and temporally, more so than other vegetation indices used in our analysis, making it the most suitable variable for change analysis.

ELEVATION, ASPECT, DISTANCE-TO-STREAM

The watershed was discretized into three elevation classes (LOW, MID, HIGH) using Iso Cluster Unsupervised Classification with a digital elevation map (DEM) from 1/3 arc second elevation data from the Shuttle Rader Topography Mission (SRTM) (USGS 2006). Aspect was determined for each 30 x 30 m cell in the watershed using the SRTM DEM with the aspect tool in ArcGIS 10.2 with each cell classified as North, Northeast, East, etc. Distance from stream was calculated for each cell using the Euclidean distance tool in ArcGIS 10.2.

Absolute NDVI values for 1986 and 2011 along with changes in NDVI from linear trend analysis were compared across elevation and aspect class (and the interaction of aspect and elevation) using an analysis of variance (ANOVA); NDVI values were compared across elevation classes with distance-to-stream as a covariate using an analysis of covariance (ANCOVA) in R 3.2.2 (R Core Team, 2015). Significant differences between classes were determined with Tukey's test for Honest Significant Differences using the TukeyHSD test in R 3.2.2. Our analysis of differences in NDVI with respect to landscape variables was restricted to data derived from the 1986 and 2011 Landsat scenes in order to make beginning and end of time-series comparisons.

R. maximum has a strong association with streams and riparian areas. To evaluate spatial effects of distance-to-stream on NDVI, change-point analysis employing piecewise regression with the segmented package in R 3.2.2 was used to parse the watershed into riparian and upland areas based on breakpoints derived using NDVI and distance-to-stream as model inputs. Riparian and upland areas were then evaluated using linear regression and Pearson's Correlation Coefficient to evaluate effects of distance-to-stream on NDVI.

RESULTS

VEGETATION INDICES

Mean winter NDVI for the Weimer Run watershed in 1986 was 0.44 (Fig. 4.1), and by 2011, mean winter NDVI increased to 0.53. Median values of NDVI shifted from 0.43 to 0.52. First and third quartile values of NDVI increased from 1986 to 2011 as well, while maximum values fluctuated, but remained relatively constant. The distribution of NDVI values shift upwards each year from 1986 to 2011 (Fig. 4.2). Winter greening increases throughout the watershed with time (Fig. 4.3). Endmember analysis of the difference between each pixel from 1986 to 2011 shows that 95.2% of the watershed increased in winter NDVI from 1986 to 2011. Mean NDVI increased from 0.44 in 1986 to 0.54 in 2011 for pixels with positive differences. For the remainder of the watershed mean NDVI was 0.43 in 1986 and 0.41 in 2011.

Mean Greenness decreased from 1986 (-0.003) to 2011 (-0.022) with 4.8% of the watershed showing increases in Greenness (Fig. 4.3). Brightness decreased from 0.258 to 0.171, with 99.8% of the watershed decreasing. Wetness increased from -0.126 to -0.098 with 97.3% of the watershed showing increases as did G+W, from -0.128 to -0.120 with 64.3% of the watershed increasing.

MODEL CLASSIFICATION COMPARISON

Iso Cluster Unsupervised Classification analysis shows that NDVI is initially the most conservative model (with respect to identifying shrub pixels), classifying 103.7 ha of the watershed as shrub in 1986, but it shows a relative increase in shrub cover of 54.3% over the period of the satellite record, with a final areal shrub coverage of 160 ha for 2011 (Table 4.3). DI has the highest initial shrub cover at 133.8 ha of the watershed in 1986 and a final shrub cover of 239.9 ha in 2011, a 41.3% increase. Both Greenness and G+W are more similar to NDVI, with increases of 39% and 33.6%, respectively (Table 4.3). Combining models yields a mean initial shrub coverage in the watershed of 114.9 ha in 1986 and a final shrub coverage of 162.4 ha in 2011with an increase in coverage of 41.3% or an increase in areal shrub coverage of 47.5 ha. Composite analysis shows that 43.7% of the watershed is classified as shrub by at least one model, 30.8% by at least two models, 25.7% by at least three models, and 22.1% by all four models. Composite analysis shows that 56.2% of the watershed is classified as non-shrub by all four models (Fig. 4.4).

CHANGES IN CLASSIFICATION FROM 1986 TO 2011

Total classification change for the watershed, determined by comparing spatial classifications of 1986 and 2011 NDVI shrub and non-shrub cover, derived using Iso Cluster Unsupervised Classification analysis, shows that 17.4% of the watershed area changed from non-shrub to shrub coverage (Fig. 4.5). 54.7% of the watershed remained absent of shrub coverage, while 25.3% of the watershed was originally classified as shrub in 1986 and remained shrub in 2011 (Fig. 4.5). Only 2.4% of the watershed went from shrub to non-shrub classification. Moving from 25.3% shrub coverage in 1986 to 42.7% in 2011—a 68.7% relative increase in shrub coverage.

LINEAR REGRESSION CHANGE ANALYSIS

NDVI change analysis using linear regression shows that 353.5 ha of the watershed (94.5%) had increased winter NDVI values from 1986 to 2011 for an increase in mean winter NDVI of 0.076 for the entire watershed. For the 353.5 ha area that shows winter greening, there is a mean NDVI increase of 0.082, while the remainder of the watershed shows a decrease in winter NDVI of 0.019. 46.9% of the scene pixels, or 174.7 ha of the watershed, have significant slopes based on an alpha of 0.05.

ELEVATION

In both 1986 and 2011, NDVI shows strong differences among elevation classes (1986, $F = 33.3$, $p = <<0.001$; 2011, $F = 86.9$, $p = <<0.001$). In 1986, mean NDVI was greatest at the LOW and MID elevation class (0.45) and lowest at the HIGH elevation level (0.43). The HIGH elevation NDVI was significantly different than both MID and LOW NDVI values. By 2011, NDVI at the LOW elevation had increased to 0.55, at MID to 0.54 and the HIGH to 0.51. Each elevation level was significantly different from each other in 2011. The HIGH elevation class showed the lowest increase in mean winter NDVI (0.06) based on linear trend analysis and was statistically significantly different from both the MID (0.08) or LOW (0.08) classes ($F = 57.4$, $p = <<0.001$).

ASPECT

In 1986, NDVI is lowest on southerly and westerly facing slopes in the watershed, with mean values of 0.42. Easterly and northeasterly facing slopes have the highest mean values of NDVI, at 0.46. When contrasted by elevation, southerly facing slopes at mid elevations have the highest mean NDVI at 0.53 followed by flat areas low in the watershed, 0.48. Southwesterly facing slopes high in the watershed have the lowest NDVI (0.37). ANOVA results show significant

differences among aspect (F = 27.6, p = <<0.001) and aspect by elevation class (F = 16.8 p = <<0.001) for 1986.

For 2011, northerly, southerly, westerly, and northeasterly facing slopes and flat areas have mean NDVI ranging from 0.51 to 0.52, southeasterly and southwesterly facing slopes are the highest at 0.54. When contrasted by elevation class, southerly facing slopes at mid elevations are again the highest at 0.66 while southwesterly and southerly facing slopes at high elevations have the lowest values of NDVI (0.47). ANOVA results show significant differences among aspect (F = 2.8, p = 0.004) and aspect by elevation class (F = 18.2 p = <<0.001) for 2011.

Southwesterly facing slopes show the greatest increase in winter NDVI from our linear trend analysis, increasing by an average of 0.11 (Fig. 4.7), while northeasterly slopes show the lowest increase, 0.05. When contrasted by elevation, southerly slopes at the mid and low elevations show high increases, 0.13 and 0.11 respectively. Increases are quite notable at southwesterly facing slopes at the mid (0.10) and low (0.12) elevations as well. ANOVA results show significant differences in NDVI change among aspect (F = 38.4, p = <<0.0001) and aspect by elevation class (F = 7.9 p = <<0.001).

DISTANCE-TO-STREAM

Change-point analysis indicates NDVI versus distance-to-stream breakpoints of 136.7 m ±5.7 for 1986 and 142.4 ±4.5 for 2011 (error estimates are standard error). This indicates a bifurcation of influence whereby below this threshold, NDVI values are statistically influenced by distance-to-stream. Based on this analysis, a conservative estimate of 150 m was used as a classification threshold whereby pixels in a scene 150 m or closer to a stream were classified as riparian, while pixels farther than 150 m from a stream were classified as upland. In riparian areas, NDVI has a negative correlation with distance-to-stream (1986, r = -0.415; 2011, r = -

0.588) indicating that NDVI values decrease with increasing distance from the stream. In 2011 in riparian areas, a greater amount of variance in NDVI values is explained by distance-to-stream (r^2 = 0.345) than in 1986 (r^2 = 0.172) (Fig. 4.6). In upland areas, NDVI shows a positive correlation with distance-to-stream (1986, *r* = 0.18; 2011, *r* = 0.20). However, in upland areas, little of the model variance is explained with distance-to-stream (1986, r^2 = 0.03; 2011, r^2 = 0.03).

LANDSCAPE VARIABLE COVARIANCE

ANCOVA results indicated significant interactive effects of elevation and distance-to-stream on NDVI values across the watershed for both 1986 and 2011 (1986, *F* = 77.43, *p* = <<0.001; 2011, *F* = 165.66, *p* = <<0.001) where distance-to-stream is a more influential variable at LOW and MID elevations. A Tukey's test for Honest Significant Differences for 1986 shows that areas at HIGH elevation in the watershed are different from MID and LOW elevation area, but that MID and LOW are not significantly different from each other. For 2011, each elevation level is significantly different from every other.

DISCUSSION

To verify the observed Landsat TM+ derived winter NDVI values (Fig. 4.2) for 2011 (captured on November 8, 2011), we compared MODIS derived NDVI from November 8, 2011 with our Landsat TM+ derived NDVI. MODIS derived NDVI showed a minimum NDVI of 0.46 in the pixels within the Weimer Run watershed. The minimum Landsat TM+ derived NDVI value for 2011 was 0.15 with 25% of all NDVI values in the scene at or below 0.46. While MODIS resolution is far coarser than Landsat, this gives us confidence in these values.

There is a distinct increase in winter NDVI from 1986 to 2011 within the Weimer Run watershed that we attribute to an increase in evergreen understory shrub coverage and density primarily driven by *R. maximum*. This increase in NDVI is also accompanied by a notable decrease

in tasseled cap Brightness—which is strongly correlated with the reflectance of bare soil (Fig. 4.3C); a sharp decrease in Brightness can be interpreted as a decrease in the spatial extent of bare soil in the scene (Crist and Cicone, 1984). Tasseled cap Wetness also increases sharply, indicating an increase in vegetation cover, stand complexity, and shadowing within the forest (Cohen and Spies, 1992) (Fig 4.3D). However, there is a decrease in absolute Greenness values from 1986 – 2011 (Fig. 4.3B). Tasseled cap Greenness was initially derived to capitalize on the wide scattering of infrared radiation that results from the cellular structure within green vegetation (Crist and Cicone, 1984). Higher values of Greenness typically indicate high densities of green vegetation as more of the visible spectra is absorbed in plant pigments, such as chlorophyll (Crist and Cicone, 1984). Greenness may not be attenuated sufficiently for the darker, sclerophyllous leaves of the understory evergreen shrub cover in this watershed. Variations in chlorophyll content within rhododendron leaves may be driving this relationship as well (Whittaker and Garfine, 1962). Surface leaf waxes found in some evergreen species do have light-scattering properties sufficient to affect surface reflectance (Reicosky and Hanover, 1978). The thick, waxy nature of *Rhododendron* leaves may be affecting Greenness through physiological effects on reflectance.

By using Iso Cluster Unsupervised Classification analysis the within-scene distribution and variance of Greenness shows an increase in the area of the watershed classified as shrub over the period of satellite record concordant with increases seen in the other models despite absolute decreases in Greenness. This discrepancy may be described by some seasonality in using pre- and post-winter Landsat scenes or in the spectral signature of *Rhododendron* that is not adequately attenuated by the Greenness index. This increase in Greenness is greater at

lower Wetness values, with a greater number of pixels with increases in Wetness from 1986 to 2011, and saturates at higher values of Wetness with more pixels tending towards marginal to minimal increases (Fig. 4.3D). There are increases in the G+W values at low and medium values of G+W with more pixels above the 1:1 line than below (Fig. 4.3F). The G+W model shows that areas that are the most "wet" and most "green" did not increase markedly over the 25 year study period—those values may have already been saturated (Fig. 4.3F). Our DI model shows similar results to both G+W and NDVI, albeit with tighter data grouping and less variance (Fig. 4.3E) (note that DI values are inverted compared to other models, with more negative values indicating more dense canopy).

Given the spatial agreement in shrub and non-shrub classification among all of the considered models and the similarities between 1986 to 2011 comparisons of G+W, DI, and NDVI, the G+W model represents a new recombination method of potential value in ecological and vegetation changes studies that incorporates more information for each Landsat scene than NDVI alone. Further, utilizing DI on winter, snow-free Landsat scenes, offers another potential method for tracking and quantifying evergreen shrub expansion. The advantage to using DI is that it also includes tasseled cap Brightness in its derivation.

IMPACTS OF UNDERSTORY SHRUB EXPANSION

Our analysis shows an estimated increase in areal shrub extent of between 33.6 and 54.3% in the Weimer Run watershed during the available 25-year satellite record based on comparing NDVI, G+W, DI, and Greenness using Iso Cluster Unsupervised Classification analysis. Our understanding of species richness and diversity within this and similar watersheds across West Virginia gives us strong cause to believe a majority, if not all, of this evergreen expansion is driven by *R. maximum* expansion. *R. maximum* increases stocks of soil carbon and soil nitrogen

and increases soil porosity while decreasing soil bulk density (Atkins et al. 2015). *R. maximum* also influences soil respiration by lowering soil bulk density and increasing soil porosity, creating more potential of oxidation of soil organic matter while contributing concomitant root respiration, resulting in higher soil carbon fluxes during periods of low to medial soil moisture. *R. maximum* also changes soil moisture and soil temperature while raising soil C:N ratios and lowering decomposition rates (Atkins et al. 2015). An increase in evergreen shrub coverage, even at the low end of our estimates, represents a vegetation and ecosystem change of potential significance.

R. maximum directly inhibits regeneration and growth of silivculturally and socially important species such as *P. rubens*. *R.* maximum also has strong associations with ericoid mycorrhizae, allowing it to outcompete species that depend on ectomycorrhizae, such as *P. rubens* for available organic N (Bending and Read, 1997). Habitat suitability studies have acknowledged the importance of the inclusion of evergreen shrub coverage in projections of suitability for *P. rubens* (Walter et al. in prep) however, the change in spatial extent of *R. maximum* distribution and its concordant impacts on the ecosystem have not been fully considered. Our analysis indicates that using winter NDVI change analysis allows for a potentially viable means of quantifying the spatial dynamics of evergreen shrub coverage that could further inform additional studies and management practices.

SHRUB EXPANSION AND LANDSCAPE VARIABLES

Increases in winter NDVI were stronger in areas closer to streams. Change-point analysis shows a linear increase in the influence of distance-to-stream (Fig. 4.5) that indicates the expansion of *R. maximum* along stream corridors and in riparian areas, giving further credence to our assumption that increases in NDVI are driven by *R. maximum* expansion. *R. maximum* can

reproduce clonally (Elliott and Vose, 2012)—spatial expansion of shrubs would correspond with the patterns of NDVI increases seen in our data (Fig. 4.2). We also see greater increases in winter NDVI at lower elevations in the watershed. Great increases in winter NDVI and shrub coverage are occurring on southerly, southeasterly, and southwesterly oriented slopes in the watershed. There are also notable and complex interactions occurring between aspect and elevation. *R. maximum* typically favors cooler, northerly facing slopes (Anderson, 2008). The northerly facing slopes in the Weimer Run watershed have high winter NDVI and evergreen shrub coverage, yet the greatest increases we are seeing are occurring on southerly oriented slopes. Annual precipitation has been increasing in this watershed (Atkins et al. 2015) and could be contributing to this trend, with soil moisture no longer being limiting on southerly oriented slopes due to greater increases of moisture into the system. Though projected warming for this region would be expected to limit the expansion of species like *R. maximum*, precipitation is also expected to increase, obfuscating possible trajectories (IPCC, 2013).

EVERGREEN SHRUBS WITHIN THE SECONDARY FOREST

The primeval forest of Canaan Valley, West Virginia and surrounding areas is characterized as a towering canopy of *P. rubens* populated by a dense understory of "big laurel" (Fortney, 1993) ("big laurel" in this case a colloquial reference to *R. maximum*). The influx of European settlement coupled with widespread logging and fire between 1800 and 1930, fundamentally altered the composition of the upland forests of Canaan Valley and throughout West Virginia. The past extent of *P. rubens* forests, estimated to have been on the order of 200,000 ha, are now estimated to be approximately 20,000 ha. Over the past century, secondary hardwood species such as *B. alleghaniensis*, *A. rubrum*, and *F. grandifolia* have become the canopy dominants within the forest, with *R. maximum* (and to a lesser extent *K. latifolia*)

populating the understory. Gaps that open within the forests, are quickly populated by *R. maximum*.

Our understanding and concept of the upland forests of these regions is influenced by our prior knowledge of the pre-settlement forest state, wherein a possible bias exists. The current forest has evolved under post-settlement, post-disturbance, heavily anthropogenically influenced conditions. The evergreen understory has developed concordantly with the current dominant mesic hardwood species. *R. maximum* may be acting as an ecosystem engineer within this system by altering the forest micrometorology along with available light and nutrients. There is potential here that *R. maximum* has fundamentally altered these forests sufficiently that the current forest represents an alternate, stable ecosystem state; without *R. maximum* in the system, species such as *P. rubens* could more readily take hold, expand, and eventually, following senescence and death of current canopy species (e.g. *B. alleghaniensis*, *A. rubrum*), dominate the forest overstory. Seed production does not typically occur for *P. rubens* until an individual tree is 30 – 40 years of age and dispersal distances are often less than 100 m from the parent tree. This limits the expansion of this slow growing species to areas adjacent to existing patches of current *P. rubens.* However, seedling establishment and growth are inhibited by the presence of *R. maximum* which directly and indirectly outcompetes *P. rubens* for nutrients, light, and water in the forest (Philips and Murdy, 1985; Clinton and Vose, 1996, Van Lear et al. 2002). The current state of the forest, which includes this dominate, expanding evergreen shrub component, is a by-product of immense anthropological disturbance that has resulted in a shift in the ecosystem state (Groffman et al. 2006). The few, isolated communities of relict species (e.g. *P. rubens*) may only be present due to a lag effect. Determination of whether a fundamental ecosystem state

change has occurred can be difficult, with time being an important issue as there is a mismatch in scale between what we consider relevant in human terms and what occurs in the natural environment. These considerations are important not only for the basic theoretical and ecological framework with which we view forest systems in the mid Appalachians but also to applied science and management strategies.

Restoration efforts may need to employ substantive measures, such as widespread thinning and removal of *R. maximum*, to achieve desired results. However, sufficient pause should be taken when considering the employment of these or similar management strategies. More work and more time is needed to evaluate both the ecological effects of evergreen shrub expansion and the potential of habitat restoration in light of changing climate and vegetation change.

CONCLUSIONS

By evaluating a time series of Landsat scenes for the Weimer Run watershed, near Canaan Valley, WV, we were able to show an increase in mean winter NDVI of 0.44 to 0.53 over the period of the satellite record (1986-2011) with 95.2% of the watershed exhibiting greening. We attribute this increase in NDVI to evergreen shrub expansion, predominately driven by *R. maximum*. NDVI increases are greater along streams, at lower elevations, and along southerly oriented slopes. The expansion of evergreen shrub coverage within this and similar watersheds has potentially profound management and ecological consequences. However, our current understanding of the forest present versus the forest prior needs careful consideration.

TABLES AND FIGURES

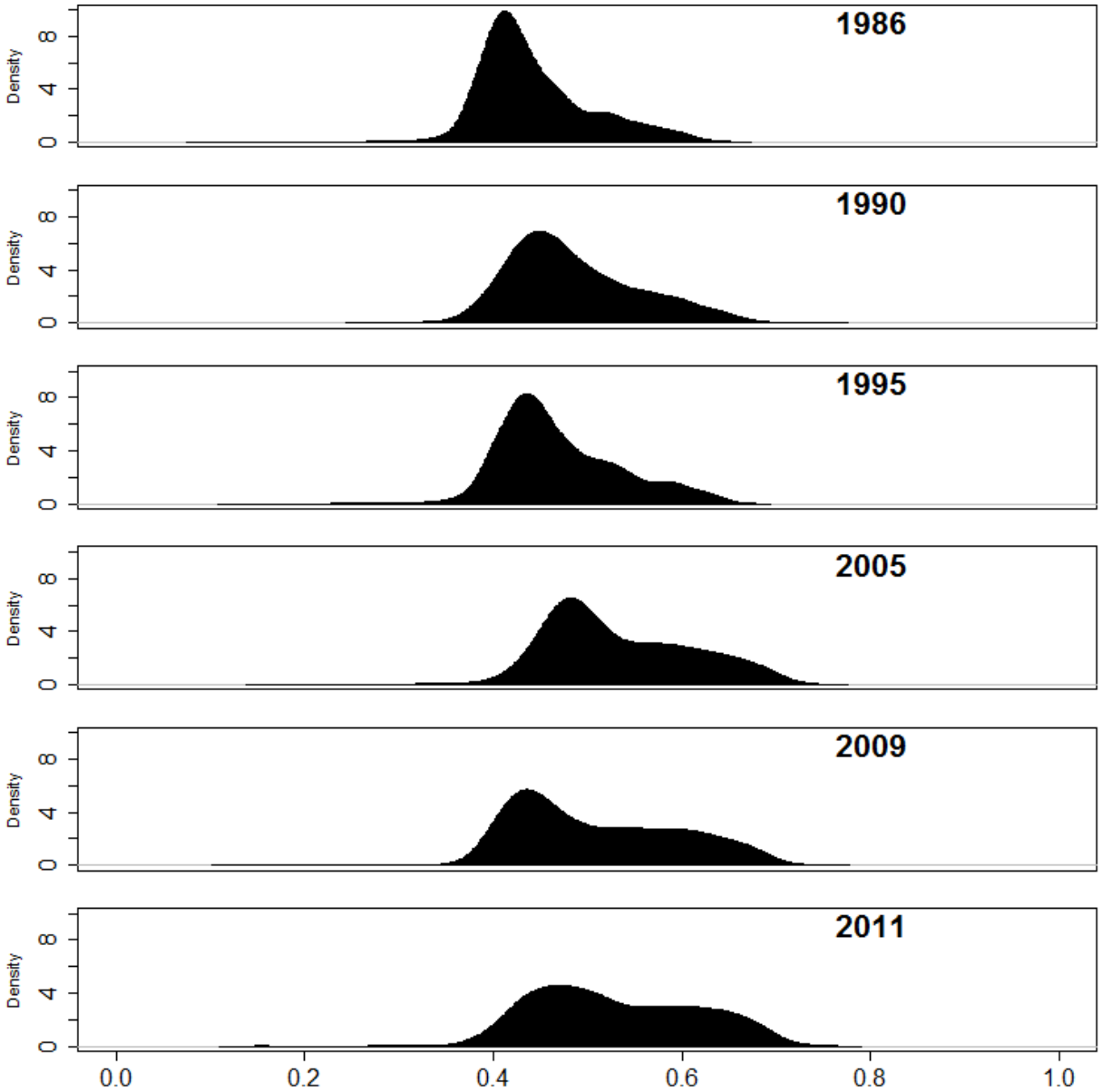

Figure 4.1. Density plots of NDVI for all scenes showing the distribution of NDVI values for each scene in the analysis (n = 4153).

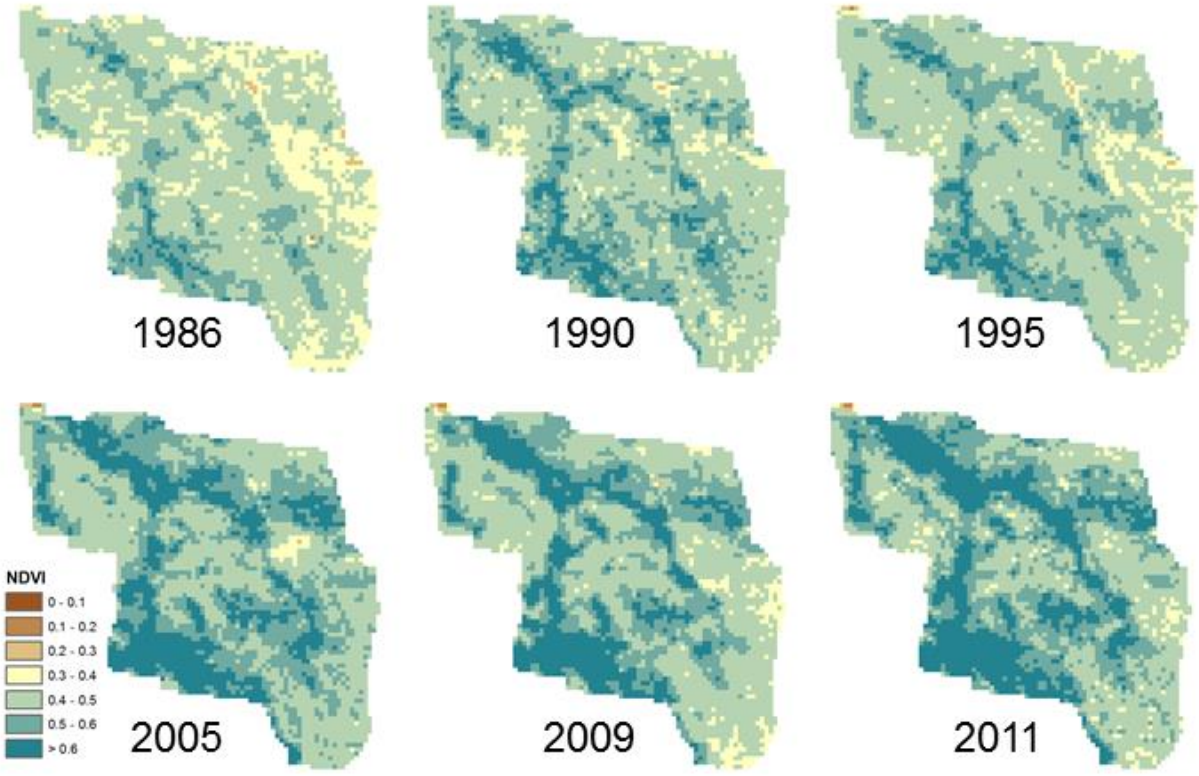

Figure 4.2. NDVI from 1986 through 2011 for each Landsat TM scene.

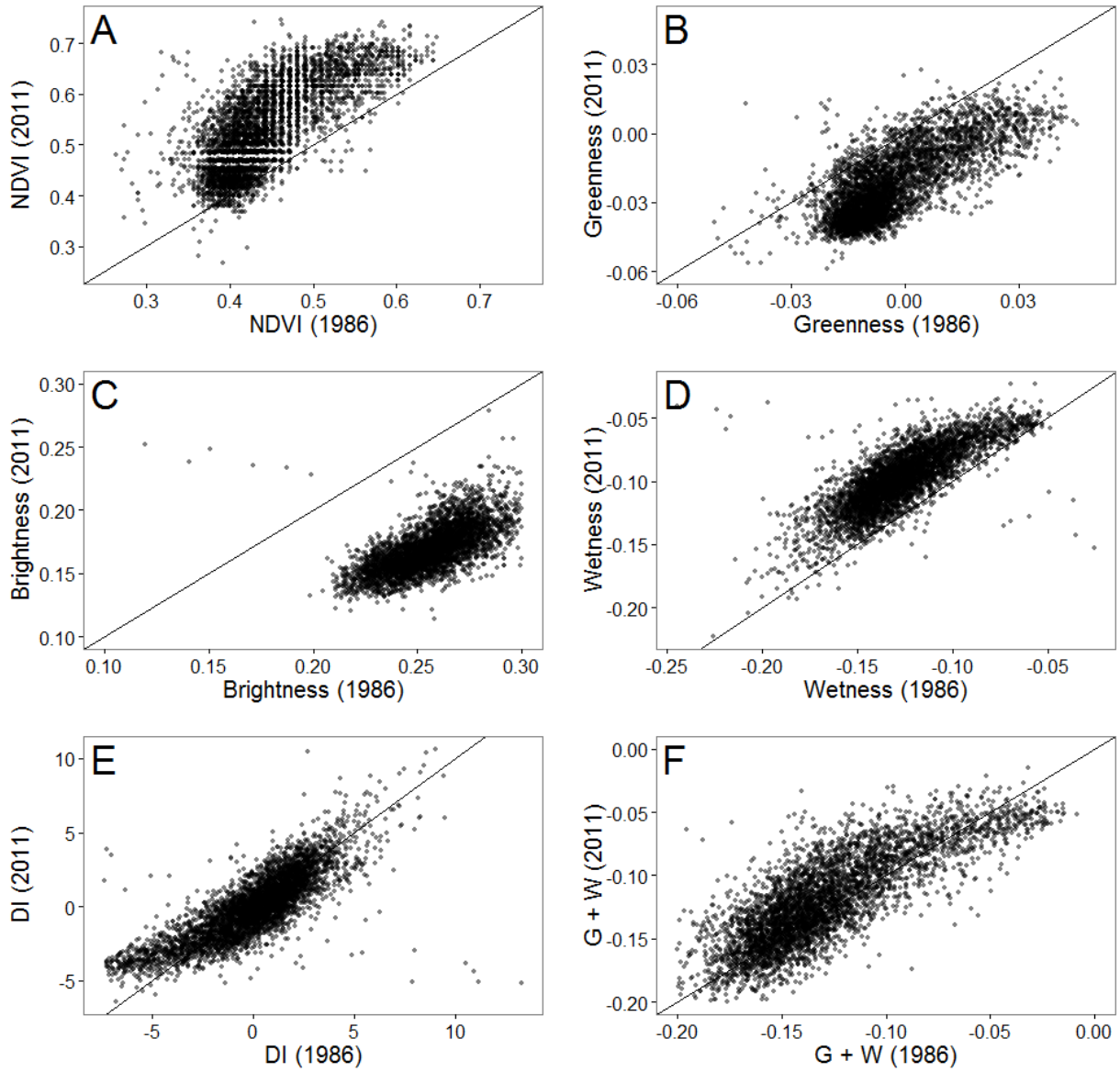

Figure 4.3. Each plot shows values from 1986 on the x-axis compared to 2011 on the y-axis. All values above the 1:1 line in each plot indicate an increase from 1986 to 2011, conversely, values below indicate a decrease. (A) NDVI, (B) Greenness, (C) Brightness, (D) Wetness, (E) DI (Disturbance Index), (F), G + W (Greenness + Wetness).

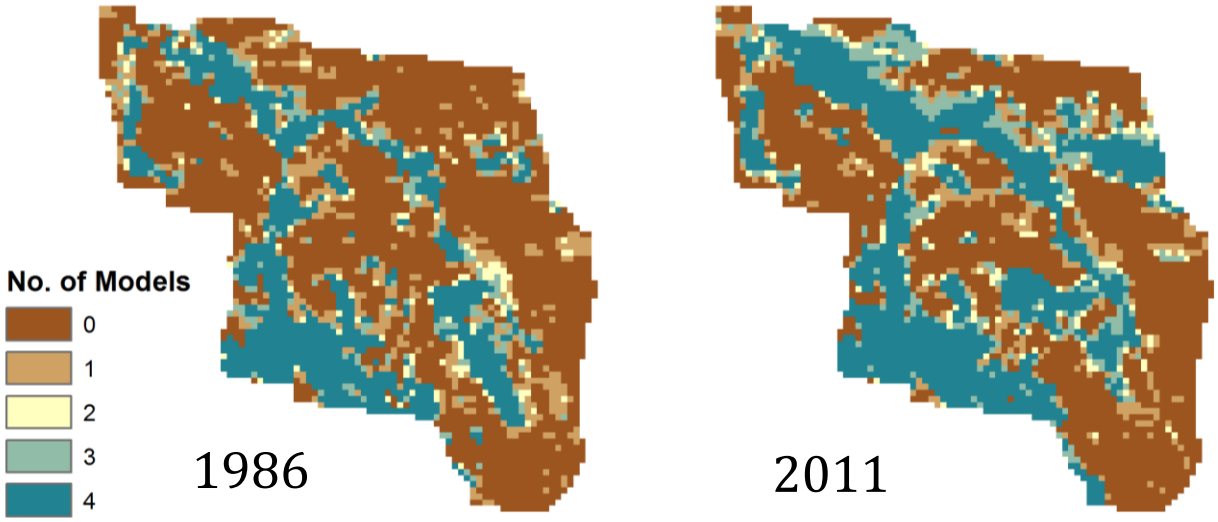

Figure 4.4. Comparison of all four models (NDVI, DI, Greenness, and Greenness + Wetness) indicating shrub coverage for the 2011 Landsat TM scene based on Iso Cluster Unsupervised Classification. Scale ranges from 0 (no models predict evergreen shrub coverage) to 4 (all models indicate shrub coverage).

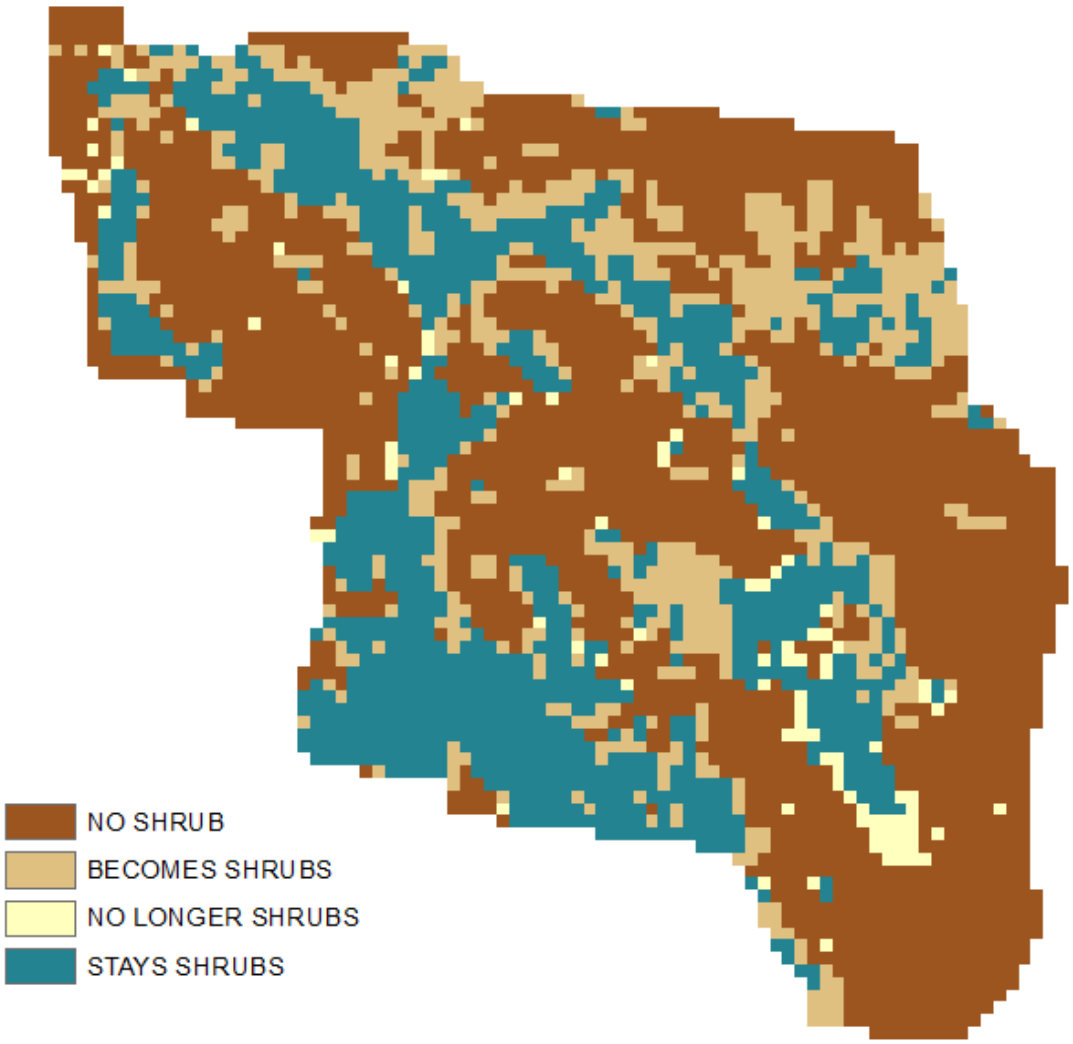

Figure 4.5. Change in shrub/non-shrub classification from 1986 to 2011 using NDVI coupled with Iso Cluster Unsupervised Classification. In absolute watershed area (374 ha total): NO SHRUB – 54.7%; BECOMES SHRUB – 17.4%; NO LONGER SHRUBS – 2.4%; STAYS SHRUBS – 25.3%.

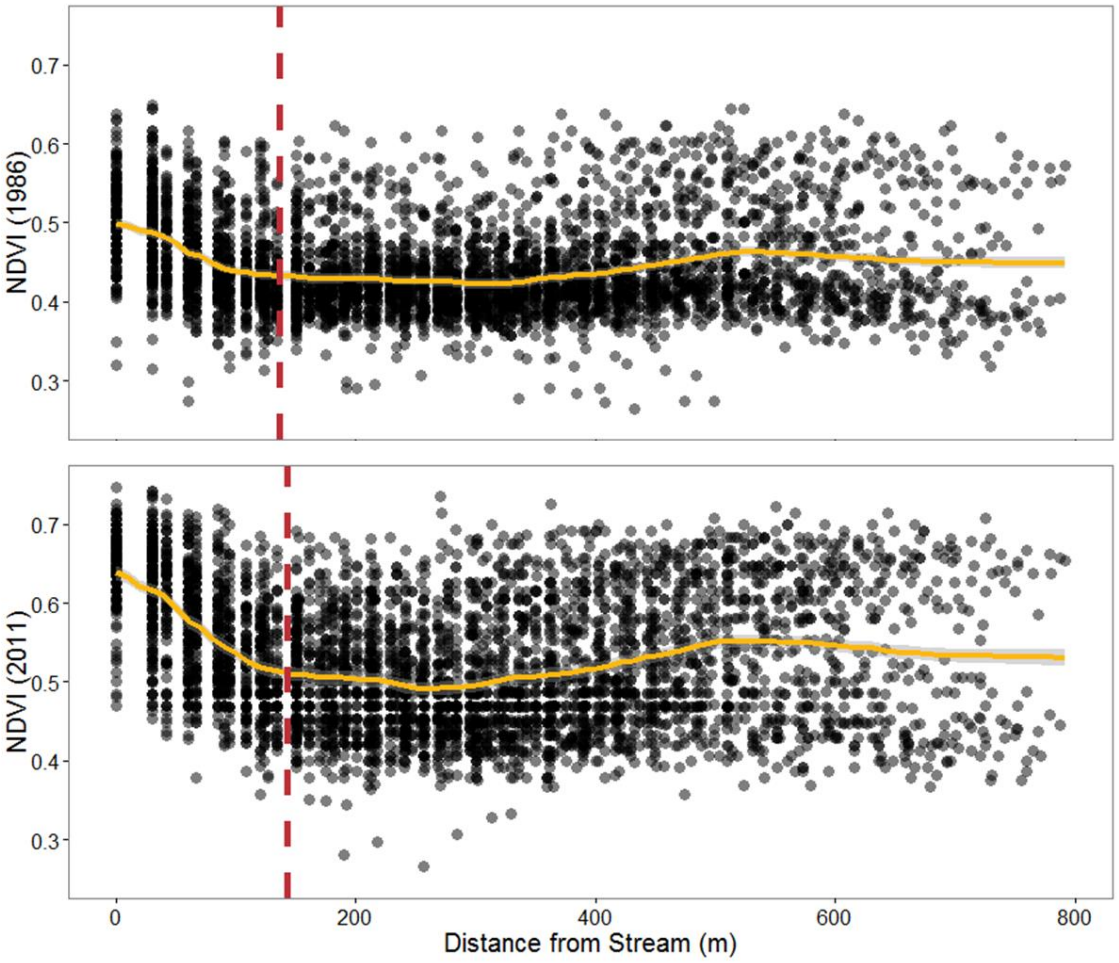

Figure 4.6. NDVI values by distance-from-stream (m), with breakpoints indicated by dashed red lines.

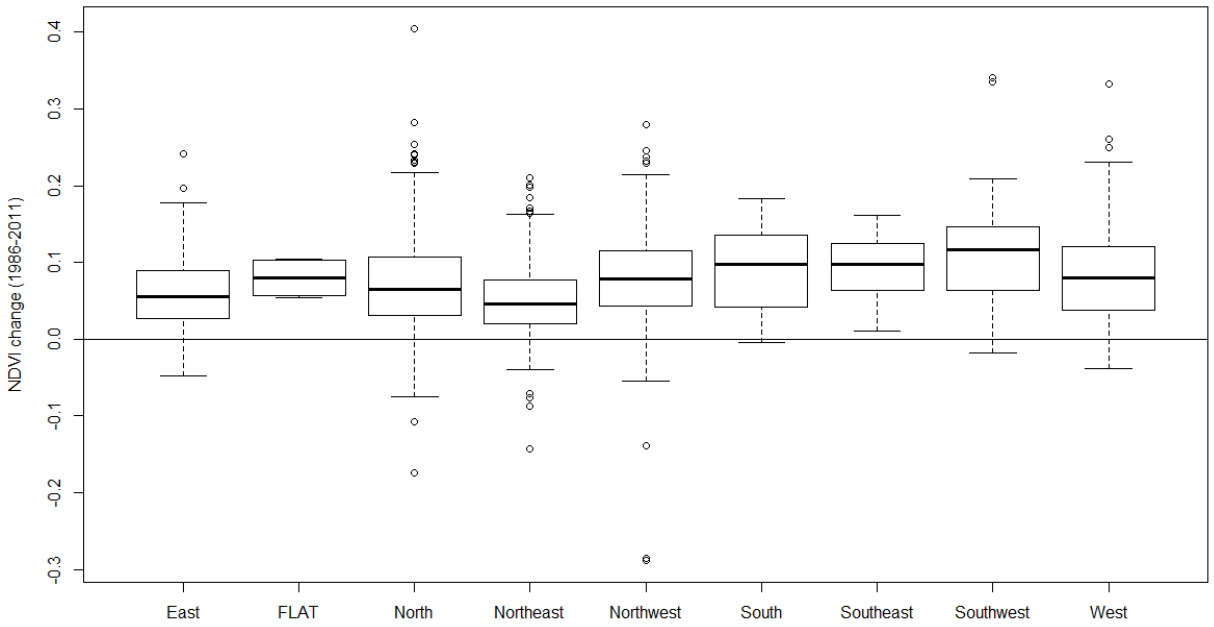

Figure 4.7. Boxplot of change in NDVI by aspect class based on linear regression model.

Table 4.1. Landsat 5 TM scenes used in analysis.

Acquisition Date	Acquisition Quality	Acuisition Time	Cloud Cover
March 24, 1986	7	1524	0%
November 14, 1990	9	1518	0%
March 17, 1995	9	1508	0%
November 7, 2005	9	1546	15.7%
March 23, 2009	9	1545	0%
November 8, 2011	9	1546	0.1%

Table 4.2. Tasseled cap coefficients for brightness, greenness, and brightness for Landsat 4-5 TM data (Huang et al. 2002).

Index	Band 1	Band 2	Band 3	Band 4	Band 5	Band 7
Brightness	0.3561	0.3972	0.3904	0.6966	0.2286	0.1596
Greenness	-0.3344	-0.3544	-0.4556	0.6966	-0.0242	-0.2630
Wetness	0.2626	0.2141	0.0926	0.0656	-0.7629	-0.5388

Table 4.3. Inter-model comparison of Greenness, G+W, NDVI, and DI by pixel at top, area (ha) middle, and percentage of entire watershed bottom.

*table showing total no. of pixels (n = 4153) for each scene after unsupervised iso cluster classification

	GREENNESS		G+W		NDVI		DI		ALL MODELS (mean)	
YEAR	SHRUB	NON-SHRUB	SHRUB	NON-SHRUB	SHRUB	NON-SHRUB	SHRUB	NON-SHRUB	SHRUB	NON-SHRUB
1986	1205	2948	1262	2891	1153	3000	1487	2666	1276.75	2876.25
1990	1294	2859	1928	2225	1501	2652	2134	2019	1714.25	2438.75
1995	1221	2932	1386	2767	1344	2809	1652	2501	1400.75	2752.25
2005	1492	2661	1735	2418	1637	2516	*	*	1621.33	2531.67
2009	1657	2496	1622	2531	1767	2386	1669	2484	1678.75	2474.25
2011	1675	2478	1686	2467	1779	2374	2076	2077	1804.00	2349.00

*same table in hectares (total area = 374 ha)

	GREENNESS		G+W		NDVI		DI		ALL MODELS (mean)	
YEAR	SHRUB	NON-SHRUB	SHRUB	NON-SHRUB	SHRUB	NON-SHRUB	SHRUB	NON-SHRUB	SHRUB	NON-SHRUB
1986	108.45	265.32	113.58	260.19	103.77	270.00	133.83	239.94	114.91	258.86
1990	116.46	257.31	173.52	200.25	135.09	238.68	192.06	181.71	154.28	219.49
1995	109.89	263.88	124.74	249.03	120.96	252.81	148.68	225.09	126.07	247.70
2005	134.28	239.49	156.15	217.62	147.33	226.44	*	*	145.92	227.85
2009	149.13	224.64	145.98	227.79	159.03	214.74	150.21	223.56	151.09	222.68
2011	150.75	223.02	151.74	222.03	160.11	213.66	186.84	186.93	162.36	211.41

*same table in percentage of the watershed

	GREENNESS		G+W		NDVI		DI		ALL MODELS (mean)	
YEAR	SHRUB	NON-SHRUB	SHRUB	NON-SHRUB	SHRUB	NON-SHRUB	SHRUB	NON-SHRUB	SHRUB	NON-SHRUB
1986	29.02	70.98	30.39	69.61	27.76	72.24	35.81	64.19	34.64	65.36
1990	31.16	68.84	46.42	53.58	36.14	63.86	51.38	48.62	38.38	61.62
1995	29.40	70.60	33.37	66.63	32.36	67.64	39.78	60.22	31.71	68.29
2005	35.93	64.07	41.78	58.22	39.42	60.58	*	*	39.33	60.67
2009	39.90	60.10	39.06	60.94	42.55	57.45	40.19	59.81	42.87	57.13
2011	40.33	59.67	40.60	59.40	42.84	57.16	49.99	50.01	41.26	58.74

APPENDIX

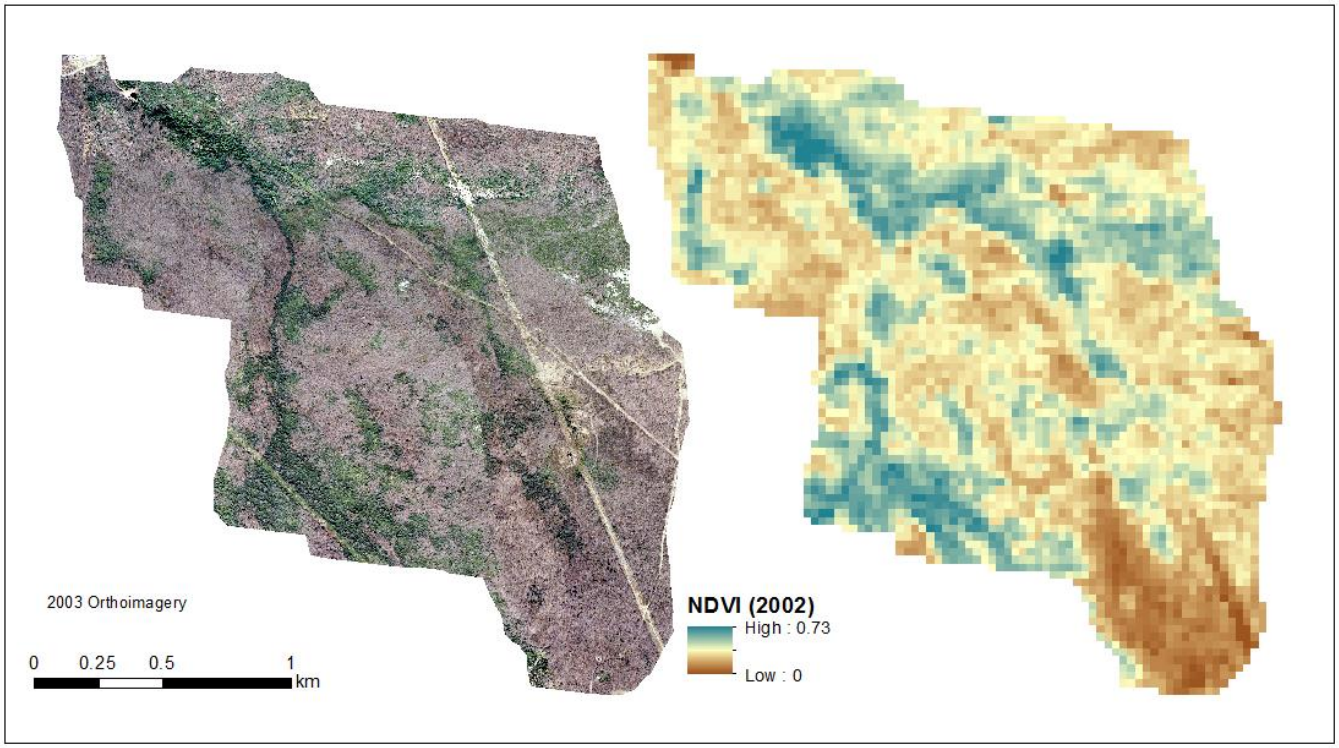

Appendix 4.A. The image to the left is the Orthoimagery taken on March 10, 2003. The NDVI scene is from February 16, 2002—the closest high-quality image that we have. Below is the greenness raster for this scene. 2002 was eliminated from analysis because there is evidenced of snow at the higher values when you isolate certain bands.

REFERENCES

Abrams, M. D., & McCay, D. M. (1996). Vegetation-site relationships of witness trees (1780-1856) in the presettlement forests of eastern West Virginia. Canadian Journal of Forest Research, 26(2), 217-224.

Allard, H. A., & Leonard, E. C. (1952). The Canaan and the Stony River valleys of West Virginia, their former magnificent spruce forests, their vegetation and floristics today. Castanea, 1-60.

Anagnostakis, S. L. (1987). Chestnut blight: the classical problem of an introduced pathogen. Mycologia, 23-37.

Anderson, Michelle D. (2008). Rhododendron maximum. In: Fire Effects Information System, [Online]. U.S. Department of Agriculture, Forest Service, Rocky Mountain Research Station, Fire Sciences Laboratory (Producer). Available: http://www.fs.fed.us/database/feis/

Atkins, J. W., Epstein, H. E., & Welsch, D. L. (2015). Vegetation and elevation influence the timing and magnitude of soil CO_2 efflux in a humid, topographically complex watershed. Biogeosciences, 12(10), 2975-2994.

Baker, T. T., & Van Lear, D. H. (1998). Relations between density of rhododendron thickets and diversity of riparian forests. Forest Ecology and Management, 109(1), 21-32.

Beier, C. M., Horton, J. L., Walker, J. F., Clinton, B. D., & Nilsen, E. T. (2005). Carbon limitation leads to suppression of first year oak seedlings beneath evergreen understory shrubs in Southern Appalachian hardwood forests. Plant Ecology, 176(1), 131-142.

Bending, G. D., & Read, D. J. (1997). Lignin and soluble phenolic degradation by ectomycorrhizal and ericoid mycorrhizal fungi. Mycological Research, 101(11), 1348-1354.

Chander, G., Markham, B. L., & Helder, D. L. (2009). Summary of current radiometric calibration coefficients for Landsat MSS, TM, ETM+, and EO-1 ALI sensors. Remote sensing of environment, 113(5), 893-903.

Clinton, B. D., & Vose, J. M. (1996). Effects of Rhododendron maximum L. on Acer rubrum L. seedling establishment. Castanea, 38-45.

Cohen, W. B., & Spies, T. A. (1992). Estimating structural attributes of Douglas-fir/western hemlock forest stands from Landsat and SPOT imagery. Remote Sensing of Environment, 41(1), 1-17.

Crist, E. P., & Cicone, R. C. (1984). A physically-based transformation of Thematic Mapper data---The TM Tasseled Cap. Geoscience and Remote Sensing, IEEE Transactions on, (3), 256-263.

Crist, E. P. (1985). A TM tasseled cap equivalent transformation for reflectance factor data. Remote Sensing of Environment, 17(3), 301-306.

Day, F. P., & Monk, C. D. (1974). Vegetation patterns on a southern Appalachian watershed. Ecology, 1064-1074.

Dymond, C. C., Mladenoff, D. J., & Radeloff, V. C. (2002). Phenological differences in Tasseled Cap indices improve deciduous forest classification. Remote Sensing of Environment, 80(3), 460-472.

Elliott, K. J., Hendrick, R. L., Major, A. E., Vose, J. M., & Swank, W. T. (1999). Vegetation dynamics after a prescribed fire in the southern Appalachians. Forest Ecology and Management, 114(2), 199-213.

Elliott, K. J., & Vose, J. M. (2012). Age and distribution of an evergreen clonal shrub in the Coweeta Basin: Rhododendron maximum L. 1. The Journal of the Torrey Botanical Society, 139(2), 149-166.

Fensholt, R., & Proud, S. R. (2012). Evaluation of earth observation based global long term vegetation trends—Comparing GIMMS and MODIS global NDVI time series. Remote sensing of Environment, 119, 131-147.

Flatley, W. T., Lafon, C. W., Grissino-Mayer, H. D., & LaForest, L. B. (2013). Fire history, related to climate and land use in three southern Appalachian landscapes in the eastern United States. Ecological applications, 23(6), 1250-1266.

Fortney, R. H. (1993). Canaan Valley–An area of special interest within the upland forest region. Upland forests of West Virginia. McClain Printing Co, Parsons.

Fowler, C., & Konopik, E. (2007). The history of fire in the southern United States. Human Ecology Review, 14(2), 165-176.

Frost, G. V., Epstein, H. E., & Walker, D. A. (2014). Regional and landscape-scale variability of Landsat-observed vegetation dynamics in northwest Siberian tundra. Environmental Research Letters, 9(2), 025004.

Groffman, P. M., Baron, J. S., Blett, T., Gold, A. J., Goodman, I., Gunderson, L. H., ... & Poff, N. L. (2006). Ecological thresholds: the key to successful environmental management or an important concept with no practical application?. Ecosystems, 9(1), 1-13.

Healey, S. P., Cohen, W. B., Zhiqiang, Y., & Krankina, O. N. (2005). Comparison of Tasseled Cap-based Landsat data structures for use in forest disturbance detection. Remote Sensing of Environment, 97(3), 301-310.

Huang, C., Wylie, B., Yang, L., Homer, C., & Zylstra, G. (2002). Derivation of a tasselled cap

transformation based on Landsat 7 at-satellite reflectance. International Journal of Remote Sensing, 23(8), 1741-1748.

IPCC (2013): Kirtman, B., Power, S. B., Adedoyin, J. A., Boer, G. J., Bojariu,R., Camilloni, I., Doblas-Reyes, F. J., Fiore, A. M., Kimoto, M.,Meehl, G. A., Prather, M., Sarr, A., Schär, C., Sutton, R., van Oldenborgh, G. J., Vecchi, G., and Wang, H. J.: Near-term Climate Change: Projections and Predictability, in: Climate Change 2013: The Physical Science Basis, Contribution of Working Group I to the Fifth Assessment Report of the Intergovernmental Panel on Climate Change, edited by: Stocker, T. F., Qin, D..Plattner, G.-K., Tignor, M., Allen, S. K., Boschung, J., Nauels, A., Xia, Y., Bex , V., and Midgley, P. M., Cambridge University Press, Cambridge, United Kingdom and New York, NY, USA, 953–1028, 2013.

Kennedy, P. P. (1853). The Blackwater Chronicle. Redfield. p. 223.

Knapp, R., & Casey, T. M. (1986). Thermal ecology, behavior, and growth of gypsy moth and eastern tent caterpillars. Ecology, 598-608.

Koo, K. A., Madden, M., & Patten, B. C. (2014a). Projection of red spruce (Picea rubens Sargent) habitat suitability and distribution in the southern appalachian mountains, USA. Ecological Modelling, 293, 91-101.

Koo, K. A., Patten, B. C., Teskey, R. O., & Creed, I. F. (2014b). Climate change effects on red spruce decline mitigated by reduction in air pollution within its shrinking habitat range. Ecological Modelling, 293, 81-90.

Koo, K. A., Patten, B. C., & Madden, M. (2015). Predicting Effects of Climate Change on Habitat Suitability of Red Spruce (Picea rubens Sarg.) in the Southern Appalachian Mountains of the USA: Understanding Complex Systems Mechanisms through Modeling. Forests, 6(4), 1208-1226.

Lillesand, M. T., Kieffer, W. R., & Chipman, W. J. (2008). Digital Image Interpretation and Analysis. Remote Sensing and Image Interpretation, 6, 545-81.

Masek, J. G., Huang, C., Wolfe, R., Cohen, W., Hall, F., Kutler, J., & Nelson, P. (2008). North American forest disturbance mapped from a decadal Landsat record. Remote Sensing of Environment, 112(6), 2914-2926.

Maxwell, H. (1884). History of Tucker County, West Virginia. Kingwood, West Virginia.

McClure, M. S., Salom, S. M., & Shields, K. S. (2001). Hemlock wooly adelgid. Forest Health Technology Enterprise Team. US Forest Service Publication FHTET–2001–03. Morgantown, WV.

McGee, C. E., & Smith, R. C. (1967). Undisturbed rhododendron thickets are not spreading. Journal of Forestry, 65(5), 334-335.

Monk, C. D., McGinty, D. T., & Day Jr, F. P. (1985). The ecological importance of Kalmia latifolia and Rhododendron maximum in the deciduous forest of the southern Appalachians. Bulletin of the Torrey Botanical Club, 187-193.

Nilsen, E. T., Clinton, B. D., Lei, T. T., Miller, O. K., Semones, S. W., & Walker, J. F. (2001). Does Rhododendron maximum L.(Ericaceae) reduce the availability of resources above and belowground for canopy tree seedlings?. The American Midland Naturalist, 145(2), 325-343.

Phillips, D. L., & Murdy, W. H. (1985). Notes: effects of Rhododendron (Rhododendron maximum L.) on regeneration of Southern Appalachian hardwoods. Forest Science, 31(1), 226-233.

Reicosky, D. A., & Hanover, J. W. (1978). Physiological effects of surface waxes I. Light reflectance for glaucous and nonglaucous Picea pungens. Plant Physiology, 62(1), 101-104.

Strother, D. H. (1857). Virginia Illustrated. New York, Harper and Brothers, Publishers.

Tucker, C. J. (1979). Red and photographic infrared linear combinations for monitoring vegetation. Remote sensing of Environment, 8(2), 127-150.

Van Lear, D. H., Vandermast, D. B., Rivers, C. T., Baker, T. T., Hedman, C. W., Clinton, B. D., & Waldrop, T. A. (2002). American chestnut, rhododendron, and the future of Appalachian cove forests. In Proceedings of the eleventh biennial southern silvicultural research conference, Gen Tech Rep SRS-48, USDA Forest Service, Southern Research Station, Asheville, NC (pp. 214-220).

Vogelmann, J. E., Howard, S. M., Yang, L., Larson, C. R., Wylie, B. K., & Van Driel, N. (2001). Completion of the 1990s National Land Cover Data Set for the conterminous United States from Landsat Thematic Mapper data and ancillary data sources. Photogrammetric Engineering and Remote Sensing, 67(6).

Walker, D. A., Epstein, H. E., Raynolds, M. K., Kuss, P., Kopecky, M. A., Frost, G. V., ... & Khitun, O. V. (2012). Environment, vegetation and greenness (NDVI) along the North America and Eurasia Arctic transects. Environmental Research Letters, 7(1), 015504.

Weiss, J. L., Gutzler, D. S., Coonrod, J. E. A., & Dahm, C. N. (2004). Long-term vegetation monitoring with NDVI in a diverse semi-arid setting, central New Mexico, USA. Journal of Arid Environments, 58(2), 249-272.

Whittaker, R. H. (1956). Vegetation of the Great Smoky Mountains. Ecological Monographs, 26(1), 1-80.

Wittaker, R. H., & Garfine, V. (1962). Leaf characteristics and chlorophyll in relation to exposure and production in Rhododendron maximum. Ecology, 120-125.

Woods, F. W., & Shanks, R. E. (1959). Natural replacement of chestnut by other species in the

Great Smoky Mountains National Park. Ecology, 349-361.

Wurzburger, N., & Hendrick, R. L. (2007). Rhododendron thickets alter N cycling and soil extracellular enzyme activities in southern Appalachian hardwood forests. Pedobiologia, 50(6), 563-576.

Chapter Five: Synthesis and Conclusions

In this dissertation, I have evaluated the controls exerted by landscape position and vegetation heterogeneity on carbon cycling within a cool, humid watershed in West Virginia. I have also explored the impacts of climatic variability, nitrogen availability, decomposition, and the spatial and temporal dynamics of the evergreen shrub understory and its associated ecological effects. I have utilized three broad approaches to address my research questions: 1) plot-based measurements of soil CO_2 efflux, soil moisture, and soil temperature over three years coupled with extensive quantification of the soils within my study watershed by both field and laboratory methods; 2) a two year litterbag study and estimations of soil nitrogen availability; 3) derivation and comparison of multiple vegetation indices from a time-series of remotely sensed Landsat images. Combined, these approaches create the narrative of ecological dynamics driving carbon cycling within the Weimer Run watershed in West Virginia and have added to the broader theoretical constructs and process understanding of the interaction between vegetation and landscape position in affecting biogeochemical cycling within complex terrain.

LANDSCAPE CONTROLS ON SOIL CO_2 EFFLUX

Past research into soil CO_2 efflux and soil respiration in complex terrain has not fully or explicitly considered the role of vegetation heterogeneity or its interaction with landscape position (e.g. elevation) in affecting fluxes. Areas of complex terrain fail to meet many of the assumptions of eddy covariance flux methods (Baldocchi et al. 2000) due to significant advection (Novick et al. 2014), resulting in the need for plot-based measurements to better estimate surface soil carbon fluxes. Research concerning landscape controls on soil CO_2 fluxes within complex terrain have not specifically evaluated the controls exerted by vegetation heterogeneity. In the case of the semi-arid, Rocky Mountains of Montana, where much of the

vegetation consists of even-aged stands of lodge-pole pine, landscape morphology plays a significant role in modulating soil water availability, resulting in differential surface soil CO_2 fluxes (Pacific et al. 2009; Riveros-Iregui et al. 2012). Other work has focused on successional stages or climatic gradients (Stoy et al. 2008; Anderson-Teixeira et al. 2011). One of the major findings in Chapter Two of my dissertation is that vegetation can exert strong controls on fluxes within elevation classes. Within elevation and year, plots located beneath shrubs had greater soil CO_2 fluxes. For areas with varying forest and ecological structure, this is potentially a key consideration for future research. Another key finding from Chapter Two is the interaction of inter-annual climatic variability to control the magnitude of fluxes across the watershed, a line of research that has received recent attention (Berryman et al. 2015) and will be of marked interest in the years to come given changes in precipitation regimes driven by anthropogenically forced climate change that are already being seen (Zhang et al. 2007).

LANDSCAPE CONTROLS ON DECOMPOSITION, NUTRIENT CYCLING, AND THE ORGANIC LAYER

Decomposition is a significant component of the carbon cycle and nutrient cycling. While broadly decomposition is controlled by climate, litter chemistry, and substrate quality (Meetenmeyer, 1978; Melillo et al. 1982; Aerts, 1997; Zhang et al. 2008; Silver and Miya, 2000), forest structure and landscape position exert controls at finer scales (Hastwell and Morris, 2013). It is important to quantify and understand the ecological drivers of nutrient cycling within complex terrain, particularly with respect to vegetation heterogeneity. It is apparent that changing vegetation dynamics, driven by climate change, may be affecting nutrient cycling in many areas of the globe (Cornelissen and Cornwall, 2014; Ward et al. 2015), and understanding the mechanisms behind these changes is an exciting, yet complex line of inquiry. In Chapter

Three, I show that a two-year litter bag experiment in the Weimer Run watershed using yellow birch litter provides mixed results. While elevation exerts significant controls on initial decomposition (after one month), with areas lower in the watershed having significantly faster rates of decomposition, these effects lessen during the remainder of the experiment. There is the indication of a potential interaction between winter decomposition driven by snowfall and snowpack development. However, this was not a specific hypothesis I set out to test, and the data are inconclusive. Nitrogen remains quite high in the leaf litter during the course of the experiment, suggesting a system dominated more by fungal components than bacterial. Nitrogen availability is also influenced by vegetation cover, with higher N availability associated with closed-canopy areas. Here, there is the potential of interactions between the ericoid mycorrhizae associated with *R. maximum* and other associations within the system driving these differences.

CHARACTERIZING THE EVERGREEN SHRUB COMMUNITY

The evergreen shrub layer is a strong component of the Weimer Run watershed and many other areas of the mountains of the mid and southern Appalachians. *R. maximum* is a significant component of this shrub layer that affects the ecology of the system by altering forest species richness, forest structure, forest diversity, soil chemical and physical properties, and soil carbon fluxes (Clinton and Vose, 1996; Nilsen et al. 2001; Wurzberger and Hendrick, 2007; Atkins et al. 2015). Accurate quantification of the spatial and temporal dynamics of this shrub layer are difficult, as *R. maximum* branches close to the ground, in dense, nearly impenetrable thickets that make ground-based measurements tedious, expensive, or practically impossible. Through this work, I have shown the utility of using winter NDVI and other remotely sensed vegetation indices to quantify evergreen shrub expansion throughout the period of available satellite data

(1986-2011). I have also shown that *R. maximum* is expanding into areas of the forests where it was formerly limited by evapotranspiration demands on soil moisture (southerly oriented slopes). This work has contributions not only to forest and terrestrial ecology, but also to applied watershed management.

FUTURE DIRECTIONS

One of the key findings of this dissertation is the impact that vegetation has on carbon cycling within complex terrain through mediating micrometeorology and driving soil and ecological changes. The plot based measurements outlined in Chapter Two, if paired with concurrent measurements of soil CO_2 pore space taken below the soil surface (not explicitly presented in this dissertation) could be used to develop a process-based, spatially explicit soil carbon flux model providing weighted, watershed scale measurements of soil respiration. Paired with past climatic information (e.g. NCDC database) and knowledge of the changing vegetation dynamics of the watershed (informed from Chapter Four of this dissertation), this model could then estimate spatially explicit fluxes through time, with projections of how changing vegetation and climate could further impact carbon cycling in the Weimer Run watershed and other watersheds.

There is also a need to examine the bi-directionality of watershed scale response of soil CO_2 efflux or soil respiration to soil moisture. Where and when do soil carbon fluxes increase in response to increasing moisture? Is there a common threshold of soil moisture at which soil carbon fluxes begin to decrease or is that threshold watershed specific? By pairing soil CO_2 efflux, soil temperature, and soil moisture data from this study with data from other studies there is the potential to generate a broad, macroscale understanding of watershed response of soil carbon fluxes to soil moisture.

Understanding how changing climate will impact our forests and our landscapes will be a pressing concern for many years. We have likely passed a threshold where we are committed to significant warming over the next century or more that will drastically alter the world as we know it. By leveraging research into fundamental carbon cycling, specifically in vulnerable areas, as outlined in this dissertation, we can inform mitigation strategies, develop an understanding of process and resilience, confront change, and inform the research questions to come.

REFERENCES

Aerts, R. (1997). Nitrogen partitioning between resorption and decomposition pathways: a trade-off between nitrogen use efficiency and litter decomposibility?. Oikos, 603-606.

Anderson-Teixeira, K. J., Delong, J. P., Fox, A. M., Brese, D. A., & Litvak, M. E. (2011). Differential responses of production and respiration to temperature and moisture drive the carbon balance across a climatic gradient in New Mexico. Global Change Biology, 17(1), 410-424.

Atkins, J. W., Epstein, H. E., & Welsch, D. L. (2015). Vegetation and elevation influence the timing and magnitude of soil CO2 efflux in a humid, topographically complex watershed. Biogeosciences, 12(10), 2975-2994.

Baldocchi DD, Finnigan JJ, Wilson KW, Paw U KT, Falge E (2000) On measuring net ecosystem carbon exchange in complex terrain over tall vegetation. Boundary Layer Meteorology. 96: 257-291.

Berryman EM, Barnard HR, Adams HR, Burns MA, Gallo E, Brooks PD (2015) Complex terrain alters temperature and moisture limitations of forest soil respiration across a semiarid to subalpine gradient. JGR: Biogeosciences, 120, 707-723.

Clinton, B. D., & Vose, J. M. (1996). Effects of Rhododendron maximum L. on Acer rubrum L. seedling establishment. Castanea, 38-45.

Cornelissen, J. H., & Cornwell, W. K. (2014). The Tree of Life in ecosystems: evolution of plant effects on carbon and nutrient cycling. Journal of Ecology, 102(2), 269-274.

Hastwell, G. T., & Morris, E. C. (2013). Structural features of fragmented woodland communities affect leaf litter decomposition rates. Basic and Applied Ecology, 14(4), 298-308.

Meentemeyer, V. (1978). Macroclimate and lignin control of litter decomposition rates. Ecology, 59(3), 465-472.

Melillo, J. M., Aber, J. D., Muratore, J. F. (1982) Nitrogen and Lignin Control of Hardwood Leaf Litter Decomposition Dynamics. Ecology 63:621–626. http://dx.doi.org/10.2307/1936780

Nilsen, E. T., Clinton, B. D., Lei, T. T., Miller, O. K., Semones, S. W., & Walker, J. F. (2001). Does Rhododendron maximum L.(Ericaceae) reduce the availability of resources above and belowground for canopy tree seedlings?. The American Midland Naturalist, 145(2), 325-343.

Novick, K., Brantley, S., Miniat, C. F., Walker, J., & Vose, J. M. (2014). Inferring the contribution of advection to total ecosystem scalar fluxes over a tall forest in complex terrain. Agricultural and Forest Meteorology, 185, 1-13.

Pacific VJ, McGlynn BL, Riveros-Iregui DA, Epstein HE, Welsch DL (2009). Differential soil respiration responses to changing hydrologic regimes. Water Resources Research, 45(7), W07201. doi:10.1029/2009WR007721.

Riveros-Iregui, D. A., McGlynn, B. L., Emanuel, R. E., & Epstein, H. E. (2012). Complex terrain leads to bidirectional responses of soil respiration to inter-annual water availability. Global Change Biology, 18(2), 749-756.

Silver, W. L., & Miya, R. K. (2001). Global patterns in root decomposition: comparisons of climate and litter quality effects. Oecologia, 129(3), 407-419. http://www.jstor.org/stable/3546886

Stoy, P. C., Palmroth, S., Oishi, A. C., Siqueira, M., JUANG, J. Y., Novick, K. A., ... & Oren, R. A. M. (2007). Are ecosystem carbon inputs and outputs coupled at short time scales? A case study from adjacent pine and hardwood forests using impulse–response analysis. Plant, Cell & Environment, 30(6), 700-710.

Ward, S. E., Orwin, K. H., Ostle, N. J., Briones, M. J., Thomson, B. C., Griffiths, R. I., ... & Bardgett, R. D. (2015). Vegetation exerts a greater control on litter decomposition than climate warming in peatlands. Ecology, 96(1), 113-123.

Wurzburger, N., & Hendrick, R. L. (2007). Rhododendron thickets alter N cycling and soil extracellular enzyme activities in southern Appalachian hardwood forests. Pedobiologia, 50(6), 563-576.

Zhang, D., Hui, D., Luo, Y., & Zhou, G. (2008). Rates of litter decomposition in terrestrial ecosystems: global patterns and controlling factors. Journal of Plant Ecology, 1(2), 85-93.

Zhang, X., Zwiers, F. W., Hegerl, G. C., Lambert, F. H., Gillett, N. P., Solomon, S., ... & Nozawa, T. (2007). Detection of human influence on twentieth-century precipitation trends. Nature, 448(7152), 461-465.